# DEVELOPMENT AND VALIDATION OF A CONDITIONAL LOCALIZATION DOMAIN TO CONTROL TRAFFICKING OF SECRETORY PROTEINS IN *PLASMODIUM FALCIPARUM*

by
Aleah D. Roberts

A dissertation submitted to Johns Hopkins University in conformity with the requirements for the degree of Doctor of Philosophy

Baltimore, Maryland
July 2017

**ABSTRACT**

The apicoplast is an essential organelle of *P. falciparum*. Currently, there are few molecular tools to identify and validate specific essential apicoplast proteins. We have therefore developed a molecular tool to probe the function of apicoplast-targeted proteins.

Nuclear-encoded proteins that are targeted to the apicoplast contain a transit peptide sequence that is essential for sorting proteins from the endoplasmic reticulum, into vesicles that fuse with the apicoplast outer membrane. Transit peptides have a unique requirement that they are unstructured during apicoplast import; furthermore, formation of structure in the transit peptide region blocks import. The goal of my thesis was to use this feature of transit peptides to design a conditional localization domain (CLD) tag that can control the localization of an apicoplast targeted protein. The CLD replaces the natural transit peptide of the target protein and traffics to the apicoplast under permissive conditions. An interacting ligand is added to the cell to bind the domain and cause the CLD to become secreted.

We tested several proteins as potential CLDs and analyzed their ability to control trafficking of a fluorescent cargo protein using microscopy. Chapters 2 and 3 describe our efforts to design a suitable CLD from Dihydrofolate Reductase (DHFR) enzymes and the FK-506 Binding Protein (FKBP). The candidate domains we designed from DHFR were not suitable CLDs because they did not traffic to the apicoplast. Our initial design of a CLD from FKBP was also not a suitable CLD because it was too unstable to respond to the interacting ligand, although it was able to traffic to the apicoplast. We modified the original CLD designed from FKBP to generate three successful domains (CLD1, 2, and 3) that can be used to control the trafficking of apicoplast-targeted proteins. In Chapter 4 we analyzed the trafficking dynamics of CLD1, 2, and 3 in detail. Results show that CLD2 and CLD3

traffic to the apicoplast more efficiently than CLD1; we found that CLD1's leaky apicoplast trafficking is caused by a higher protein stability compared to CLD2 or CLD3.

To validate this system, we tested whether CLD1 or CLD2 could conditionally localize a parasite biotin ligase called Holocarboxylase Synthetase 1 (HCS1) without interfering with the function of the enzyme. HCS1 biotinylates the acetyl-CoA carboxylase, a protein that is only biotinylated in the apicoplast of liver stage parasites. In parasite lines that express CLD1-HCS1 or CLD2-HCS1, we were able to control protein biotinylation in the apicoplast in a ligand-dependent manner, demonstrating the full functionality of the CLD tool.

**ACKNOWLEDGEMENTS**

I would like to thank my PhD thesis advisor Dr. Sean Prigge for his helpful advice and support throughout my PhD. Dr. Prigge always makes time to talk with his students and is a great resource. I would also like to thank the members of my thesis committee for their help in driving the direction of my thesis and providing valuable feedback. Past and current Prigge lab members have been very supportive throughout my PhD and the Prigge lab meetings in particular were imperative to helping me prepare for presentations and molding my data into a cohesive story.

I would like to thank a few lab members in particular who contributed significantly to the work described in this thesis. During my first few months in the lab Dr. Krista Matthews helped me to get the transfection methods working and was a patient and invaluable resource. Also, during the early days of my graduate career, Dr. Gustavo Afanador was a great help with some of the biophysical studies of the candidate CLD proteins. Finally, Dr. Alfredo Guerra taught me all of the protein purification and thermal shift assay techniques. I could not have completed the *in vitro* protein studies without his guidance.

Finally, I would like to thank all of my family and friends who supported me over the last few years of pursuing my PhD.

**TABLE OF CONTENTS**

**List of Tables**

**List of Figures**

**List of Abbreviations**

ACC = acetyl-CoA carboxylase

Acetyl-CoA/Ac-CoA = acetyl-coenzyme A

ACP = acyl carrier protein

ACS = acetyl-CoA synthetase

BSD = blasticidin S-deaminase

CAD = conditional aggregation domain

CLD = conditional localization domain

dFKBP = destabilized FKBP

DHF = dihydrofolate

DHFR = dihydrofolate reductase

DMAPP = dimethylallyl pyrophosphate

ER = endoplasmic reticulum

ERAD = endoplasmic reticulum associated degradation

FAME = fatty acid methyl ester

FASII = type 2 fatty acid synthesis

FKBP = FK-506 binding protein

GFP = green fluorescent protein

HCS1 = holocarboxylase synthetase 1

HPTLC = high performance thin layer chromatography

IPP = isopentenyl pyrophosphate

KDH = α-ketoglutarate dehydrogenase

Lipl1 = Lipoate Ligase 1

Lipl2 = Lipoate Ligase 2

$M_1$ = Mander's Overlap Coefficient

Malonyl-CoA = malonyl-coenzyme A

MBP = maltose binding protein

MEP = 2-C-methyl-D-erythritol 4-phosphate

MTX = methotrexate

mPDH = mitochondrial pyruvate dehydrogenase

NADPH = nicotinamide adenine dinucleotide phosphate

PATS = predictor of apicoplast targeted sequences

PCC = Pearson's correlation coefficient

PEP = phosphoenolpyruvate

PPT = PEP/phosphate translocator

RBC = red blood cell

RNAi = RNA interference

sbFKBP = shield1 binding FKBP

SFG = super folder green

SPP = stromal processing peptidase

TetR = tetracycline repressor

TEV = Tobacco Etch Virus

THF = tetrahydrofolate

$T_m$ = melting temperature

TMP = trimethoprim

# Chapter 1

# Introduction

## *Plasmodium falciparum* Malaria

Malaria is a disease caused by 5 species of the Plasmodium parasite that infects humans. *Plasmodium falciparum* is the most prevalent Plasmodium species in Africa and according to the World Health Organization's most recent report, 90 % of the 438,000 deaths from malaria in 2015 occurred in the African region[1]. Typical symptoms of Malaria include anemia, splenomegaly, and cyclical fevers but infection with *P. falciparum* can trigger more severe forms of disease such as cerebral malaria, which can lead to death in infants and children who are less than 5 years old. Given the severe impact of *P. falciparum* infection on young children, studies of the cell biology and immune response to this parasite are imperative to develop new treatments for the disease.

*P. falciparum* has a complex life cycle that requires two hosts: female Anopheles mosquitos and humans. Humans are the intermediate host and are required for asexual replication and transmission of the parasite. The human stages of the parasite life cycle begin when a mosquito injects sporozoites into the skin while blood feeding. Sporozoites travel to the liver, and undergo a period of development in hepatocytes that lasts 5-6 days. Morphological changes occur in hepatocytes that allow the parasite to enter the blood stream, where it begins repeated cycles of asexual division in red blood cells[2]. Some parasites circulating in the blood split off from the asexual cycle and become gametocytes. Gametocytes are required for transmission of the parasite back to the mosquito during blood feeding.

There are four stages of parasite development in the asexual blood cycle. Merozoites are the infectious stage that primarily invades reticulocytes (Figure 1-1 [1]). After invasion, the parasite enters the ring stage and begins catabolizing hemoglobin that is imported from the red blood cell cytosol (Figure 1-1 [2]) [3]. Increases in parasite size and shape, as well as the

generation of Maurer's clefts which are involved in export of parasite proteins to the red blood cell surface, mark the transition to the trophozoite stage (Figure 1-1 [3]) [4]. In the final phase of development, schizonts prepare to release 16 or more newly formed merozoites (Figure 1-1 [4]). During the schizont stage the nucleus and other organelles required for cell survival and invasion are replicated and segregated into daughter merozoites [3] that are released from ruptured red blood cells.

Most of the canonical and severe symptoms of malaria have been linked to parasite biology that occurs in the asexual cycle in red blood cells. For example, the release of merozoites at the end of each 48 hour cycle stimulates a pro-inflammatory immune response that causes cyclical fevers [5]. This pro-inflammatory immune response also contributes to the development of severe anemia that is associated with Plasmodium infection. Pro-inflammatory molecules negatively impact the maturation of erythroid cells, which leads to a reduction in erythropoesis[6]. Additionally, sequestration of late stages – trophozoites and schizonts – on brain endothelium is a major factor in the development of cerebral malaria [7]. Sequestered parasites reduce perfusion around the brain tissue and cause hypoxia which exacerbates the symptoms of cerebral malaria[8].

Given that the symptoms associated with malaria are caused by the erythrocytic cycle, it is not surprising that several classes of antimalarial compounds target the erythrocytic cycle. For example, Quinolines are a class of anti-malarials that interfere with hemoglobin digestion, and Atovaquone collapses the mitochondrial membrane potential in blood stage parasites. Between the late 1950s and early 1980s however, widespread resistance to Chloroquine – a quinolone compound – arose, and resistance to several other classes of anti-malarials has been documented since then[9]. Due to Plasmodium's historic ability to acquire drug resistance, it is important to continue to advance efforts to develop new anti-

malarial compounds. One ideal target for development of novel anti-malarials is the apicoplast organelle.

**The Essential Apicoplast Organelle**

An ancient eukaryotic ancestor of Plasmodium engulfed a algal cell which was reduced through evolution to the current apicoplast[10]. The apicoplast is a non-photosynthetic plastid that is essential for parasite survival at all stages of development in the human host. Most of the protein coding genes previously encoded in the apicoplast have been transferred to the nucleus of the parasite[11]. As a result, nuclear encoded proteins that still function in the apicoplast must be post-translationally trafficked back to the organelle to perform their function.

Proteins that are active in the apicoplast perform essential functions at multiple stages of parasite development in the human host; and targeting apicoplast proteins for drug development could impact both the liver and blood stages of the parasite life cycle. For example, Plasmodium relies on the Type II Fatty Acid Synthesis (FASII) pathway in the apicoplast for production of lipids[12,13]. Studies of the FASII pathway in Plasmodium have revealed that FASII activity is required for progression from the liver stage to the blood stage of the parasite life cycle [14,15]. Since mammalian cells rely on the Type I FAS pathway for lipid synthesis, targeting proteins required by the FASII pathway could inhibit growth of liver stage parasites and also prevent progression to the blood stage, without harming host cells.

The apicoplast also houses the MEP (2-C-methyl-D-erythritol 4-phosphate) pathway for synthesis of isoprenoid precursors: isopentenyl pyrophosphate (IPP) and dimethylallyl pyrophosphate (DMAPP)[16]. Studies have shown that IPP and DMAPP are the only essential

products of the apicoplast in blood stage *P. falciparum* and treatment with drugs that inhibit the MEP pathway, kill the parasite[17,18]. Humans use a different pathway to synthesize isoprenoid precursors, and drugs that target the MEP pathway specifically, such as Fosmidomycin, have been successfully used to treat malaria in clinical trials[19].

Another group of proteins that has the potential to provide new drug targets against Plasmodium are proteins that are required for maintenance of the apicoplast organelle. Antibiotics inhibit apicoplast maintenance by blocking the activity of the ribosome in the apicoplast, which is responsible for translating a small number of proteins encoded in the apicoplast genome[20,21]. Studies from our lab have shown that the iron-sulfur (Fe-S) cluster synthesis pathway is also required for parasites to maintain the apicoplast and interfering with Fe-S cluster synthesis through expression of a dominant negative protein kills the parasite[22]. Other pathways could potentially be targeted inside the apicoplast that are essential for maintaining the apicoplast genome, organelle morphology, and protein import. Targeting proteins that are essential for apicoplast maintenance could be effective against both liver and blood stage parasites, since the apicoplast is essential at both stages of parasite development.

Despite the importance of the apicoplast at multiple stages in the lifecycle, current knowledge of essential apicoplast biochemistry is largely based on predictions of the putative presence of nuclear-encoded proteins that contain the appropriate targeting motifs to allow them to be trafficked to the apicoplast [16]. Increasing our knowledge of the essential pathways that are required for apicoplast maintenance and cell survival will improve our understanding of parasite biology and could provide insight into new drug targets for malaria treatment.

**Protein Trafficking to the Apicoplast**

Soluble proteins are trafficked to the apicoplast via an N-terminal signal sequence and transit peptide motif [23–25]. The signal sequence directs the protein to the endoplasmic reticulum (ER), where it is cleaved to reveal the transit peptide[24]. The transit peptide then further directs the protein to the apicoplast [25]. A model of how proteins are trafficked to the apicoplast is shown in Figure 1-2 A.

Several studies have helped to elucidate the characteristics of apicoplast transit peptides. Initially, researchers hypothesized that apicoplast transit peptides might have some features similar to the transit peptides of chloroplasts in plant cells. Apicoplast transit peptides however, do not appear to be similar to chloroplast transit peptides, and do not have a requirement for specific serine or threonine residues for trafficking[24]. Further studies showed that there is no specific amino acid sequence that is required for apicoplast trafficking. *P. falciparum* transit peptides must maintain a net positive charge near the N-terminus, but the exact sequence of the positively charged residues is not important[26]. Our lab investigated whether there were any structural requirements for apicoplast transit peptides[27]. Nuclear magnetic resonance studies and mutational analysis of a confirmed apicoplast transit peptide sequence led to the discovery that transit peptides are unstructured during apicoplast import. These studies also showed that formation of structure in the transit peptide region blocks proteins from being imported to the apicoplast. Finally, bioinformatics analysis of a group of putative apicoplast trafficked proteins revealed that transit peptides are typically between 24 and 150 amino acids in length[28].

The Acyl-Carrier Protein (ACP) was identified and verified early on as an apicoplast trafficked protein[12,28]. ACP is involved in fatty acid synthesis and is expressed in both liver and blood stage parasites[29]. Consequently, ACP is often used as a marker for the apicoplast and the trafficking motif from ACP has been appended to multiple fluorescent proteins to

illuminate the morphology of the apicoplast[30]. Figure 1-2 B, shows one such experiment where the targeting motif from ACP is appended to a green fluorescent protein and expressed in blood stage parasites. The pattern of fluorescence in Figure 1-2 B shows the morphology of the apicoplast at the ring, trophozoite and schizont stages of development. At the ring stage, the apicoplast appears as a small dot that is usually located at the edge of the cell. In the trophozoite stage, the apicoplast branches out and can form almost any shape. In the schizont, the apicoplast divides into multiple daughter organelles that get segregated into each budding merozoite.

Although there has been significant progress in defining the characteristics of transit peptides and the morphology of the apicoplast, there is still some debate about exactly how transit peptides direct trafficking to the apicoplast from the endoplasmic reticulum. Once the transit peptide is revealed in the endoplasmic reticulum, one hypothesis is that a currently unidentified receptor protein binds the transit peptide and sorts it into vesicles bound for the apicoplast outer membrane without trafficking through the Golgi[31]. This hypothesis is supported by experiments that showed that treating parasites with Brefelden A (Brefelden A collapses the Golgi complex) does not inhibit apicoplast trafficking[31]. More recent studies have conflicted with this model by showing that addition of an ER retrieval sequence to an apicoplast trafficked protein, reduces trafficking to the apicoplast[32]. This is significant because ER retrieval sequences are recognized in the Golgi and then trafficked back to the ER; In order for an ER retrieval sequence that is added on to an apicoplast targeted protein to be effective, the apicoplast targeted protein must traffic through the Golgi. This suggests that there may be a sorting branch point in the Golgi for apicoplast-targeted proteins.

**Molecular tools to investigate apicoplast-targeted proteins in *P. falciparum***

Currently there are only a few options for molecular tools to investigate apicoplast-targeted proteins. Some of these options include genetic knockouts, which can only be applied to non-essential proteins, and conditional degradation domain tags [33,34]. Conditional degradation domains are used to control the level of a specific protein in the cell. The protein of interest is tagged with the degradation domain and in the absence of an interacting ligand the domain destabilizes the protein and causes it to be degraded. When the ligand is added to cell culture media, the degradation domain stabilizes, which allows the protein to avoid degradation by the proteasome. Conditional degradation domains work well to control the level of cytosolic proteins, but are not as effective at controlling the level of proteins that traffic through the secretory pathway – this includes apicoplast-targeted proteins. Degradation domains may be less effective when tagging secretory proteins because they rely on the proteasome complex in the cytosol to reduce protein levels. Secretory proteins are co-translationally imported into the ER and must be must be recognized and exported by the ER-associated degradation (ERAD) pathway before they can be degraded by the proteasome in the cytosol. The ERAD pathway may have differences in regulation or kinetics that prevents secretory proteins tagged with the degradation domain from being efficiently recognized or exported for degradation.

RNA interference (RNAi) is a cellular pathway that is also commonly used to control protein levels in eukaryotic organisms [35]. RNAi is not applicable in *P. falciparum* because the parasite does not encode any of the essential RNAi pathway genes and lacks a functional RNAi pathway [36].

Recently, a translational control molecular tool was designed for use in *P. falciparum*. This system requires the introduction of an aptamer sequence at the 3' and 5' ends of the target mRNA [37]. Under permissive conditions the aptamers interact with the Tet-repressor

(TetR) protein fused to a translational repressor (*Pf*DOZI) to block translation of the target mRNA. Addition of anhydrotetracycline to the culture, prevents the TetR-*Pf*DOZI repressor complex from interacting with the aptamer and allows the mRNA to be translated [37]. This methodology may be difficult to implement with apicoplast-targeted proteins because introduction of an aptamer at the 5' end of the mRNA, if translated with the leader peptide, could interfere with proper trafficking to the apicoplast.

Given the small number of molecular tools available to control protein levels in Plasmodium, and the limitations of the current tools, the goal of my thesis was to develop a conditional localization system that would allow us to control the localization of apicoplast-targeted proteins, and add to the field of molecular tools used in *P. falciparum*. The conditional localization system developed in this thesis is based on the use of a conditional localization domain (CLD) tag that we designed to be added as an N-terminal modification to a protein of interest and control its localization. Under permissive conditions the CLD traffics to the apicoplast and when an interacting ligand is added to the cell culture media, the CLD changes localization and is secreted from the cell. To design the CLD we tested two modified proteins as potential domains based on their previous use as degradation domains in *P. falciparum*. Chapter 2 described our initial attempts to design a CLD from the Dihydrofolate Reductase (DHFR) protein and Chapter 3 describes our final design of the CLD from the FK-506 Binding Protein (FKBP).

**Dihydrofolate Reductase Protein and Ligands**

DHFR is an essential enzyme in the folate metabolism pathway of both prokaryotic and eukaryotic cells. DHFR binds dihydrofolate (DHF) and the cofactor NADPH, and generates tetrahydrofolate (THF) and $NADP^+$. THF is an essential cofactor for synthesis of

purine molecules, some amino acids, and most importantly, thymidine nucleotides[38]. DHFR activity supports the growth of rapidly dividing cells in cancer by maintaining high levels of THF for thymidine synthesis. Specific inhibitors of DHFR activity, such as methotrexate (MTX) are used as chemotherapeutic agents[39] .

The crystal structure of DHFR in complex with MTX and NADPH is shown in Figure 1-3 A. DHFR has a complex structure made up of four alpha helices and an 8-strand beta sheet that fold to create two binding domains. The discontinuous loop domain (violet colored structure in Figure 1-3 A) binds DHF or a folate analog (MTX), and the adenosine-binding domain (cyan colored structure in Figure 1-3 A) binds NADPH[40]. The structure in Figure 1-3 A shows that the DHFR interaction domains bring folate and NADPH into close association when bound to DHFR, and studies have shown that NADPH facilitates cooperative binding between DHFR and another folate analog, trimethoprim (TMP)[41]. TMP (structure shown in Figure 1-3 B) has enhanced specificity for bacterial DHFR enzymes and is used as an antibiotic[38]. In our studies we expressed DHFR in parasites as a candidate CLD and we used TMP as the interacting ligand in these experiments.

**FK-506 Binding Protein and Ligands**

FKBP is a prolyl isomerase that is normally active in the cytosol as a protein folding chaperone[42]. FKBP was identified as the target of two immunosuppressive agents isolated from bacteria: FK-506 and Rapamycin. Both of these compounds form complexes with FKBP that interfere with the cellular immune response by blocking signal transduction pathways that are required for T-cell activation[42]. FKBP has a much simpler structure than DHFR that consists of a 5-strand anti-parallel beta sheet that wraps in a right handed twist around a short alpha helix (Figure 1-4 A)[43]. The side chains of the beta sheet form a

hydrophobic pocket where the FK-506 ligand binds.

The FKBP/FK-506 protein and ligand combination has been re-purposed for use as a molecular tool in multiple eukaryotic cell systems[44]. FKBP and FK-506 have both been modified in many of these molecular tools to create a more high affinity protein-ligand interaction[45]. The structure of FK-506 is shown in Figure 1-4 B with the conserved core region highlighted in red. This conserved core region binds in the hydrophobic pocket of FKBP and is maintained in most FK-506 derivatives. Studies of the carbonyl oxygen highlighted with an arrow in Figure 1-4 B have found that this region of the compound interacts with the amino acid side chains depicted in Figure 1-4 A (Tyr26, Phe36, and Phe99)[45]. Mutating the phenylalanine at position 36 to valine creates a hole in the hydrophobic pocket of FKBP that is compensated by the replacing the highlighted carbonyl oxygen in FK-506 with a trimethoxyphenyl group to create the Shield1 ligand (Shield1 structure is shown in the bottom panel of Figure 4-1 B). Shield1 is an FK-506 derivative that has a binding affinity ($K_d$) of 0.094 nM for the $FKBP_{F36V}$ mutant, compared to 67 nM for the wild type protein[45]. Shield1 is commonly used as the ligand for $FKBP_{F36V}$ when FKBP is used as a molecular tool in *P. falciparum* and in other eukaryotic cells.

**Thesis Rationale**

This thesis will describe the design, evaluation, and validation, of a conditional localization domain tag that can be used to control the localization of specific apicoplast targeted proteins. Previous studies in our laboratory on the targeting motifs required for apicoplast trafficking were instrumental in the conceptualization of the apicoplast conditional localization domain[27].These studies showed that *P. falciparum* transit peptides must be unstructured to traffic to the apicoplast, and that the formation of structure in the

transit peptide region blocks apicoplast import [27]. My thesis builds on this understanding of the structural requirements of transit peptides to engineer a conditional localization domain that can be added as an N-terminal tag to a protein of interest and replace the transit peptide motif. In the absence of an effector ligand the CLD mimics a natural transit peptide region, and is unstructured to allow the protein to traffic to the apicoplast. When the effector ligand, binds to the CLD, it stabilizes the structure of the protein and causes the CLD to be secreted from the cell. A model of the conditional localization system designed in this thesis is shown in Figure 1-5.

To engineer a CLD, we designed and tested multiple proteins as candidate CLDs. We reasoned that a destabilized protein would be an ideal starting point for the design of the CLD. Our overall hypothesis was that the destabilized version of the CLD could mimic an unstructured transit peptide region and traffic to the apicoplast, and addition of a binding ligand to stabilize the structure of the CLD could cause the protein to be secreted. Two destabilized proteins have been expressed in *P. falciparum* as conditional degradation domains: Dihydrofolate Reductase and FK-506 Binding Protein [33,34]. We modified both of these proteins to more closely mimic a *P. falciparum* transit peptide and expressed them in *P. falciparum* to test if they were suitable candidates to be the conditional localization domain tag. Studies of the DHFR protein (Chapter 2) showed that DHFR could not be used as a CLD because it does not traffic to the apicoplast. We were however, able to design three successful CLDs by modifying the FKBP sequence (Chapter 3). We characterized the trafficking dynamics of each CLD designed from the FKBP protein in Chapter 4. And finally, in Chapter 5 we validated two of the CLDs by tagging the active parasite biotin ligase, Holocarboxylase Synthetase 1 (HCS1; PlasmoDB PF3D7_1026900). We were able to control the localization and activity of this enzyme in the apicoplast using the conditional

localization domain. The apicoplast conditional localization system designed in this thesis can be added to the list of molecular tools for investigating the molecular biology of *P. falciparum* and will be useful in future studies of the function of specific apicoplast targeted proteins that could provide novel drug targets for Malaria.

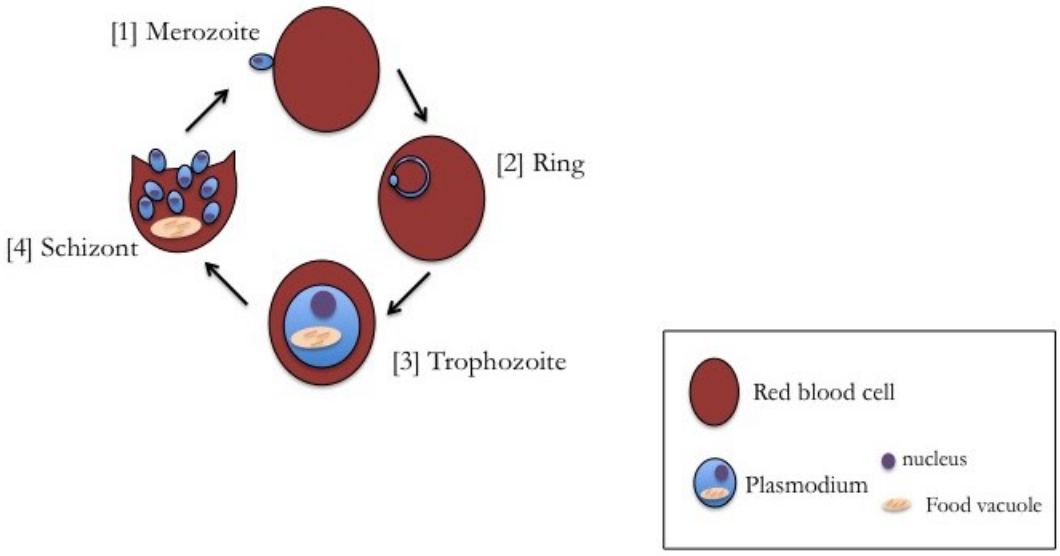


**Figure 1-1 The erythrocytic cycle of *P. falciparum***

[1] Merozoites actively invade red blood cells (RBC) to begin the asexual division cycle.

[2] After invasion the ring stage parasite begins to feed on the red blood cell cytosol.

[3] The trophozoite expands in size and sets up export machinery for parasite proteins in the RBC cytosol.

[4] Mature schizonts have replicated the cellular DNA and organelles required for invasion and separated them into daughter merozoites. Merozoites are released from the ruptured RBC and invade new red blood cells.

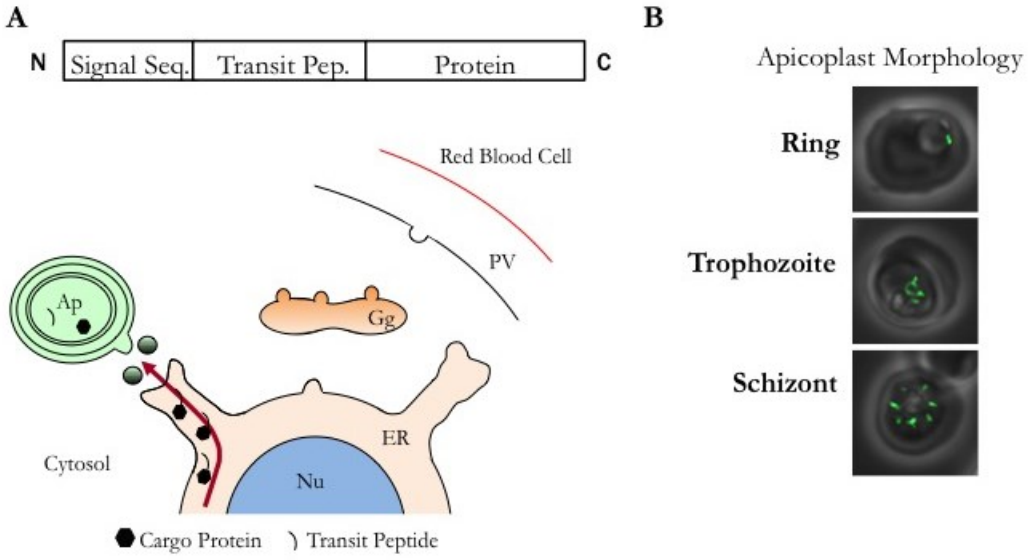


**Figure 1-2 Protein trafficking in Plasmodium**

A) Nuclear encoded proteins that are trafficked to the apicoplast contain an N-terminal signal sequence and transit peptide. The signal sequence directs the protein to be co-translationally imported into the ER, where it is cleaved to reveal the transit peptide. The transit peptide then further directs the protein to the apicoplast.

Ap = Apicoplast, PV = Parasitophorous Vacuole, ER = Endoplasmic Reticulum,
Nu = Nucleus, Gg = Golgi, Signal Seq. = Signal Sequence, Transit Pep. = Transit Peptide

B) Live fluorescence images of a transgenic parasite line that expresses the Super Folder Green fluorescent protein with an N-terminal trafficking motif from a verified apicoplast resident protein (the Acyl-Carrier Protein). This parasite line allows us to visualize the apicoplast morphology at each stage of parasite development. Images are 10 microns wide by 10 microns long.

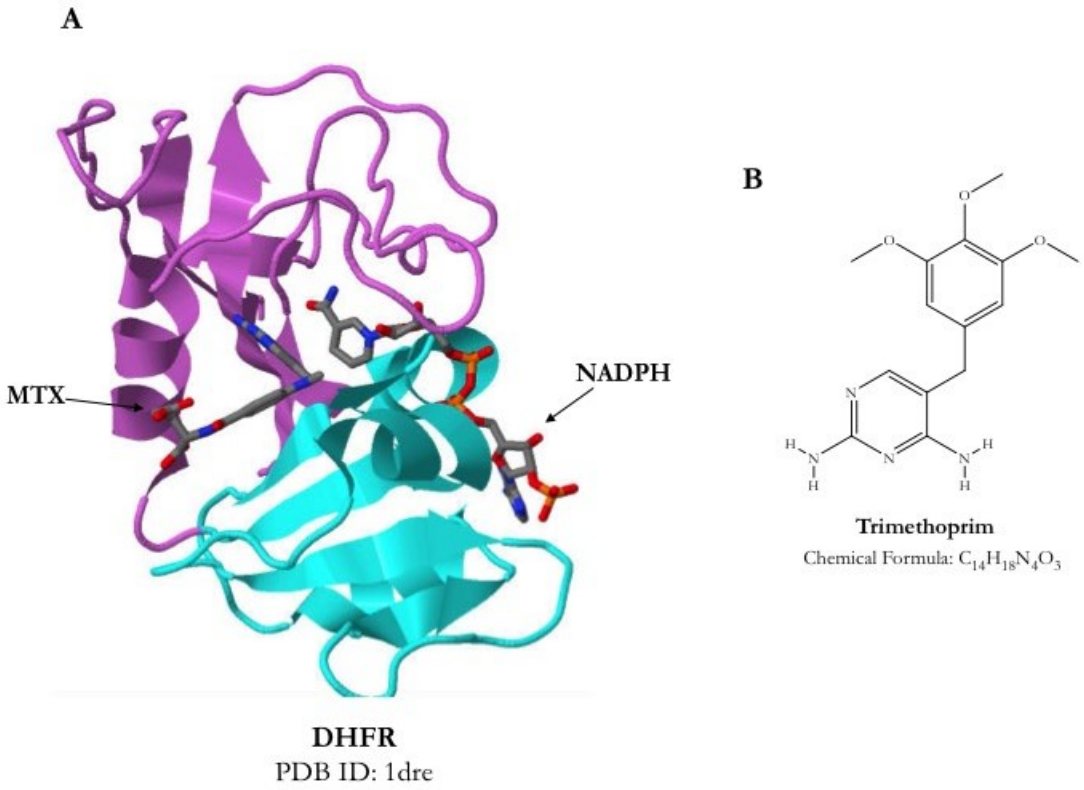


**Figure 1-3 Structure of Dihydrofolate Reductase and Trimethoprim**

A) Crystal structure of the *E. coli* DHFR protein in a complex with methotrexate (MTX) and the co-factor NADPH[46].

B) Chemical structure of Trimethoprim (PubChem CID: 5578)

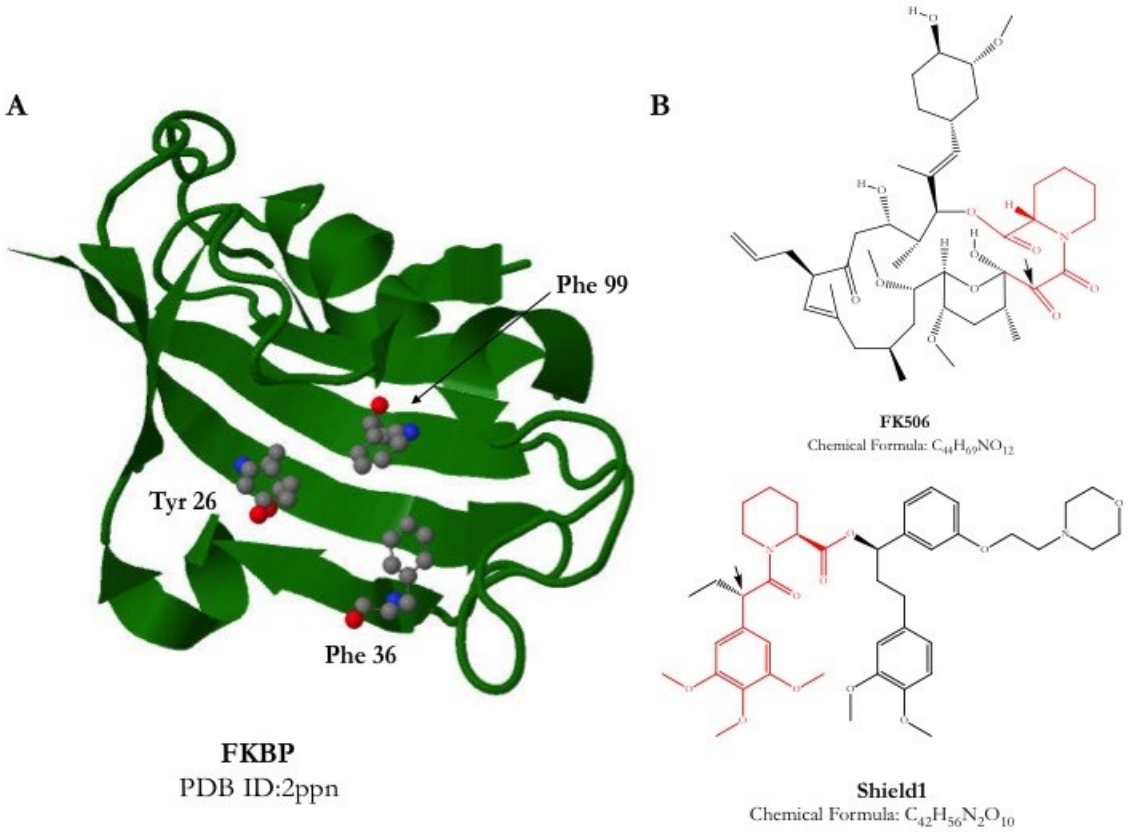


**Figure 1-4 Structure of FK-506 Binding Protein, FK-506, and Shield1**

A) Crystal structure of the human FKBP protein. Amino acid side chains that directly interact with the modified carbonyl oxygen highlighted in the FK-506 structure are shown. The phenylalanine at position 36 was mutated to valine to create a cavity in the hydrophobic pocket.

B) Top panel shows the chemical structure of FK-506 that was first isolated from *Streptomyces tsukubaensis* (CID: 445643). The region colored in red is a conserved core region that binds in the hydrophobic pocket of FKBP. The arrow points to a carbonyl oxygen that was modified to create Shield1. Bottom panel shows the chemical structure of Shield1 (CID: 44455162). Shield1 is an FK-506 derivative that has a higher binding affinity for $FKBP_{F36V}$ than the wild type FKBP.

**Figure 1-5 Model of the apicoplast conditional localization system**

The CLD is added as an N-terminal tag to a protein of interest and replaces the natural protein trafficking motif. In the absence of an interacting ligand (− Ligand, left side) the CLD is unstructured and mimics a natural transit peptide, which allows the cargo protein to

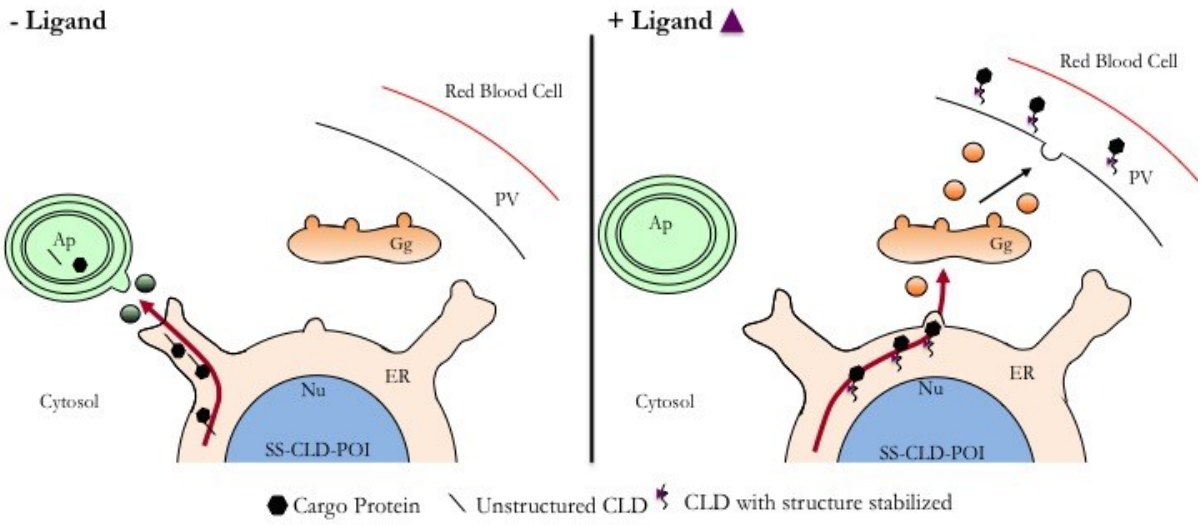


traffic to the apicoplast. When an interacting ligand is added to the culture media (+ Ligand, right side), the structure of the CLD is stabilized and this causes the cargo protein to be secreted from the cell. Proteins that are secreted accumulate in the parasitophorous vacuole space that separates the red blood cell cytosol from the parasite.

Ap = Apicoplast, PV = Parasitophorous Vacuole, ER = Endoplasmic Reticulum,
Nu = Nucleus, SS = Signal Sequence, CLD = Conditional Localization Domain,
POI = Protein of Interest, Gg = Golgi

## REFERENCES


1. *World Malaria Report 2016*. Geneva; 2016.

2. de Koning-Ward TF, Dixon MWA, Tilley L, Gilson PR. Plasmodium species: master renovators of their host cells. *Nat Rev Microbiol*. 2016;14(8):494-507. doi:10.1038/nrmicro.2016.79.

3. Bannister LH, Hopkins JM, Fowler RE, Krishna S, Mitchell GH. A Brief Illustrated Guide to the Ultrastructure of. *Parasitol Today*. 2000;16(10):427-433.

4. Bhattacharjee S, Van Ooij C, Balu B, Adams JH, Haldar K. Maurer's clefts of *Plasmodium falciparum* are secretory organelles that concentrate virulence protein reporters for delivery to the host erythrocyte. *Blood*. 2008;111(4):2418-2425. doi:10.1182/blood-2007-09-115279.

5. Ferreira MU, Nunes S, Wunderlich G. Antigenic Diversity and Immune Evasion by Malaria Parasites MiniReviews Antigenic Diversity and Immune Evasion by Malaria Parasites. *Clin Diagn Lab Immunol*. 2004;11(6):987-995. doi:10.1128/CDLI.11.6.987.

6. Haldar K, Mohandas N. Malaria, erythrocytic infection, and anemia. *Hematology*. 2009:87-93. doi:10.1182/asheducation-2009.1.87.

7. Ponsford MJ, Medana IM, Prapansilp P, et al. Sequestration and microvascular congestion are associated with coma in human cerebral malaria. *J Infect Dis*. 2012;205:663-671. doi:10.1093/infdis/jir812.

8. Idro R, Marsh K, John CC, Newton CRJ. Cerebral Malaria : Mechanisms Of Brain Injury And Strategies For Improved Neuro-Cognitive Outcome. *Pediatr Res*. 2010;68(4):267-274. doi:10.1203/PDR.0b013e3181eee738.Cerebral.

9. Mita T, Tanabe K. Evolution of *Plasmodium falciparum* drug resistance: implications for the development and containment of artemisinin resistance. *Jpn J Infect Dis*. 2012;65:465-475. http://www.ncbi.nlm.nih.gov/pubmed/23183197.

10. Gould SB, Waller RF, McFadden GI. Plastid evolution. *Annu Rev Plant Biol*. 2008;59:491-517. doi:10.1146/annurev.arplant.59.032607.092915.

11. Tonkin CJ, Foth BJ, Ralph SA, Struck N, Cowman AF, Mcfadden GI. Evolution of malaria parasite plastid targeting sequences. *Proc Natl Acad Sci U S A*. 2008;105(12):4781-4785.

12. Waller RF, Keeling PJ, Donald RG, et al. Nuclear-encoded proteins target to the plastid in *Toxoplasma gondii* and *Plasmodium falciparum*. *Proc Natl Acad Sci U S A*. 1998;95:12352-12357. doi:10.1073/pnas.95.21.12352.

13. Shears MJ, Botté CY, McFadden GI. Fatty acid metabolism in the Plasmodium

apicoplast: Drugs, doubts and knockouts. *Mol Biochem Parasitol*. 2015;199:34-50. doi:10.1016/j.molbiopara.2015.03.004.

14. Vaughan AM, O'neill MT, Tarun AS, et al. Type II fatty acid synthesis is essential only for malaria parasite late liver stage development. *Cell Microbiol*. 2009;11(3):506-520. doi:10.1111/j.1462-5822.2008.01270.x.

15. Yu M, Kumar TRS, Nkrumah LJ, et al. The fatty acid biosynthesis enzyme FabI plays a key role in the development of liver-stage malarial parasites. *Cell Host Microbe*. 2008;4:567-578. doi:10.1016/j.chom.2008.11.001.

16. Ralph SA, Dooren GG Van, Waller RF, et al. Metabolic Maps and Function of the *Plasmodium Falciparum* Apicoplast. *Nat Rev Microbiol*. 2004;2:203-216. doi:10.1038/nrmicro843.

17. Yeh E, Derisi JL. Chemical Rescue of Malaria Parasites Lacking an Apicoplast Defines Organelle Function in Blood-Stage *Plasmodium falciparum*. *PLoS Biol*. 2011;9(8):e1001138. doi:10.1371/journal.pbio.1001138.

18. Jomaa H, Wiesner J, Sanderbrand S, et al. Inhibitors of the Nonmevalonate Pathway of Isoprenoid Biosynthesis as Antimalarial Drugs. *Science (80- )*. 1999;285(5433):1573-1576.

19. Borrmann S, Issifou S, Esser G, et al. Fosmidomycin-clindamycin for the treatment of *Plasmodium falciparum* malaria. *J Infect Dis*. 2004;190(9):1534-1540. doi:10.1086/424603.

20. Dahl EL, Shock JL, Shenai BR, Gut J, DeRisi JL, Rosenthal PJ. Tetracyclines specifically target the apicoplast of the malaria parasite *Plasmodium falciparum*. *Antimicrob Agents Chemother*. 2006;50(9):3124-3131. doi:10.1128/AAC.00394-06.

21. Dahl EL, Rosenthal PJ. Multiple antibiotics exert delayed effects against the *Plasmodium falciparum* apicoplast. *Antimicrob Agents Chemother*. 2007;51(10):3485-3490. doi:10.1128/AAC.00527-07.

22. Gisselberg JE, Dellibovi-Ragheb T a, Matthews K a, Bosch G, Prigge ST. The suf iron-sulfur cluster synthesis pathway is required for apicoplast maintenance in malaria parasites. *PLoS Pathog*. 2013;9(9):e1003655. doi:10.1371/journal.ppat.1003655.

23. Przyborski JM, Lanzer M. Protein transport and trafficking in *Plasmodium falciparum* - infected erythrocytes. *Parasitology*. 2005;130:373-388. doi:10.1017/S0031182004006729.

24. Waller RF, Reed MB, Cowman AF, Mcfadden GI. Protein trafficking to the plastid of *Plasmodium falciparum* is via the secretory pathway. *EMBO J*. 2000;19(8):1794-1802.

25. Parsons M, Karnataki A, Feagin JE, DeRocher A. Protein trafficking to the apicoplast: deciphering the apicomplexan solution to secondary endosymbiosis.

*Eukaryot Cell*. 2007;6(7):1081-1088. doi:10.1128/EC.00102-07.

26. Tonkin CJ, Roos DS, McFadden GI. N-terminal positively charged amino acids, but not their exact position, are important for apicoplast transit peptide fidelity in *Toxoplasma gondii*. *Mol Biochem Parasitol*. 2006;150:192-200. doi:10.1016/j.molbiopara.2006.08.001.

27. Gallagher JR, Matthews K a, Prigge ST. *Plasmodium falciparum* apicoplast transit peptides are unstructured *in vitro* and during apicoplast import. *Traffic*. 2011;12:1124-1138. doi:10.1111/j.1600-0854.2011.01232.x.

28. Zuegge J, Ralph S, Schmuker M, McFadden GI, Schneider G. Deciphering apicoplast targeting signals--feature extraction from nuclear-encoded precursors of *Plasmodium falciparum* apicoplast proteins. *Gene*. 2001;280:19-26. http://www.ncbi.nlm.nih.gov/pubmed/11738814.

29. Waters NC, Kopydlowski KM, Guszczynski T, et al. Functional characterization of the acyl carrier protein (PfACP) and beta-ketoacyl ACP synthase III (PfKASIII) from *Plasmodium falciparum*. *Mol Biochem Parasitol*. 2002;123:85-94. doi:10.1016/S0166-6851(02)00140-8.

30. Tilley L, Mcfadden G, Cowman A, Klonis N. Illuminating *Plasmodium falciparum* - infected red blood cells. *TRENDS Parasitol*. 2007;23(6):268-277. doi:10.1016/j.pt.2007.04.001.

31. Tonkin CJ, Struck NS, Mullin KA, Stimmler LM, McFadden GI. Evidence for Golgi-independent transport from the early secretory pathway to the plastid in malaria parasites. *Mol Microbiol*. 2006;61(3):614-630. doi:10.1111/j.1365-2958.2006.05244.x.

32. Heiny SR, Pautz S, Recker M, Przyborski JM. Protein traffic to the *Plasmodium falciparum* apicoplast: Evidence for a sorting branch point at the Golgi. *Traffic*. 2014;15:1290-1304. doi:10.1111/tra.12226.

33. Armstrong CM, Goldberg DE. An FKBP destabilization domain modulates protein levels in *Plasmodium falciparum*. *Nat Methods*. 2007;4(12):1007-1009. doi:10.1038/nmeth1132.

34. Muralidharan V, Oksman A, Iwamoto M, Wandless TJ, Goldberg DE. Asparagine repeat function in a *Plasmodium falciparum* protein assessed via a regulatable fluorescent affinity tag. *Proc Natl Acad Sci U S A*. 2011;108(11):4411-4416. doi:10.1073/pnas.1018449108.

35. Kolev NG, Tschudi C, Ullu E. RNA interference in protozoan parasites: Achievements and challenges. *Eukaryot Cell*. 2011;10(9):1156-1163. doi:10.1128/EC.05114-11.

36. Baum J, Papenfuss AT, Mair GR, et al. Molecular genetics and comparative genomics reveal RNAi is not functional in malaria parasites. *Nucleic Acids Res*. 2009;37(11):3788-

3798. doi:10.1093/nar/gkp239.

37. Ganesan SM, Falla A, Goldfless SJ, Nasamu AS, Niles JC. Synthetic RNA-protein modules integrated with native translation mechanisms to control gene expression in malaria parasites. *Nat Commun*. 2016;7:1-10. doi:10.1038/ncomms10727.

38. Hawser S, Lociuro S, Islam K. Dihydrofolate reductase inhibitors as antibacterial agents. *Biochem Pharmacol*. 2006;71:941-948. doi:10.1016/j.bcp.2005.10.052.

39. Huennekens FM. In search of dihydrofolate reductase. *Protein Sci*. 1996;5:1201-1208. doi:10.1002/pro.5560050626.

40. Ionescu RM, Smith VF, O'Neill JC, Matthews CR. Multistate Equilibrium Unfolding of *Escherichia coli* Dihydrofolate Reductase: Thermodynamic and Spectroscopic Description of the Native, Intermediate, and Unfolded Ensembles. *Biochemistry*. 2000;39:9540-9550.

41. Sasso SP, Gilli RM, Sari JC, Rimet OS, Briand CM. Thermodynamic study of dihydrofolate reductase inhibitor selectivity. *Biochim Biophys Acta*. 1994;1207:74-79.

42. Holt DA, Luengo JJI, Yamashita DS, et al. Design, Synthesis, and Kinetic Evaluation of High-Affinity FKBP Ligands and the X-ray Crystal Structures of Their Complexes with FKBP12. *J Am Chem Soc*. 1993;115(22):9925-9938.

43. Duyne GD Van, Standaert RF, Karplus PA, Schreiber SL, Clardy J. Atomic Structure of FKBP-FK506 , an Immunophilin-Immunosuppressant Complex. *Science (80- )*. 1991;252(5007):839-842.

44. Pollock R, Clackson T. Dimerizer-regulated gene expression. *Curr Opin Biotechnol*. 2002;13:459-467.

45. Clackson T, Yang W, Rozamus LW, et al. Redesigning an FKBP-ligand interface to generate chemical dimerizers with novel specificity. *Proc Natl Acad Sci U S A*. 1998;95:10437-10442. doi:10.1073/pnas.95.18.10437.

46. Sawaya MR, Kraut J. Loop and subdomain movements in the mechanism of *Escherichia coli* dihydrofolate reductase: crystallographic evidence. *Biochemistry*. 1997;36:586-603. http://www.ncbi.nlm.nih.gov/pubmed/9012674.

# Chapter 2

# Design and Evaluation of Dihydrofolate Reductase as a Candidate Conditional Localization Domain

**ABSTRACT**

This chapter will describe our attempts to engineer a Conditional Localization Domain (CLD) from the Dihydrofolate Reductase (DHFR) proteins of *Escherichia coli* (CLD:*Ec*DHFR) and *Mus Musculus* (CLD:*Mm*DHFR). To determine if a candidate CLD is suitable for our conditional localization system we expressed each candidate CLD in parasites with a C-terminal fluorescent cargo protein. We then analyzed the localization of the protein in the presence and absence of an interacting ligand. The candidate CLD must traffic to the apicoplast under permissive conditions and change localization when the ligand is added to cell culture media in order to be considered a suitable domain for further studies. CLD:*Ec*DHFR failed to traffic to the apicoplast or change localization when the ligand was added to cell culture media. While CLD:*Mm*DHFR also failed to traffic to the apicoplast under permissive conditions, it was able to change localization and become secreted upon the addition of an interacting ligand. Both candidate CLDs appear to accumulate in the secretory space under permissive conditions.

We hypothesized that the failure of CLD:*Ec*DHFR and CLD:*Mm*DHFR to traffic to the apicoplast could be because the DHFR protein is toxic in the apicoplast organelle. We investigated this hypothesis by attempting to generate a transgenic parasite line that constitutively over-expresses DHFR in the apicoplast. Multiple transfections in *P. falciparum* failed to over-express *Ec*DHFR or *Mm*DHFR in the apicoplast. This suggested to us that the enzymatic activity of DHFR might be harmful to the apicoplast.

Ultimately, neither of the candidate CLDs tested in this chapter were successful because they did not traffic to the apicoplast and were eliminated as candidates to be the final domain. Our analysis of these domains however, informed and helped refine our studies of the next candidate CLD (described in Chapter 3).

## INTRODUCTION

To design a CLD that is effective for our apicoplast conditional localization system we tested multiple proteins as candidate conditional localization domains. Our goal in the design of each candidate CLD was to mimic an apicoplast transit peptide under permissive conditions to allow the CLD to traffic to the apicoplast. Our second major design goal was to give the CLD structural properties that could be altered experimentally to change the localization of the CLD. Once we designed a candidate CLD we generated transgenic parasite lines that express the domain fused to a fluorescent cargo protein, so that we could evaluate its localization using live fluorescence microscopy. When analyzing protein localization we expect to see the typical branched apicoplast morphology (Figure 2-1 A) to indicate that the CLD is trafficking to the apicoplast. After addition of an interacting ligand to alter the structure of the CLD we looked for a change in trafficking pattern (Figure 2-1 B) to indicate that the CLD is secreted from the cell.

We began our studies with two candidate CLDs designed from Dihydrofolate Reductase (DHFR). DHFR is a highly studied enzyme that is involved in folate metabolism and is required for synthesis of thymidine nucleotides[1,2]. DHFR proteins from multiple species have been successfully expressed in *P. falciparum* as molecular tools. The human DHFR gene is most often expressed in *P. falciparum* as a selection cassette to generate transgenic parasite lines[3,4]. Human DHFR can be used to select transgenic parasites because anti-folate compounds have different specificities for vertebrate and bacterial DHFR proteins[5]; The DHFR protein from *P. falciparum* is targeted by some anti-folates, such as WR99210, that are active against bacterial DHFR proteins but not the human DHFR [3]. In

general, to create a transgenic parasite line through homologous recombination, parasites are transfected with a plasmid that contains the human DHFR gene, in addition to the homologous region of the gene that researchers are trying to disrupt. To promote integration of the transfection plasmid, parasites are treated with WR99210, which forces the parasites to integrate or maintain the transfection plasmid in order to express the human DHFR protein that is not affected by WR99210. Parasites that integrate the transfection plasmid are selected over time by cycling on and off of WR99210.

A conditionally destabilized mutant of *E. coli* DHFR (*Ec*DHFR) is commonly expressed in *P. falciparum* as a conditional degradation domain tag [6–8]. This degradation domain was used to show that the proteasome lid subunit *Pf*Rpn6, is essential for ubiquitin related protein degradation and parasite survival in the blood stage[7]. *Pf*ATG7 is an autophagy related gene that was also tagged with the degradation domain and was found to be essential for normal parasite growth in the blood stage[8]. The first candidate CLD we tested was designed from the destabilized *Ec*DHFR protein. Destabilized *Ec*DHFR was modified to mimic an apicoplast transit peptide and expressed in *P. falciparum* (CLD:*Ec*DHFR). We hypothesized that the destabilized *Ec*DHFR would resemble an unstructured transit peptide and allow the CLD to traffic to the apicoplast in the absence of a ligand. We further hypothesized that addition of the binding ligand Trimethoprim (TMP) to stabilize the structure of CLD:*Ec*DHFR would block import to the apicoplast and cause the CLD to be secreted from the cell.

The DHFR protein form *M. musculus* (*Mm*DHFR) has also been used as a molecular tool in *P. falciparum*. In a study of how proteins are exported to the red blood cell cytosol, *Mm*DHFR was used to show that proteins must be unfolded to cross the parasitophorous vacuole membrane[9]. In this study, researchers expressed a green fluorescent protein fused to

*Mm*DHFR in the secretory pathway of parasites. In the absence of the binding ligand (TMP), *Mm*DHFR could be unfolded to allow GFP to cross the vacuolar membrane through the PTEX translocon. When TMP was added to cell culture media, *Mm*DHFR stabilized and prevented GFP from crossing the vacuolar membrane. Although *Mm*DHFR has not been used as a conditional destabilization domain, we hypothesized that the change in stability of the wild type protein in the presence of TMP might be sufficient to change the localization of the CLD. We therefore tested *Mm*DHFR as our second candidate CLD (CLD:*Mm*DHFR).

To get an idea of how well each CLD sequence meets the requirements of a *P. falciparum* transit peptide, we input the amino acid sequences into the Predictor of Apicoplast Targeted Sequences (PATS) computer program[10]. The PATS algorithm analyzes amino acid sequences to determine if an apicoplast trafficking motif is present and gives an output score between 0 and 1. A score of 0 indicates that the input sequence does not contain an apicoplast trafficking motif and is not likely to traffic to the apicoplast. A score of 1 indicates that the sequence does appear to contain an apicoplast trafficking motif and is likely to traffic to the apicoplast. Although the PATS program is a useful tool to evaluate whether the CLD sequences we design are similar in terms of amino acid sequence features to a natural apicoplast transit peptide, there are some limitations of the algorithm. The PATS algorithm was developed before the full *P. falciparum* genome sequence was completed and only uses information from chromosomes 1 and 2 to make its predictions. The algorithm was trained from 84 likely apicoplast trafficked and 102 non-apicoplast trafficked sequences[10]. Information from the complete sequence of the *P. falciparum* nuclear genome has revealed that there are over 500 nuclear encoded proteins that are likely trafficked to the apicoplast[11]. Additional training of the PATS algorithm, based on the full genome sequence of *P.*

*falciparum* could improve the accuracy of its predictions. The PATS algorithm also does not consider structural features of the transit peptide region, which our lab has shown in previously described studies (Chapter 1), are an important characteristic of transit peptides. Despite these limitations of the PATS program, we still found it to be a useful tool to guide the design of each candidate CLD.

We analyzed protein trafficking in parasite lines that express either CLD:EcDHFR or CLD:MmDHFR fused to a fluorescent cargo protein. Both of these CLDs were tested with the interacting ligand TMP. Neither CLD trafficked to the apicoplast under permissive conditions (- TMP) and CLD:*Ec*DHFR did not change localization when TMP was added to cell culture media. CLD:*Mm*DHFR however, did change localization when TMP was added and was secreted from the cell.

Since DHFR is not usually expressed in the apicoplast of wild type parasites, we investigated whether over-expression of DHFR in the apicoplast could be toxic to parasites. The apicoplast houses essential biochemical pathways that could be perturbed by the over expression of an enzyme that is not normally present in the organelle. To test if DHFR can be over-expressed in the apicoplast we attempted to generate transgenic parasite lines that constitutively traffic DHFR to the apicoplast using a verified apicoplast trafficking motif from ACP. Multiple transfections using high and low strength promoters failed to express DHFR in the apicoplast compartment. This suggested to us that there could be some toxicity associated with over-expressing DHFR in the apicoplast. Since both of the candidate CLDs designed from DHFR proteins also failed to traffic to the apicoplast, we did not do any further analysis of either of the candidate CLDs tested in this chapter.

**RESULTS**

**Design and Expression of CLD:*Ec*DHFR**

To design our first candidate conditional localization domain we mutated the destabilized *Ec*DHFR to mimic a *P. falciparum* transit peptide. As discussed in Chapter 1 transit peptides must maintain a net positive charge near the N-terminus and they must be unstructured to traffic to the apicoplast. To meet the positive charge requirement of transit peptides, we mutated a negatively charged aspartic acid at position 11 and a glutamic acid at position 17 to positively charged lysine (*Ec*DHFR$_{D11K, E17K}$). This increased the overall charge near the N-terminus of the CLD +4 (Figure 2-2 A). The destabilized EcDHFR that has been used as a degradation domain in other studies has an asparagine to threonine mutation at residue 18 and an alanine to valine mutation at position 19 (*Ec*DHFR$_{N18T, A19V}$) [7]. These mutations were also made in the CLD:*Ec*DHFR sequence to conditionally destabilize the CLD. There are no specific sequence motifs required for recognition of apicoplast trafficked proteins and so no further changes to the *Ec*DHFR sequence were applied to generate the CLD. CLD:*Ec*DHFR received a PATS score of 0.89, which is comparable to PATS scores computed from known apicoplast trafficked sequences. This suggested to us that the sequence of CLD:*Ec*DHFR closely mimics an apicoplast trafficking peptide and could potentially traffic the test cargo protein to the apicoplast.

We expressed CLD:*Ec*DHFR in parasites with an N-terminal signal sequence to allow the protein to be co-translationally imported into the endoplasmic reticulum (Figure 2-2 A). We also added a C-terminal Green Fluorescent Protein (GFP) tag to the CLD so that we could track its localization. We investigated the localization of GFP in the presence and absence of the interacting ligand (TMP) using live fluorescence imaging. In Figure 2-2 B, the top panel shows that GFP does not take on the branched localization pattern that is

indicative of apicoplast trafficking in the absence of the interacting ligand TMP. Instead, GFP appears to accumulate in the secretory space, which suggests that CLD:*Ec*DHFR is not recognized as a transit peptide by the parasite. When TMP is added to the culture media (Figure 2-2 B, bottom panel), there is no change in localization of GFP.

We also analyzed fixed cells in immunofluorescence images to confirm that CLD:*Ec*DHFR does not traffic to the apicoplast. Co-localization analysis of cells stained with anti-ACP (ACP is an apicoplast marker discussed in Chapter 1) and anti-GFP antibodies revealed no significant co-localization between these two proteins (Figure 2-2 C), confirming that CLD:*Ec*DHFR does not traffic to the apicoplast.

**Design and Expression of CLD:*Mm*DHFR**

The second candidate CLD we tested was the wild type sequence of the *Mm*DHFR protein. The wild type *Mm*DHFR sequence does not contain any negatively charged residues near the N-terminus, and so we did not make mutations to alter the charge (Figure 2-3 A). Although *Mm*DHFR has not been engineered to create a conditionally destabilized version of the protein, it has been used as a molecular tool in *P. falciparum* (see description in introduction), and we tested this protein as a candidate CLD without any destabilizing mutations. We also put the CLD:*Mm*DHFR sequence into the PATS program to estimate its likelihood of trafficking to the apicoplast. CLD:*Mm*DHFR got a score of 0.97 from the PATS program, which suggests that the wild type *Mm*DHFR sequence has basic sequence similarities with other apicoplast transit peptide motifs.

We expressed CLD:*Mm*DHFR in parasites with an N-terminal signal sequence and the Super Folder Green (SFG) fluorescent protein at the C-terminus. SFG is an enhanced green fluorescent protein that has been optimized for expression in the secretory

pathway[12,13]. In the absence of TMP, CLD:*Mm*DHFR appears to accumulate in the secretory space (Figure 2-3 B, top panel), similar to the trafficking pattern of CLD:*Ec*DHFR. When TMP is added to cell culture media however, CLD:*Mm*DHFR does change localization. CLD:*Mm*DHFR is secreted from the cell and accumulates in the parasitophorous vacuole space (Figure 2-3 B, bottom panel). We confirmed that CLD:*Mm*DHFR does not traffic to the apicoplast in the absence of TMP, by staining fixed cells with anti-ACP and anti-GFP antibodies in immunofluorescence assays. No significant co-localization was observed between SFG and the apicoplast marker ACP (Figure 2-3 C), indicating that CLD:*Mm*DHFR does not traffic to the apicoplast.

**Expression of DHFR in the Apicoplast**

In our next experiment, we investigated whether over-expression of DHFR in the apicoplast is toxic to parasites. Parasites were transfected with plasmids that contain the full-length apicoplast trafficking motif (signal sequence and transit peptide) from the Acyl-Carrier Protein (ACP) fused to the wild type sequence of *Ec*DHFR or *Mm*DHFR. Both of the DHFR proteins were exogenously expressed from a high (calmodulin) or low (ribosomal L2 protein) strength promoter. Our lab's experience with protein over-expression in the apicoplast has been that some enzymes are not tolerated in the apicoplast when expressed from a high strength promoter like the *P. falciparum* calmodulin promoter. In these cases, switching expression of the transgene to a lower strength promoter like the ribosomal L2 promoter can rescue the viability of the parasites. However, this was not the case with DHFR. Out of four successful transfections where drug resistant parasites were selected, none of the parasites expressed *Ec*DHFR or *Mm*DHFR in the apicoplast from a high or low strength promoter (Table 2-1). In each of these experiments, parasites have presumably

found a way to turn off expression of the transgene (Apicoplast trafficked DHFR), while maintaining expression of the selection cassette. This suggests that over-expression of DHFR in the apicoplast, even at low levels, is toxic to the parasite, possibly because of the enzymatic activity of the protein.

## CONCLUSIONS AND DISCUSSION

Analysis of protein trafficking by CLD:*Ec*DHFR and CLD:*Mm*DHFR as potential CLDs revealed that neither of these domains were able to traffic a test protein (GFP or SFG) to the apicoplast (Figure 2-2 and 2-3 respectively). CLD:*Mm*DHFR was moderately more successful as a CLD because it could change localization of the test protein when TMP was added to cell culture media. This result supported our hypothesis that stabilizing the structure of the CLD could change the localization of a protein. But, since neither of the candidate CLDs trafficked to the apicoplast, they could not be used as a conditional localization domain.

Both CLDs appear to get hung up in the secretory pathway without being recognized as an apicoplast transit peptide. This trafficking pattern could be because DHFR has the ability to bind multiple ligands – dihydrofolate and/or NADPH – independently in the endoplasmic reticulum[1]. If DHFR binds NADPH in the endoplasmic reticulum, this could stabilize the protein and prevent the CLD from trafficking to the apicoplast.

We also investigated whether DHFR has some toxic effect that would lead the parasite to avoid expressing this enzyme in the apicoplast. We attempted to generate parasite lines that over-express DHFR in the apicoplast to show that the enzyme activity is not toxic. None of the transfected parasites were able to express DHFR in the apicoplast from a high

or low strength promoter (Table 2-1). This suggests that there may be some toxicity associated with expressing the DHFR enzyme in the apicoplast. One theory to explain why DHFR is toxic is again linked to DHFR's ability to bind the cofactor NADPH. DHFR could bind NADPH in the apicoplast and reduce the pool of NADPH that is available for use by the MEP pathway. The MEP pathway is essential because it synthesizes isoprenoid precursors that are required for development of blood stage parasites[14]. Over expression of DHFR in the apicoplast may sufficiently reduce the pool of available NADPH so that the apicoplast is no longer able to synthesize isoprenoids and the cell dies.

At this point in the progression of my thesis, we decided not to further investigate CLD:*Ec*DHFR or CLD:*Mm*DHFR. Our overall goal was to design a CLD that could be used to control trafficking of apicoplast targeted proteins and it was clear from these studies that DHFR could not easily be converted into a CLD because it does not readily traffic to the apicoplast. Our analysis of these failed CLDs was useful however, to inform our design specifications for the next candidate CLD.

One feature of DHFR proteins in general that may not have worked in our favor for these studies is that DHFR can bind multiple ligands (most significantly, NADPH) that could be present in the ER and apicoplast compartments. NADPH binding would affect DHFR stability, but it would also increase the affinity of other ligands like DHF or TMP since these ligands bind in a cooperative manner. As previously discussed, this activity of DHFR could interfere with trafficking of DHFR to the apicoplast, or disrupt essential pathways that function in the apicoplast. When considering the design of our next candidate CLD we chose a protein that does not have as many potential binding partners in the cell.

A second feature of both of the CLDs tested in this chapter that may have contributed to their inability to traffic to the apicoplast is that they are both quite stable.

Although degradation domain mutations were introduced into the *Ec*DHFR sequence, preliminary studies in which we purified destabilized *Ec*DHFR found that the melting temperature of the CLD was not significantly different from that of the wild type protein. The level of instability required for apicoplast trafficking has not been precisely measured, but we reasoned that starting from a more severely destabilized protein for our next candidate CLD could increase its likelihood of trafficking to the apicoplast.

A third feature of DHFR proteins that may have contributed to their inability to traffic to the apicoplast is the amino-terminal structure of DHFR. The amino-terminus of DHFR is buried in the binding domain of the protein and may not be available for recognition as a transit peptide even if the protein is slightly destabilized (Figure 2-4 A).

A final feature of both DHFR proteins tested is that they are longer than the typical size of a natural *P. falciparum* transit peptide. The maximum length of most *P. falciparum* transit peptides is about 150 amino acids long while *Ec*DHFR is 159 amino acids and *Mm*DHFR is 187 amino acids long. Transit peptide length may be more important for recognition than we anticipated with these candidate CLDs, and in our next study we chose a protein that is significantly smaller than DHFR.

Our next candidate CLD was designed to take most of the previously discussed pitfalls of DHFR into account. The human FK-506 Binding Protein (FKBP) is within the normal size range of a transit peptide, it does not bind a co-factor to perform its normal function in the cell and it has a degradation domain mutation that is significantly more severe than the destabilized *Ec*DHFR protein. FKBP also has a less complex structure near the amino-terminus which is likely to be more available for recognition as a transit peptide because it does not fold into the core of the protein (Figure 2-4 B).

## METHODS

### Generation of plasmid constructs

The wild type *E. coli* DHFR gene was harmonized for expression in *P. falciparum* (Table 2-2) and synthesized by GeneArt (Life Technologies). Adaptamers were then used to insert the signal sequence from the ACP gene (see Apico20.AvrNdeF and Apico20Avr.NdeR sequences in Table 2-3) at the N-terminus of *Ec*DHFR. To generate N-terminal lysine mutations and degradation domain mutations in the *Ec*DHFR sequence, Akk.MutUF and Akk.mutUR primers from Table 2-3 were used with Pfu DNA polymerase for mutagenesis in the GeneArt cloning vector. The entire CLD:EcDHFR sequence was then cut out of the GeneArt cloning vector using AvrII and BsiWI and ligated into a modified pLN [15] vector for parasite transfection that contained the lower strength ribosomal L2 protein promoter [16] instead of the calmodulin promoter.

The signal sequence and transit peptide from the ACP gene were PCR amplified from the pMALcHT-ACP plasmid [17] using the Api55.AvrII.F and Api55.NdeI.R primers listed in Table 2-3. The PCR products were then digested with AvrII and NdeI and ligated into the GeneArt cloning vector that contained the wild type *Ec*DHFR sequence using quick ligase. The entire Signal (ACP)-Transit (ACP)-*Ec*DHFR sequence was then cut out of the GeneArt cloning vector using AvrII and BsiWI and ligated into a pLN vector with either the calmodulin or ribosomal L2 promoter.

The wild type *Mm*DHFR sequence was amplified from the pMALcHT-mDHFR plasmid using the mDHFR.NdeI.F and mDHFR.BglII.R primers in Table 2-3. The PCR amplicon was digested with NdeI and BglII and ligated into the GeneArt cloning vector described above and replaced the *Ec*DHFR sequence. The signal sequence or signal

sequence and transit peptide together were inserted into the cloning vector with *Mm*DHFR using the same procedure described above. The entire targeting motif and *Mm*DHFR sequence was then digested out of the GeneArt cloning vector using AvrII and BsiWI. The fragment was finally ligated into the pLN vector with calmodulin or ribosomal L2 promoters and the super folder green sequence. All plasmids were sequenced to confirm correct insertions after ligation.

**Parasite transfection and culture**

Parasites were cultured at 2 % hematocrit in RPMI 1640 medium containing 25 mM HEPES, 0.375% sodium bicarbonate, 12.5 μg/ml hypoxanthine, 5 g/L Albumax II and 25μg/ml gentamicin. Transfections were done using the Bxb1 mycobacteriophage integrase system in the Dd2 strain of parasites that contain an attB site for recombination[15]. Uninfected red blood cells were preloaded with transfection plasmids and electroporated using the protocol from Spalding et al 2010 [18]. Electroporated red blood cells were then mixed with parasite culture and after two days of growth transgenic parasites were selected with 2.5 μg/ml Blasticidin.

**Live cell imaging**

Parasite cultures were stained with DAPI and MitoTracker Red CMX Ros (Invitrogen). 100 μl of parasite culture was incubated for 30 minutes in 1 μg/ml DAPI and 30 nM MitoTracker Red CMX Ros at 37 °C. Samples were then washed three times in culture media and pipetted onto microscope slides. A coverslip was placed over the slide and sealed with wax (2 parts paraffin, 1 part Vaseline). Samples were then taken immediately to the Nikon 90i microscope for imaging.

**Immunofluorescence assay**

Microscope slides were set up for immunofluorescence assays by drawing wells on the slide with a Super Pap Pen Liquid Blocker (Ted Pella, inc.). A .01 % poly-L-Lysine solution (Sigma-Aldrich) in water was added to each well and allowed to dry for at least 30 minutes. 300 µl of parasite culture was then pelleted and resuspended in an equal volume of fixative (4 % paraformaldehyde and .0075 % glutaraldehyde in PBS). Cells were added to each well on the slide and then incubated for 30 minutes at room temperature. After incubation, fixed cells were permeabilized by incubation in 1 % Triton X-100 for ten minutes. The samples were then reduced by incubation in 100 µg/ml $NaBH_4$ in water for 10 minutes. Next the cells were incubated in blocking solution (3 % BSA in PBS) for two hours. Before applying primary antibodies cells were washed in PBS and then incubated with appropriate antibodies overnight at 4 °C [rabbit polyclonal αACP 1:500, raised against the *P. falciparum* antigen; Living Color mouse monoclonal αGFP 1:100 (CloneTech)]. The next day, cells were washed three times in PBS and then once in 3 % BSA. Appropriate secondary antibodies [goat αrabbit AlexaFluor 594 1:1000 (Life Technologies); goat αmouse AlexaFluor 488 1:1000 (Invitrogen)] were added to cells and incubated for 2 hours in the dark at room temperature. Finally cells were washed in PBS three times and sealed with ProLong Gold antifade reagent with DAPI (Life Technologies) under a coverslip sealed with nail polish. Slides were allowed to sit overnight at room temperature before imaging analysis on the Nikin 90i microscope.

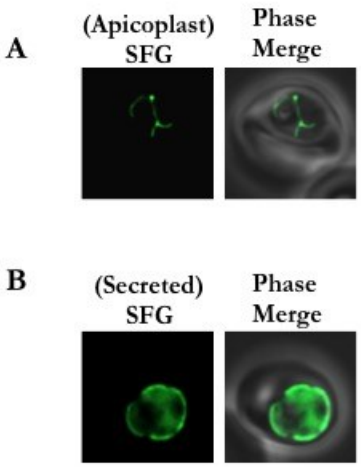


**Figure 2-1 Comparison of apicoplast and secreted protein trafficking in *P. falciparum***

Live fluorescent images of transgenic parasite lines that express the full-length apicoplast trafficking motif (signal sequence and transit peptide) from ACP fused to SFG (A) or just the signal sequence of ACP fused to SFG (B). Images are 10 microns long by 10 microns wide.

A) Typical branched structure of the apicoplast in the trophozoite stage of development in the red blood cell.

B) Secreted SFG protein that is mostly accumulated in the parasitophorous vacuole space that separates the parasite from the red blood cell. SFG signal observed inside the parasite cell is presumably in the secretory pathway, en route to be secreted from the cell.

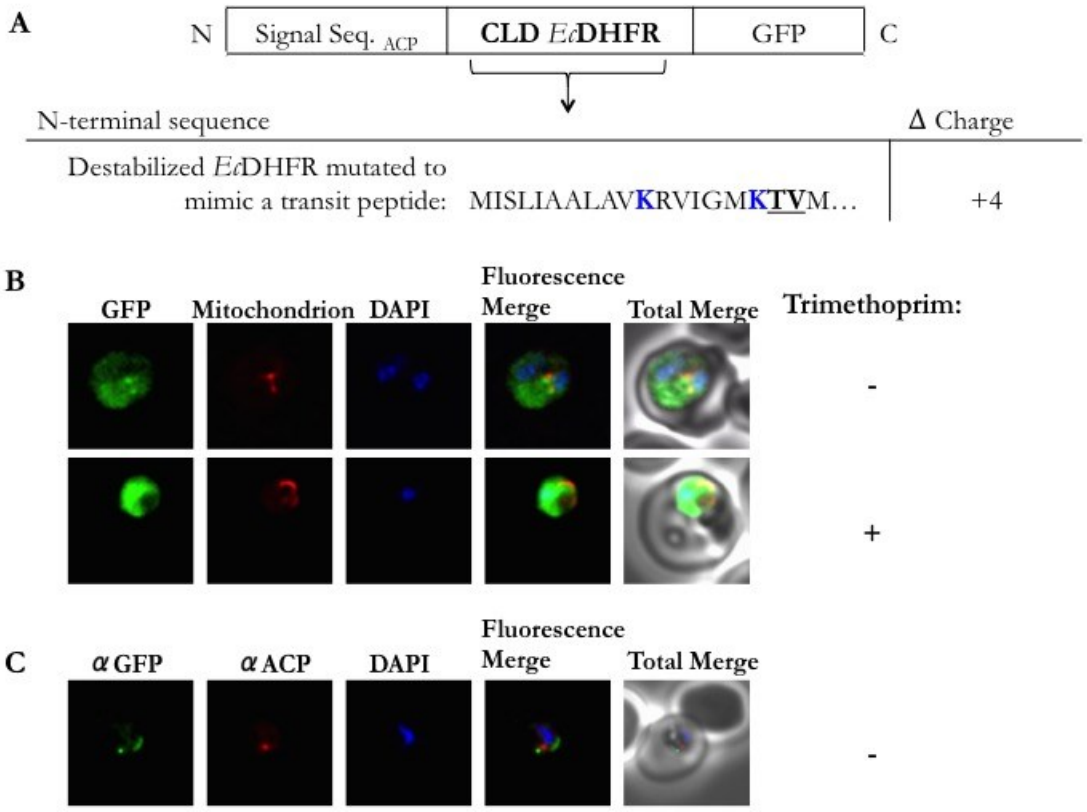


**Figure 2-2 CLD:*Ec*DHFR design and analysis of protein trafficking**

A) The first test of a candidate CLD was a destabilization domain containing *Ec*DHFR protein with additional N-terminal mutations designed to increase the net positive charge near the N-terminus. Lysine mutations in blue increase positive charge; destabilization domain mutations are underlined.

Signal Seq.$_{ACP}$ = Signal sequence from ACP
GFP = green fluorescent protein

B) Live fluorescence images of cells expressing the CLD fused to GFP. Cells treated with Trimethoprim at 5 μM for 48 hours before imaging.

C) Immunofluorescence images of fixed cells stained with anti-ACP (apicoplast marker) and anti-GFP antibodies in the absence of Trimethoprim.

Images are 10 microns long by 10 microns wide.

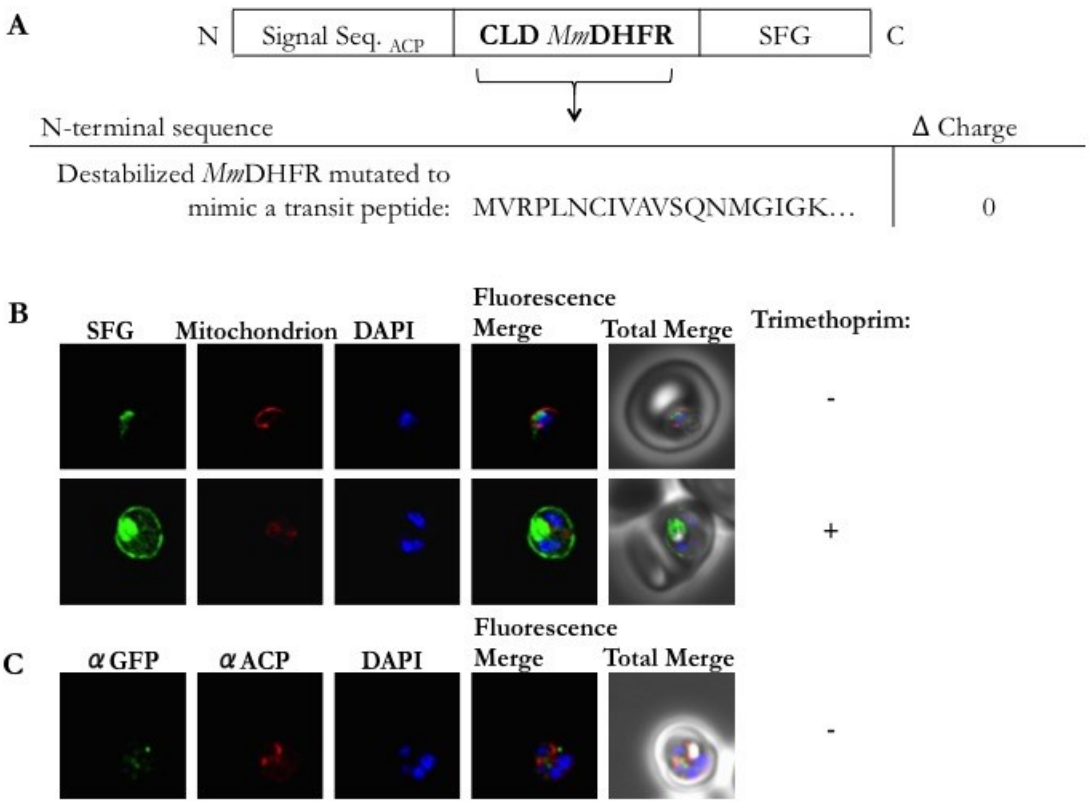


**Figure 2-3 CLD:*Mm*DHFR design and analysis of protein trafficking**

A) The second test of a candidate CLD was the wild type *Mm*DHFR protein with no mutations.

SFG = Super Folder Green (enhanced GFP)

B) Live fluorescence images of cells expressing the CLD fused to SFG. Cells treated with Trimethoprim at 5 μM for 48 hours before imaging.

C) Immunofluorescence images of fixed cells stained with anti-ACP (apicoplast marker) and anti-GFP antibodies in the absence of Trimethoprim.

Images are 10 microns long by 10 microns wide.

| Transgene | Promoter strength | # successful transfections | # lines expressing transgene |
|---|---|---|---|
| Signal Seq.$_{ACP}$-Transit Pep.$_{ACP}$-wt *Ec*DHFR-GFP | High | 1/1 | 0/1 |
| | Low | 1/3 | 0/1 |
| Signal Seq.$_{ACP}$-Transit Pep.$_{ACP}$-wt *Mm*DHFR-SFG | High | 1/1 | 0/1 |
| | Low | 1/1 | 0/1 |

**Table 2-1 Transfection log for over expression of DHFR in the apicoplast**

We attempted to express *Ec*DHFR and *Mm*DHFR in the apicoplast of *P. falciparum*. Each protein was transfected with a high (calmodulin) or low (ribosomal L2 protein) strength promoter and transfections were considered successful if parasites were able to grow back after drug selection with blasticidin. None of the four successfully transfected lines expressed the transgene. Expression was evaluated by searching for green fluorescent signal in live fluorescent microscopy analysis.

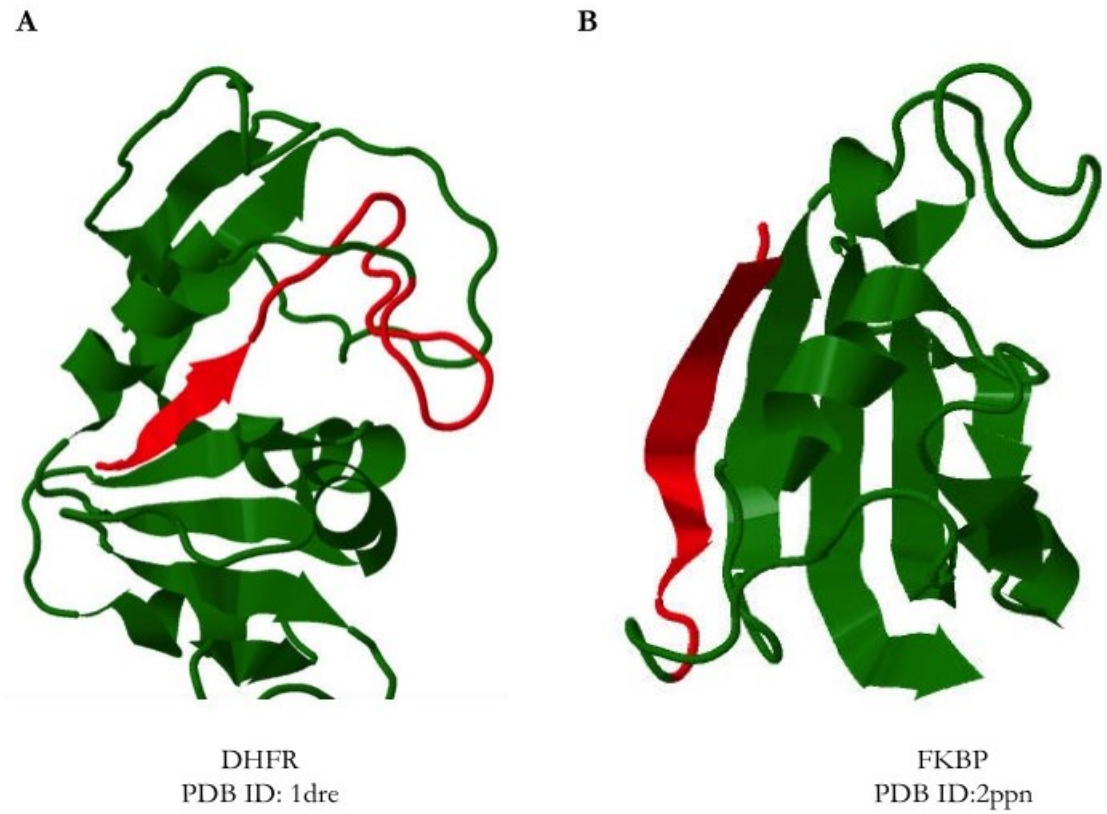


**Figure 2-4 Amino-terminal structures of DHFR and FKBP**

A) DHFR structure with the first 20 amino acids colored red. The N-terminus is a part of the loop domain that binds dihydrofolate.

B) FKBP structure with the first 10 amino acids colored red. The N-terminus is not buried in the core of the protein structure and may be more readily available when the protein is destabilized.

DHFR gene from *E. coli* harmonized for expression in *P. falciparum*:

ATGATATCCTTAATAGCGGCATTAGCAGTGGATAGAGTAATTGGTATGGAAAATGCCATGCCATGGAATTTACCTGCAGATTTA
GCTTGGTTTAAACGAAATACATTAAATAAACCAGTTATAATGGGACGACATACTTGGGAATCTATAGGCAGACCATTACCAGGT
CGAAAAAATATTATATTAAGTAGCCAACCAGGTACcGATGATAGAGTAACTTGGGTAAAATCTGTTGATGAAGCAATAGCGGCA
TGTGGAGATGTGCCAGAGATTATGGTTATAGGAGGTGGTAGAGTTTATGAACAATTTTTGCCAAAGGCTCAGAAGTTATATTT
GACACATATTGATGCGGAGGTAGAGGGAGATACACATTTTCCTGATTATGAACCAGATGATTGGGAATCAGTGTTTAGTGAGT
TCCATGATGCAGACGCCCAAAATTCACATTCTTATTGTTTTGAGATATTAGAAAGAAGG

**Table 2-2 DNA sequence of the *Ec*DHFR gene harmonized for expression in *P. falciparum***

| Primer Name | Primer Sequence |
|---|---|
| Apico20.AvrNdeF | CTAGGTGAATGAAGATCTTATTACTTTGTATAATTTTTCTATATTATGTTAACGCTTTTAAAAATCA |
| Apico20.AvrNdeR | TATGATTTTTAAAAGCGTTAACATAATATAGAAAAATTATACAAAGTAATAAGATCTTCATTCAC |
| Akk.mutUF | CAGTGaAaAGAGTAATTGGTATGaAAAcTGtCATGCCATGGAATTTACCTGC |
| Akk.mutUR | GCAGGTAAATTCCATGGCATGACAGTTTTCATACCAATTACTCTTTTCACTG |
| Api55.AvrII.F | GGTGGTCCTAGGATGAAGATCTTATTACTTTGTATAATTTTTC |
| Api55.NdeI.R | GGTGGTCATATGTGGGTTTTTATTTTTTATCAAATTGTAATC |
| mDHFR.NdeI.F | GGTGGTCATATGGTTCGACCATTGAACTGC |
| mDHFR.BglII.R | GGTGGTAGATCTGTCTTTCTTCTCGTAGACTTCAAA |

**Table 2-3 Primers used to generate CLD sequences for expression in *P. falciparum***

## REFERENCES


1. Ionescu RM, Smith VF, O'Neill JC, Matthews CR. Multistate Equilibrium Unfolding of *Escherichia coli* Dihydrofolate Reductase: Thermodynamic and Spectroscopic Description of the Native, Intermediate, and Unfolded Ensembles. *Biochemistry*. 2000;39:9540-9550.

2. Cody V, Pace J, Rosowsky A. Structural analysis of a holoenzyme complex of mouse dihydrofolate reductase with NADPH and a ternary complex with the potent and selective inhibitor 2,4-diamino-6-(2'-hydroxydibenz[b,f]azepin-5-yl)methylpteridine. *Biol Crystallogr*. 2008;64:977-984. doi:10.1107/S0907444908022348.

3. Fidock DA, Wellems TE. Transformation with human dihydrofolate reductase renders malaria parasites insensitive to WR99210 but does not affect the intrinsic activity of proguanil. *Proc Natl Acad Sci U S A*. 1997;94:10931-10936.

4. Maier AG, Braks J a M, Waters AP, Cowman AF. Negative selection using yeast cytosine deaminase/uracil phosphoribosyl transferase in *Plasmodium falciparum* for targeted gene deletion by double crossover recombination. *Mol Biochem Parasitol*. 2006;150:118-121. doi:10.1016/j.molbiopara.2006.06.014.

5. Sasso SP, Gilli RM, Sari JC, Rimet OS, Briand CM. Thermodynamic study of dihydrofolate reductase inhibitor selectivity. *Biochim Biophys Acta*. 1994;1207:74-79.

6. Iwamoto M, Björklund T, Lundberg C, Kirik D, Wandless TJ. A general chemical method to regulate protein stability in the mammalian central nervous system. *Chem Biol*. 2010;17:981-988. doi:10.1016/j.chembiol.2010.07.009.

7. Muralidharan V, Oksman A, Iwamoto M, Wandless TJ, Goldberg DE. Asparagine repeat function in a *Plasmodium falciparum* protein assessed via a regulatable fluorescent affinity tag. *Proc Natl Acad Sci U S A*. 2011;108(11):4411-4416. doi:10.1073/pnas.1018449108.

8. Walker DM, Mahfooz N, Kemme KA, Patel VC, Spangler M, Drew ME. *Plasmodium falciparum* Erythrocytic Stage Parasites Require the Putative Autophagy Protein PfAtg7 for Normal Growth. *PLoS One*. 2013;8(6):e67047. doi:10.1371/journal.pone.0067047.

9. Gehde N, Hinrichs C, Montilla I, Charpian S, Lingelbach K, Przyborski JM. Protein unfolding is an essential requirement for transport across the parasitophorous vacuolar membrane of *Plasmodium falciparum*. *Mol Microbiol*. 2009;71(3):613-628. doi:10.1111/j.1365-2958.2008.06552.x.

10. Zuegge J, Ralph S, Schmuker M, McFadden GI, Schneider G. Deciphering apicoplast targeting signals--feature extraction from nuclear-encoded precursors of *Plasmodium falciparum* apicoplast proteins. *Gene*. 2001;280:19-26. http://www.ncbi.nlm.nih.gov/pubmed/11738814.

11. Ralph SA, Dooren GG Van, Waller RF, et al. Metabolic Maps and Function of the

*Plasmodium Falciparum* Apicoplast. *Nat Rev Microbiol*. 2004;2:203-216. doi:10.1038/nrmicro843.

12. Pedelacq J-D, Cabantous S, Tran T, Terwilliger TC, Waldo GS. Engineering and characterization of a superfolder green fluorescent protein. *Nat Biotechnol*. 2006;24(1):79-89. doi:10.1038/nbt1172.

13. Aronson DE, Costantini LM, Snapp EL. Superfolder GFP Is Fluorescent in Oxidizing Environments When Targeted via the Sec Translocon. *Traffic*. 2011;12:543-548. doi:10.1111/j.1600-0854.2011.01168.x.

14. Yeh E, Derisi JL. Chemical Rescue of Malaria Parasites Lacking an Apicoplast Defines Organelle Function in Blood-Stage *Plasmodium falciparum*. *PLoS Biol*. 2011;9(8):e1001138. doi:10.1371/journal.pbio.1001138.

15. Nkrumah LJ, Muhle R a, Moura P a, et al. Efficient site-specific integration in *Plasmodium falciparum* chromosomes mediated by mycobacteriophage Bxb1 integrase. *Nat Methods*. 2006;3(8):615-621. doi:10.1038/nmeth904.

16. Gisselberg JE, Dellibovi-Ragheb T a, Matthews K a, Bosch G, Prigge ST. The suf iron-sulfur cluster synthesis pathway is required for apicoplast maintenance in malaria parasites. *PLoS Pathog*. 2013;9(9):e1003655. doi:10.1371/journal.ppat.1003655.

17. Gallagher JR, Matthews K a, Prigge ST. *Plasmodium falciparum* apicoplast transit peptides are unstructured *in vitro* and during apicoplast import. *Traffic*. 2011;12:1124-1138. doi:10.1111/j.1600-0854.2011.01232.x.

18. Spalding MD, Allary M, Gallagher JR, Prigge ST. Validation of a modified method for Bxb1 mycobacteriophage integrase-mediated recombination in *Plasmodium falciparum* by localization of the H-protein of the glycine cleavage complex to the mitochondrion. *Mol Biochem Parasitol*. 2010;172:156-160. doi:10.1016/j.molbiopara.2010.04.005.

# Chapter 3

# Design and Evaluation of FK506 Binding Protein as a Candidate Conditional Localization Domain

**ABSTRACT**

In this chapter we modified the FK506 Binding Protein (FKBP) to engineer a new group of candidate conditional localization domains. The first candidate CLD we tested was derived from a destabilized FKBP mutant that has been used as a degradation domain in *P. falciparum*. We modified the destabilized FKBP to mimic an apicoplast transit peptide and expressed the CLD (CLD:FKBP) fused to a fluorescent cargo protein. We then analyzed the localization of the CLD using live fluorescence microscopy. CLD:FKBP trafficked to the apicoplast in the absence of the interacting ligand and did not change localization when the ligand was added to cell culture media.

Because CLD:FKBP did not change localization it was not an ideal domain to use for our conditional localization system. We hypothesized that CLD:FKBP may be too unstable to effectively bind the ligand and change localization *in vivo*. To investigate this hypothesis we purified the CLD:FKBP protein and did thermal shift assays to measure thermal stability of the protein. Our results showed that CLD:FKBP is significantly less stable than the control destabilized FKBP mutant. This result led us to re-design CLD:FKBP to create more stable candidate domains. Our goal in re-designing CLD:FKBP was to increase the stability of the domain while also maintaining its ability to traffic to the apicoplast under permissive conditions.

CLD1, CLD2, and CLD3 are re-designed candidate CLDs that contain less severe destabilizing mutations than those of CLD:FKBP. We expressed CLD1, 2, and 3 in separate *P. falciparum* transgenic parasite lines fused to a fluorescent cargo protein, and analyzed their localization. All three of the candidate CLDs trafficked to the apicoplast in the absence of the interacting ligand and changed localization to become secreted when the ligand was added to cell culture media. CLD1, 2, and 3 meet the basic trafficking requirements for our

apicoplast conditional localization system. We moved forward with an in depth characterization of protein trafficking by each domain in the next chapter.

## INTRODUCTION

FK506 Binding Protein (FKBP) is a protein folding chaperone that specifically functions as a proline cis-trans isomerase[1]. FKBP structure and function have been studied extensively because it is the target of the immunosuppressive compound FK506[1–3]. FK506 forms a complex with FKBP that inhibits T-cell activation by blocking the activity of the phosphatase Calcineurin, which is required to activate transcription factors that promote in T-cell activation[4,5]. Studies have shown that FKBP has a very high affinity and specific binding interaction with FK506, which makes the FKBP/FK506 pair an appealing protein and ligand combination for engineering molecular tools[6]. Both FKBP and FK506 have been redesigned to identify mutations or modifications that further enhance their binding affinity[7]. This is appealing because FKBP mutants that bind synthetic ligands more effectively than natural ligands are less likely to interfere with endogenous pathways when expressed in the cell as a molecular tool. Two FKBP mutant and FK506 derived molecule combinations have been used in *P. falciparum* for conditional export and conditional degradation domain molecular tools[8–10].

The conditional export system uses a Conditional Aggregation Domain (CAD) tag to control the localization of exported proteins in *P. falciparum*. The CAD was designed from a mutant FKBP protein that binds the synthetic ligand AP21998 more effectively than its endogenous ligands [9]. The domain consists of four mutant FKBPs that are added as a fusion protein tag to the amino terminus of a protein of interest. In the absence of AP21998,

proteins tagged with the CAD aggregate in the endoplasmic reticulum and are blocked from being exported. When AP21998 is added to cell culture media, the CADs dissociate and allow the protein to be exported across the parasitophorous vacuole membrane into the red blood cell cytosol.

A conditional degradation domain was designed from a mutant FKBP that binds the synthetic ligand Shield1 more efficiently than its endogenous binding partners[7,11]. The conditional degradation domain is mutated so that it is unstable in the absence of Shield1 and causes proteins tagged with the domain to be degraded. When Shield1 is added to cell culture media the domain stabilizes so that the tagged protein remains in the cell. The conditional degradation domain has been successfully used as a molecular tool in *P. falciparum* to conditionally knock down proteins and show that they are essential for parasite development in the erythrocytic cycle [8,12,13]. For example, conditional knockdown of the calcium-dependent protein kinase 5 (*Pf*CDPK5) revealed that *Pf*CDPK5 is essential for schizont egress from the red blood cell[12]. The cysteine protease Caplain was also conditionally knocked down, to show that Caplain is essential for progression from the ring to trophozoite stage of parasite development[13].

We designed a candidate CLD from the destabilized FKBP that was used as a degradation domain in *P. falciparum* (CLD:FKBP). CLD:FKBP also binds the synthetic ligand Shield1. One drawback of using a Shield1 binding FKBP mutant for our CLD is that Shield1 has moderate anti-malarial effects when added to cell culture media at high concentrations[10]. Shield1 concentrations above 1 μM cause a delay in trophozoite development[10]. As a result, any molecular tool designed for use in *P. falciparum* that requires Shield1 –including our apicoplast conditional localization system – must be effective at low concentrations of this ligand.

To test CLD:FKBP as a candidate CLD, we expressed the domain with a fluorescent cargo protein so that we could visualize its localization using live fluorescence microscopy. Our analysis of protein trafficking by CLD:FKBP revealed that this candidate CLD traffics to the apicoplast regardless of the presence of the ligand Shield1. We hypothesized that CLD:FKBP may be too unstable to bind Shield1 and change localization *in vivo*. Additionally, we reasoned that if we partially stabilized CLD:FKBP without affecting its ability to traffic to the apicoplast, it could ultimately be a successful candidate for our conditional localization system.

To measure the stability of CLD:FKBP we purified the CLD:FKBP protein and determined its melting temperature using a thermal shift assay. We compared the melting temperature of CLD:FKBP to that of a stable control Shield1-binding FKBP (sbFKBP) and a destabilized FKBP (dFKBP) control. CLD:FKBP was significantly less stable and less competent to bind Shield1 than the dFKBP control. These data supported our hypothesis that CLD:FKBP is too unstable to effectively bind Shield1 *in vivo* and encouraged us to redesign CLD:FKBP to generate more stable mutants that could be successful candidate CLDs.

The redesigned CLD:FKBP proteins – CLD1, CLD2, and CLD3 – have a metastable structure that allows them to strike a balance between being unstable enough to traffic to the apicoplast under permissive conditions and also maintain the capacity to bind Shield1. CLD1, 2 and 3 were our first successful candidate CLDs. They meet the basic requirement of trafficking to the apicoplast under permissive conditions (-Shield1) and changing localization when Shield1 is added to cell culture media. In our next set of experiments described in Chapter 4, we conducted an in depth analysis of the dynamics of protein trafficking for each of the three CLDs.

## RESULTS

### Design and Expression of CLD:FKBP

We reasoned that the CLD should mimic an apicoplast transit peptide under permissive conditions to allow it to traffic to the apicoplast. As discussed in previous chapters, transit peptides must maintain a net positive charge near the N-terminus. To meet this requirement, we mutated a negatively charged glutamic acid at position 6 and an uncharged glutamine at position 4 to positively charged lysine residues ($FKBP_{Q4K,E6K}$). These mutations increase the overall charge near the N-terminus of FKBP to +3. Transit peptides are unstructured during apicoplast import and formation of structure in the transit peptide region blocks import to the apicoplast. To give the CLD structural features that can be controlled experimentally, we introduced the destabilizing degradation domain mutation ($FKBP_{L107P}$) to destabilize the protein in the absence of the ligand[8]. We hypothesized that the destabilized CLD would mimic an unstructured transit peptide and allow the CLD to traffic to the apicoplast. When we add the ligand to cell culture media we expect to stabilize the structure of the CLD and block the protein from being imported into the apicoplast. Finally, the CLD:FKBP protein also contains the Shield1 binding mutation ($FKBP_{F36V}$), this mutation allows CLD:FKBP to bind the synthetic molecule Shield1 more effectively than other potential endogenous binding partners in the cell. Each of the mutations introduced to create CLD:FKBP are highlighted in Figure 3-1 A.

The CLD:FKBP sequence was expressed in *P. falciparum* with an N-terminal signal sequence from ACP and the SFG protein at the C-terminus. We also input the CLD:FKBP amino acid sequence into the PATS algorithm (the PATS program was discussed in detail in

the introduction to Chapter 2) to determine how similar the sequence is to natural *P. falciparum* transit peptides. The PATS program gave CLD:FKBP a score of 0.94, which indicates that CLD:FKBP closely mimics the basic sequence features of a *P. falciparum* transit peptide.

We analyzed protein trafficking of CLD:FKBP using live fluorescence microscopy shown in Figure 3-1 B. In the absence of Shield1 we observed an SFG trafficking pattern that is consistent with apicoplast trafficking. The SFG signal forms a branched organelle that is distinct from the mitochondrion staining in the trophozoite stage of parasite development (Figure 3-1 B top row). We confirmed that CLD:FKBP traffics to the apicoplast by co-localizing SFG with the apicoplast marker ACP using immunofluorescence assays (A representative image is shown in Figure 3-1C). Next, we added 500 nM Shield1 to parasite culture media for 48 hours before analyzing protein localization. We did not observe a change in SFG localization with this treatment (Figure 3-1 B middle row) so we doubled the Shield1 concentration in our next experiment. We still did not observe a significant change in localization of SFG after treatment with 1 μM Shield1 (Figure 3-1B bottom row). These data show that CLD:FKBP traffics to the apicoplast regardless of the presence of Shield1 and is not an ideal domain for our conditional localization system. We hypothesized that the two N-terminal lysine mutations ($FKBP_{Q4K,E6K}$) combined with the destabilizing degradation domain mutation ($FKBP_{L107P}$) may have caused CLD:FKBP to be too unstable to effectively bind Shield1 and change localization *in vivo*. In our next set of experiments we tested this hypothesis by analyzing the thermal stability of the CLD:FKBP protein purified *in vitro*.

**Analysis of thermal stability of CLD:FKBP**

We used thermal shift assays to determine the melting temperature of the CLD:FKBP protein and compare it to the melting temperature of stable (sbFKBP) and unstable (dFKBP) control proteins. In order to get purified proteins for thermal shift assays we expressed each FKBP mutant – sbFKBP, dFKBP, and CLD:FKBP – in *E. coli* and purified them from cell lysates using Maltose Binding Protein (MBP) and Histidine tags fused to the N-terminus of the protein. We then further purified the FKBP mutants by size exclusion chromatography.

In the process of purifying the unstable FKBP mutants (dFKBP and CLD:FKBP) we encountered some difficulties that we did not encounter when purifying the stable FKBP mutant (sbFKBP). We induced expression of CLD:FKBP and dFKBP in *E. coli* and ran the cell lysate over an amylose column to concentrate the proteins with an MBP tag (Figure 3-2 A, lanes labeled "CLD:FKBP (no TEV)" and b, lane labeled "dFKBP (no TEV)" ). We then cleaved the MBP tag from CLD:FKBP or dFKBP using the Tobacco Etch Virus (TEV) protease. At this point we estimate that about 79 % of the CLD:FKBP protein precipitated out of solution (Figure 3-2 A lane labeled "P" for pellet in red box). We were not able to collect enough protein from the left over soluble fraction (Figure 3-2 A lane labeled "S" for soluble in red box) of this experiment to proceed with the thermal shift assay. In our next CLD:FKBP protein preparation, we added Shield1 to the TEV cleavage step to stabilize the CLD:FKBP protein and help maintain its solubility (Figure 3-2 A green box). Under these conditions only about 50 % of the CLD:FKBP protein precipitated out of solution (Figure 3-2 A, compare CLD:FKBP in green box in lanes labeled "P" and "S").

A similar but less severe result was observed when we purified dFKBP (Figure 3-2 B). When we did a TEV cleavage assay in the absence of Shield1, and about 66 % of the dFKBP protein precipitated out of solution (Figure 3-2 B compare dFKBP in lanes labeled

"P" and "S" in red box). In a parallel experiment we added Shield1 to the TEV cleavage assay and only 41 % of the dFKBP precipitated (Figure 3-2 B compare dFKBP in lanes labeled "P" and "S" in green box). The observation that destabilized FKBP mutants precipitate in solution without a stabilizing ligand indicate that both CLD:FKBP and dFKBP are significantly less stable than sbFKBP which did not precipitate after TEV cleavage. The higher percentage of precipitated protein in the CLD:FKBP preparation suggests that CLD:FKBP is even less stable than dFKBP.

We used Thermal Shift Assays to determine the melting temperature of the stable FKBP mutant purified without Shield1, and the unstable FKBP mutants purified with Shield1. Because we had to add Shield1 to the preparation to solubilize the dFKBP and CLD:FKBP proteins, we only compared the melting temperatures from the assays done in the presence of Shield1 in Table 3-1. Our analysis shows that dFKBP is 14.6 °C less stable than sbFKBP, while CLD:FKBP is 20.3 °C less stable. This result suggests that one or both of the N-terminal lysine mutations ($FKBP_{Q4K,E6K}$) further destabilize the CLD:FKBP protein so that it is less competent to bind Shield1 than dFKBP. These data also support our hypothesis that CLD:FKBP may be too unstable to effectively bind Shield1 *in vivo* and change localization. We redesigned CLD:FKBP and tested three new candidate CLDs that are more stable mutants of the original CLD:FKBP in the next section.

**Design and Expression of CLD1, CLD2, and CLD3**

Our goal in designing the next group of candidate CLDs (CLD1, CLD2 and CLD3) was to add back some stability to the CLD:FKBP protein, without losing the ability to traffic to the apicoplast. We reverted the destabilizing proline mutation at position 107 ($FKBP_{L107P}$) back to a leucine residue to enhance stability of the protein and tested three different

arrangements of lysine mutations near the N-terminus of the CLD to determine which mutations are most important for apicoplast trafficking. CLD1 has a mutation at residue 4 to convert an uncharged glutamine to a positively charged lysine ($FKBP_{Q4K}$); this increases the overall positive charge near the N-terminus +1. CLD2 has a mutation at residue 6 to convert a negatively charged aspartic acid to lysine ($FKBP_{E6K}$) and increase the overall charge +2. Finally, CLD3 has a mutation at both residues four and six ($FKBP_{Q4K,E6K}$) to increase the net positive charge +3. A summary of FKBP mutations made to generate CLD1, 2, and 3 is show in Figure 3-3. Based on the thermal stability analysis described in the previous section, we hypothesized that these lysine mutations might also slightly destabilize FKBP and allow it to traffic to the apicoplast when there is no Shield1 present. Because these mutations are likely not as severe as the degradation domain mutation of CLD:FKBP we expect that CLD1, 2, and 3 should also be more competent to bind Shield1 *in vivo*.

We expressed CLD1, 2 and 3 in separate parasite lines using the previously described signal sequence and SFG cargo protein that were also expressed with CLD:FKBP and allow us to monitor protein localization using fluorescent microscopy. The "-" Shield1 rows in Figure 3-4, 3-5, and 3-6 show trafficking of CLD1, 2 and 3 respectively, with no Shield1 added to the culture. A representative image at each development stage in the red blood cell – ring, trophozoite, and schizont - is shown and the pattern of fluorescence observed in these rows is consistent with previous reports of apicoplast trafficking[14]. The apicoplast is typically identified in live fluorescence images as a branched organelle that is distinct from the mitochondrion staining in the trophozoite stage. The apicoplast however, is closely associated with the mitochondria at all stages of development in the red blood cell and the two organelles occasionally touch in the images shown[14].

The "+" Shield1 rows in Figure 3-4, 3-5, and 3-6 show trafficking of CLD1, 2, and 3 respectively, after cells were treated with 500 nM Shield1 for 24 hours. The pattern of fluorescence in these rows is consistent with the protein being secreted. Proteins that are secreted from the cell accumulate in the parasitophorous vacuole space that separates the parasite from the red blood cell cytosol [14]. In many of the images collected from CLD1, 2, and 3, SFG appears to accumulate in the parasitophorous vacuole space and the digestive vacuole after the addition of Shield1. This pattern of fluorescence is similar the trafficking of the resident digestive vacuole protease Dipeptidyl Amino Peptidase I (DPAP1)[15]. DPAP1 is secreted into the parasitophorous vacuole space where it accumulates before moving to the digestive vacuole, presumably through the cytostomes. The CLD may follow a similar pattern when it is secreted into the parasitophorous vacuole space, and get taken back into the cell to the digestive vacuole through the cytostome. This experiment shows that CLD1, 2, and 3 all meet the basic trafficking requirements for our conditional localization system.

## CONCLUSIONS AND DISCUSSION

Our studies to engineer a CLD from FKBP suggest that there must be a balance in the in the stability of the CLD. The CLD must be unstable enough to mimic an unstructured transit peptide and traffic to the apicoplast while also maintaining enough stability to bind Shield1 *in vivo* and change localization.

CLD:FKBP contained three potentially destabilizing mutations ($FKBP_{Q4K, E6K, L107P}$) and was less stable than the dFKBP degradation domain used in the conditional degradation system(Table 3-1). This suggests that one or both the amino-terminal lysine mutations in CLD:FKBP further destabilize the domain, and make it less competent to bind Shield1 *in*

*vivo*. Because CLD:FKBP is not able to effectively bind Shield1, it trafficked to the apicoplast even when Shield1 was added to cell culture media (Figure 3-1) and could not be used for our conditional localization system.

We redesigned CLD:FKBP to increase its overall stability and competence to bind Shield1. CLD1, 2, and 3 each contain one or both of the lysine mutations at residues 4 and 6 from CLD:FKBP and no destabilizing degradation domain mutation (Figure 3-3). These lysine mutations increase the net positive charge near the N-terminus and our thermal stability analysis suggests that they also slightly destabilize the protein. In addition to our thermal stability analysis of CLD:FKBP, another indication that the amino terminal lysine mutations we made at residues 4 and 6 are slightly destabilizing can be found in the original publication describing how the FKBP degradation domain was generated. The degradation domain was selected from a screen of randomly mutagenized FKBPs[11]. The FKBP mutants were phenotypically screened for proteins that were unstable without Shield1 and stabilized when bound to Shield1. In the supplementary information for this study there is a list of all of the destabilizing mutation combinations identified in this screen. We found the $FKBP_{E6K}$ mutation appeared twice on this list of destabilizing FKBP mutations. And a similar mutation to $FKBP_{Q4K}$ in terms of charge, which is $FKBP_{Q4R}$, was also identified twice in the screen of destabilizing FKBP mutations. We tested the redesigned candidate CLDs in *P. falciparum* and all three of the candidate domains appear to traffic to the apicoplast in the absence of Shield1 and change localization to become secreted when Shield1 is supplemented in cell culture media (Figure 3-4, 3-5, and 3-6).

FKBP has some features that may have made it a better candidate CLD than DHFR. The first feature is its small size compared to DHFR. FKBP is 108 amino acids long while both of the DHFR proteins tested in Chapter 2 were over 150 amino acids long. Secondly,

FKBP has been modified to interact more efficiently with the synthetic ligand Shield1 than any of its endogenous binding partners in the cell. This gives FKBP an advantage over DHFR because it should not bind cellular ligands that could affect protein stability or apicoplast biochemistry.

In our next group of experiments (Chapter 4) we conducted an in depth analysis of protein trafficking and thermal stability of CLD1, 2, and 3. We were interested in determining whether CLD1, 2 and 3 were equal in their trafficking capacity to both the apicoplast and secreted compartment or if they differed in their ability to traffic to one compartment or the other. This information is valuable to determine how each CLD can be best used in validation studies to tag specific proteins of interest and answer questions about parasite biology.

## METHODS

### Generation of plasmid constructs

The human FKBP gene with Shield1 binding mutation [8] was PCR amplified using forward primers that contain nucleotide changes to produce lysine mutations at residues 4, 6, or both (to generate CLD1, 2 or 3 respectively). NdeI.FKBPq4k.for was used to generate CLD1, NdeI.FKBPe6k.for was used for CLD2, and NdeI.Fkkfor was used for CLD3. One reverse primer (FKBP.P107L.BglII.rev) was used to amplify the FKBP gene without the destabilizing degradation domain mutation ($FKBP_{L107P}$) for CLD1, 2, and 3. NdeI.Fkkfor and FKBP.BglII.rev were used to amplify CLD:FKBP. FKBP inserts were then digested using NdeI and BglII and ligated into cloning vectors (GeneArt) that contained the synthesized signal sequence from the ACP gene and the super folder green sequence [16]. The

CLD sequences were then ligated into a modified pLN [17] vector for parasite transfection that contained the lower strength ribosomal L2 protein promoter [18] instead of the calmodulin promoter.

Plasmids used for protein expression in *E. coli* were generated by PCR amplifying the human FKBP gene with the Shield1 binding mutation [8] using a forward primer that contains nucleotide changes to produce lysine mutations at residues 4 and 6 to generate CLD:FKBP (Fkk.EcoRI.LIC.for). The sbFKBP and dFKBP genes were amplified using the Fqe.EcoRI.LIC.for forward primer that does not generate any mutations at the N-terminus. A reverse primer that contains the destabilizing degradation domain mutations (FKBP.P107.HindIII.LIC.rev) was used to amplify the CLD:FKBP and dFKBP genes and a reverse primer that does not contain the $FKBP_{L107P}$ mutation was used to amplify sbFKBP (FKBP.P107L.HindIII.LIC.rev). PCR amplicons were then inserted into the pMALcHT [19] *E. coli* expression vector using ligase independent cloning with T4 DNA polymerase. DNA sequences were confirmed by sequencing after insertion.

**Protein expression and purification**

Plasmids pMALcHT-sbFKBP, pMALcHT-dFKBP, pMALcHT-CLD:FKBP were transformed into BL21-Star (DE3) cells and co-transformed with the pRIL plasmid isolated from BL21-CodonPlus-RIL cells [20]. These cells produce a protein product fused to an amino-terminal MBP tag followed by a Tobacco Etch Virus (TEV) protease cleavage site and a six-histidine tag. Cells were pelleted and then resuspended in lysis buffer (20 mM HEPES pH 7.5, 500mM NaCl, 1 mg/ml DNAse I, and 100 mg/ml Lysozyme). Cell lysates were then sonicated at amplitude of 45% for a total of six minutes broken into 2-minute intervals of 0.5 seconds on and 0.5 seconds off. After sonication cell lysates were filtered

through a 0.45 micron filter before purification. All constructs were then purified using an amylose column and eluted with 100 mM maltose followed by cleavage with TEV protease at room temperature overnight in the presence of 1 mM DTT and 0.5 mM EDTA. The cleavage product was extensively dialyzed into 20 mM HEPES pH 7.5 and 500 mM NaCl and purified from the MBP tag via nickel-affinity chromatography using a His Trap HP column (GE Life Sciences). Appropriate fractions were collected and further purified by size exclusion chromatography with a HiPrep 26/60 Sephacryl S-100 HR column (GE Life Sciences).

**Immunofluorescence assay**

Cells were fixed, permeabilized and reduced using the same protocol described in the Methods section of Chapter 2. Before applying primary antibodies, cells were washed in PBS and then incubated with appropriate antibodies overnight at 4 °C [rat polyclonal αACP 1:2000, raised against the *P. falciparum* antigen; rabbit polyclonal αGFP 1:10,000 raised against recombinant GFP protein]. The next day, cells were washed three times in PBS and then once in 3 % BSA. Appropriate secondary antibodies [goat αrabbit AlexaFluor 594 1:1000 (Life Technologies); donkey αrat AlexaFluor 488 1:3000 (Life Technologies)]

**Thermal shift assay**

Stability of the different FKBP constructs was determined using a thermal shift assay as previously described [21] with minor modifications. RT-PCR tube strips (Eppendorf) were used to hold 30 µL mixtures containing final concentrations of 40 µM (0.5 mg/mL) FKBP mutant and 200 µM Shield1. The Shield-1 compound (dissolved in 100% ethanol) was first added to the PCR tube to set up the reaction mixture and the solvent was then allowed to

evaporate at room temperature. Shield1 was re-suspended in buffer (HEPES pH 7.4 and 100 mM NaCl) followed by addition of FKBP mutant and 1 μL of Sypro Orange (Sigma, product no. S-5692). The reaction mixture was incubated in a RT-PCR machine (Applied Biosystems, Step One Plus Real-Time PCR System) for 2 min at 20 °C followed by an increase in temperature of 0.2 °C per 10 s until a final temperature of 80 °C. Fluorescence was monitored in the Step One Plus Real-Time PCR system using a TAMRA filter in which an increase in Sypro Orange fluorescence (excitation: 480 nm, emission: 568 nm) was observed upon thermal denaturation of FKBP mutant. Temperature and melt curve data points were exported from the StepOne v2.3 software program and analyzed in Excel to determine the melting temperature. All thermal shift assays were done with triplicate technical replicates for the indicated number of biological replicated given in figure legends.

**Live cell imaging**

Cells were stained for live fluorescence imaging using the same protocol described in Chapter 2. Samples were then taken to the Zeiss microscope for imaging.

**Quantification of Protein Bands**

The quantification of protein bands on the gels presented in Figure 3-2 was done using the ImageJ software program to estimate the amount of protein in each lane based on intensity of the gel staining with Simply Blue Safe Stain (Invitrogen) [22]. Briefly, the intensity of the FKBP bands in the soluble and pelleted lanes was added to calculate the total intensity and then the intensity of the pelleted lane was divided by the total intensity to get the percent of FKBP that precipitated in each sample.

- Parasite transfection and culture methods are the same as for Chapter 2

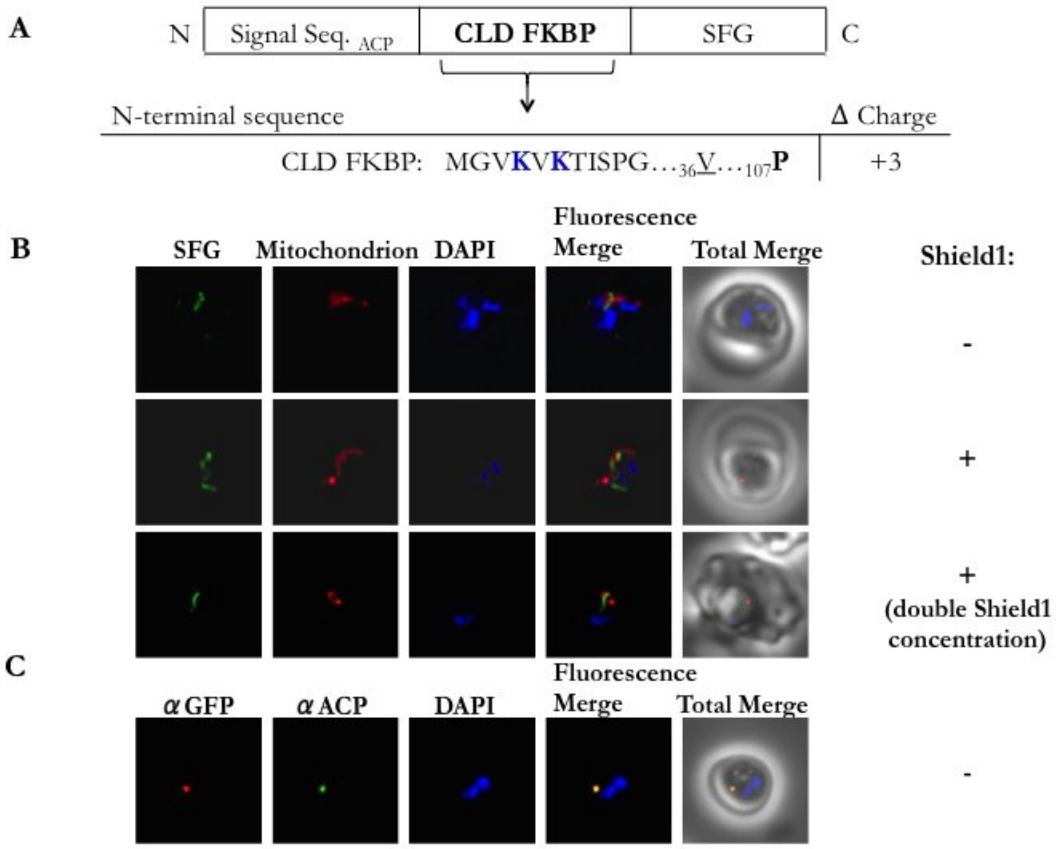


**Figure 3-1 CLD:FKBP design and analysis of protein trafficking**

A) We generated a transgenic parasite line that expresses a verified signal sequence from ACP fused to CLD:FKBP and super folder green (SFG). The N-terminal sequence of CLD:FKBP is shown. Lysine mutations in blue increase positive charge; destabilization domain mutation is in bold; Shield1 binding mutation is underlined. The overall change in charge near the N-terminus is listed in the right column.

B) Live fluorescence images of cells expressing the transgene shown in part A. Cells in the top row have not been treated with Shield1. Cells in the second row were treated with 500 nM for 48 hours and cells in the third row were treated with 1 μM Shield1 for 24 hours before imaging. Images are 10 μm long by 10 μm wide.

C) Immunofluorescence images of fixed cells stained with anti-ACP (apicoplast marker) and anti-GFP antibodies in the absence of Shield1. Images are 10μm long by 10μm wide.

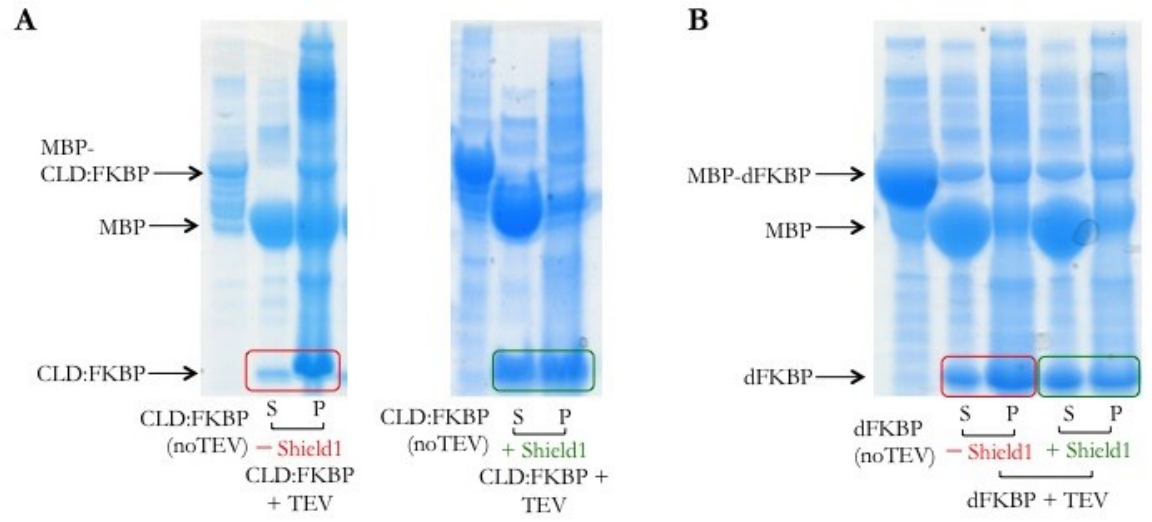


**Figure 3-2 Analysis of protein precipitation from unstable FKBP mutants**

A) An MBP tagged CLD:FKBP protein was expressed in *E. coli* and purified from cell lysates. The far left lane on both gels shows purified MBP-CLD:FKBP eluted from an amylose column. The protein solution was treated with TEV protease to separate the CLD:FKBP from MBP. At this point, CLD:FKBP precipitated and we pelleted the insoluble fraction. The boxes on both gels show the amount of CLD:FKBP protein in the pellet ("P") and supernatant ("S") after the TEV cleavage assay. The red box shows a TEV cleavage assay done without Shield1, and the green box shows the assay done in with Shield1 added at approximately 3 Shield1 molecules per CLD:FKBP protein.

B) The destabilized FKBP (dFKBP) was also expressed in *E. coli* and purified from cell lysates. The far left lane shows purified MBP-dFKBP eluted from an amylose column. The dFKBP also precipitated after cleavage with the TEV protease and the insoluble fraction was pelleted. The red box shows a TEV cleavage assay done without Shield1, and the green box shows the assay done in with Shield1 added at approximately 3 Shield1 molecules per dFKBP protein.

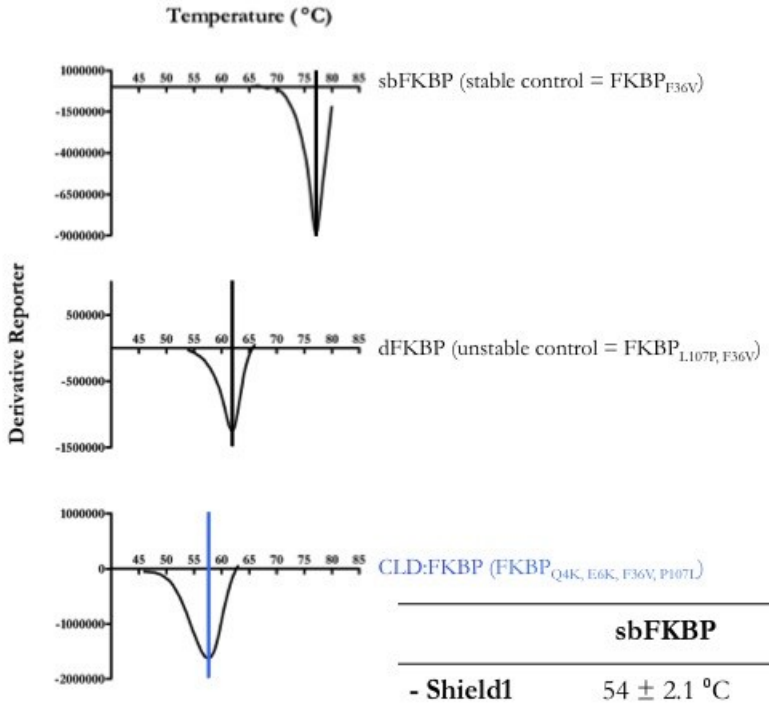


| | sbFKBP | CLD:FKBP | dFKBP |
|---|---|---|---|
| **- Shield1** | 54 ± 2.1 °C | – | – |
| **+ Shield1** | 77.5 ± 0.4 °C | 57.2 ± 0.3 °C | 62.9 ± 0.2 °C |
| **$\Delta T_m$** | – | ⁻20.3 °C | ⁻14.6 °C |

**Table 3-1 Analysis of thermal stability of CLD:FKBP**

Melting temperatures determined using Thermal Shift Assays. CLD:FKBP and dFKBP could not be purified at high concentrations without adding Shield1 during purification to stabilize the protein so only +Shield1 melting temperatures ($T_m$) are compared in this analysis. Melting temperatures are shown with standard deviations calculated from triplicate biological replicates.

Derivative reporter plots show representative data curves generated for each protein.

sbFKBP = Shield1 binding FKBP
dFKBP = destabilized FKBP
CLD:FKBP = candidate conditional localization domain designed from the FKBP protein

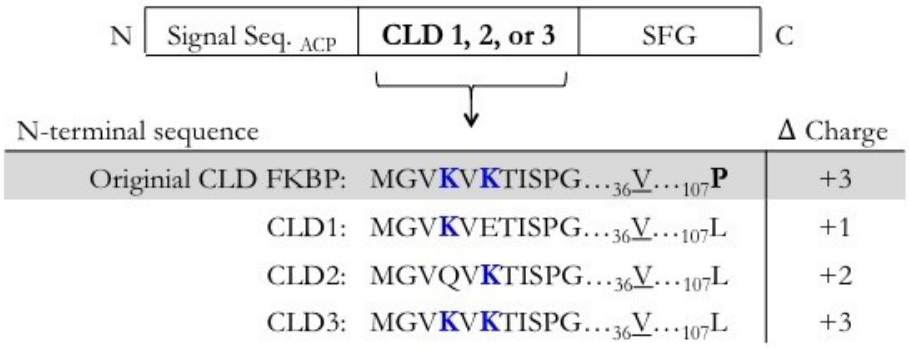


**Figure 3-3 Three candidate CLDs re-designed from the original CLD:FKBP sequence**

Test constructs for evaluation of three CLDs that were redesigned from the original CLD:FKBP sequence. The N-terminal sequence of CLD1-3 varies as shown. Lysine mutations in blue increase positive charge and the overall changes in charge near the N-terminus are listed in the right column. Shield1 binding mutation is underlined and the destabilizing degradation domain mutation is in bold in CLD:FKBP, but has been reverted in CLD1, 2, and 3.

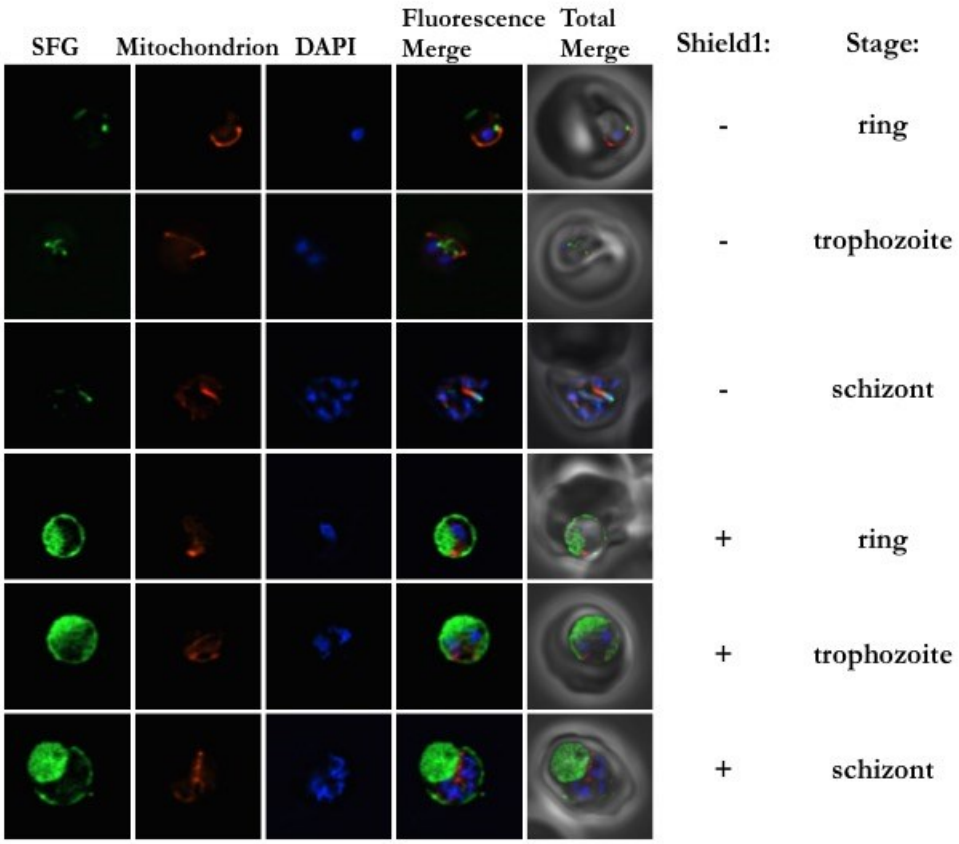


**Figure 3-4 Analysis of protein trafficking for CLD1**

Live images of transgenic parasites lines expressing CLD1. The rows labeled "-" are cells that have not been treated with Shield1 and rows labeled "+" are cells that have been treated with 500 nM Shield1 for 24 hours. The development stage of each parasite is estimated based on the number of nuclei and the size of the parasite relative to the red blood cell. Images are 10 μm long by 10 μm wide

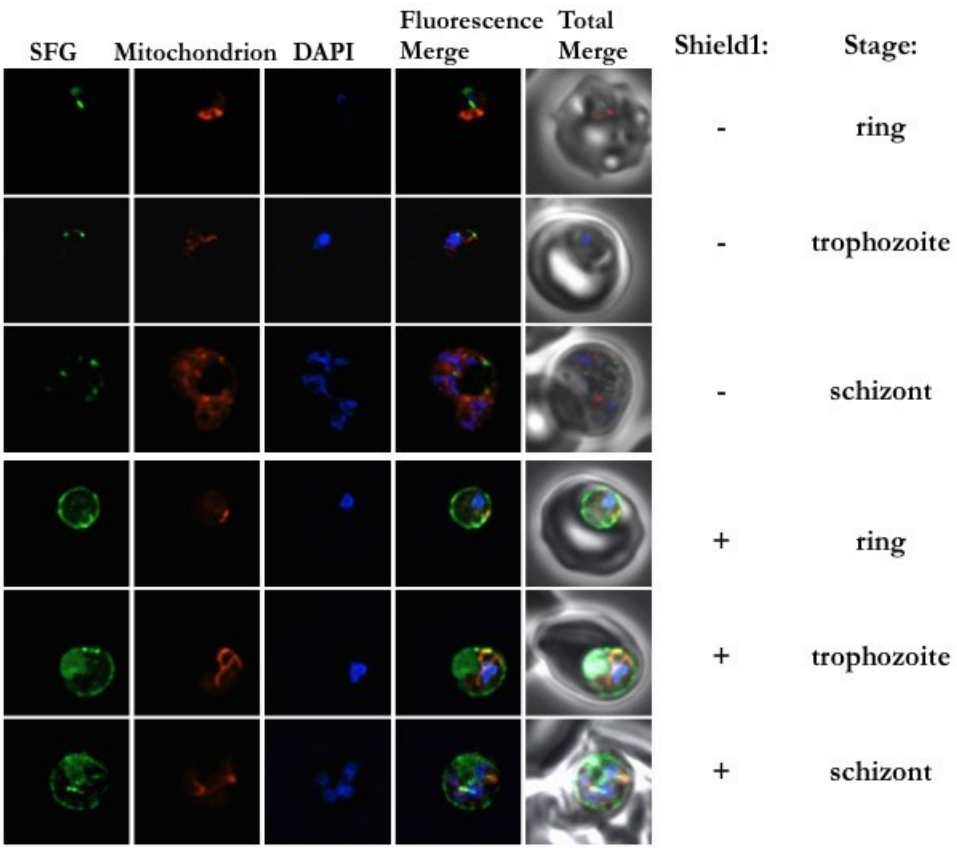


**Figure 3-5 Analysis of protein trafficking for CLD2**

Live images of transgenic parasites lines expressing CLD2. The rows labeled "-" are cells that have not been treated with Shield1 and rows labeled "+" are cells that have been treated with 500 nM Shield1 for 24 hours. The development stage of each parasite is estimated based on the number of nuclei and the size of the parasite relative to the red blood cell. Images are 10 μm long by 10 μm wide

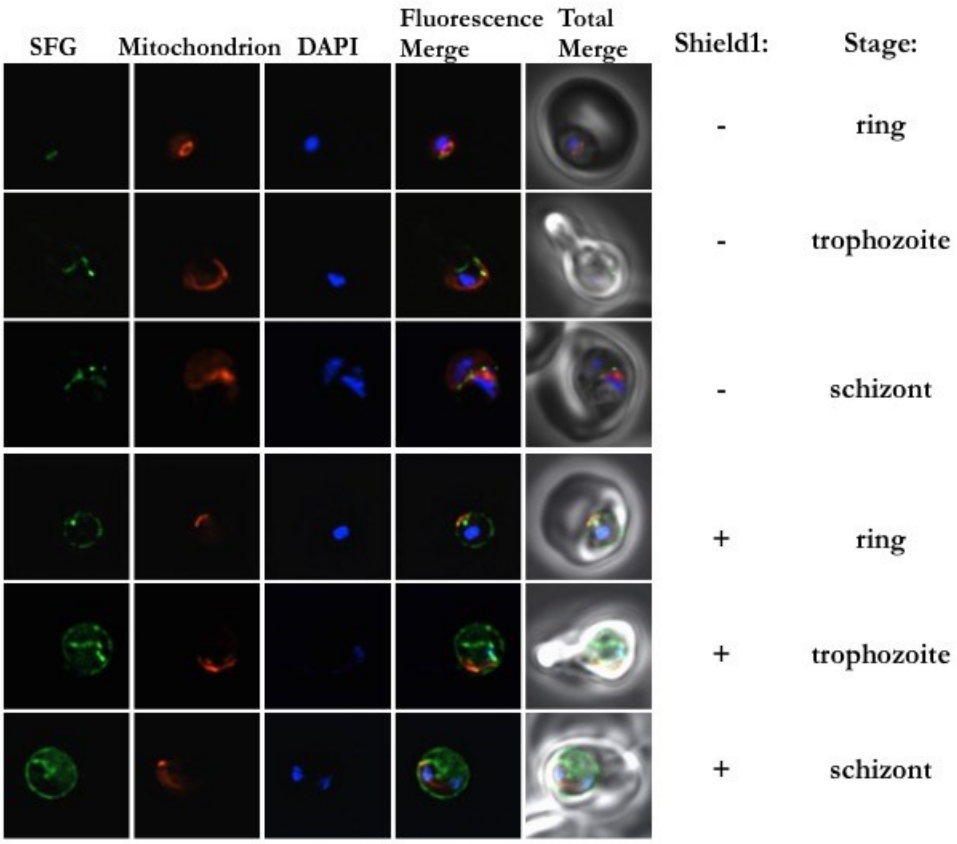


**Figure 3-6 Analysis of protein trafficking for CLD3**

Live images of transgenic parasites lines expressing CLD3. The rows labeled "-" are cells that have not been treated with Shield1 and rows labeled "+" are cells that have been treated with 500 nM Shield1 for 24 hours. The development stage of each parasite is estimated based on the number of nuclei and the size of the parasite relative to the red blood cell. Images are 10 μm long by 10 μm wide

| Primer name | Primer sequence |
|---|---|
| NdeI.FKBPq4k.for | GGTGGTCATATGGGAGTGAAGGTGGAAACCATCTCCCCAGGAGACGG |
| NdeI.FKBPe6k.for | GGTGGTCATATGGGAGTGCAGGTGAAAACCATCTCCCCAGGAGACGG |
| NdeI.Fkkfor | GGTGGTCATATGGGAGTGAAGGTGAAAACCATCTCCCCAGGAGACGG |
| FKBP.BglII.rev | GGTGGTAGATCTTTCCGGTTTTAGAAGCTCCACATCG |
| FKBP.P107L.BglII.rev | GGTGGTAGATCTTTCCAGTTTTAGAAGCTCCACATCGAAGACG |
| Fkk.EcoRI.LIC.for | CATCACCATCACGAATTCAAAAATCATATGGGAGTGAAGGTGAAAACCATC |
| Fqe.EcoRI.LIC.for | CATCACCATCACGAATTCAAAAATCATATGGGAGTGCAGGTGGAAACCATC |
| FKBP.P107L.HindIII.LIC.rev | GCCAGTGCCAAGCTTCTATTCCAGTTTTAGAAGCTCCACATCGAAGACG |
| FKBP.P107.HindIII.LIC.rev | GCCAGTGCCAAGCTTCTATTCCGGTTTTAGAAGCTCCACATCGAAGACG |

**Table 3-2 Primers used to generate CLD sequences for expression in *P. falciparum* and *E. coli***

## REFERENCES


1. Holt DA, Luengo JJI, Yamashita DS, et al. Design, Synthesis, and Kinetic Evaluation of High-Affinity FKBP Ligands and the X-ray Crystal Structures of Their Complexes with FKBP12. *J Am Chem Soc*. 1993;115(22):9925-9938.

2. Becker JW, Rotonda J, Mckeevers BM, et al. FK-506-binding Protein: Three-dimensional Structure of the Complex with the Antagonist L-685,818. *J Biol Chem*. 1993;268(15):11335-11339.

3. Duyne GD Van, Standaert RF, Karplus PA, Schreiber SL, Clardy J. Atomic Structure of FKBP-FK506 , an Immunophilin-Immunosuppressant Complex. *Science (80- )*. 1991;252(5007):839-842.

4. Hogan PG, Chen L, Nardone J, Rao A. Transcriptional regulation by calcium, calcineurin, and NFAT. *Genes Dev*. 2003;17:2205-2232. doi:10.1101/gad.1102703.GENES.

5. Müller MR, Rao A. Linking calcineurin activity to leukemogenesis. *Nat Med*. 2007;13(6):669-671.

6. Pollock R, Clackson T. Dimerizer-regulated gene expression. *Curr Opin Biotechnol*. 2002;13:459-467.

7. Clackson T, Yang W, Rozamus LW, et al. Redesigning an FKBP-ligand interface to generate chemical dimerizers with novel specificity. *Proc Natl Acad Sci U S A*. 1998;95:10437-10442. doi:10.1073/pnas.95.18.10437.

8. Armstrong CM, Goldberg DE. An FKBP destabilization domain modulates protein levels in *Plasmodium falciparum*. *Nat Methods*. 2007;4(12):1007-1009. doi:10.1038/nmeth1132.

9. Saridaki T, Sanchez CP, Pfahler J, Lanzer M. A conditional export system provides new insights into protein export in *Plasmodium falciparum*-infected erythrocytes. *Cell Microbiol*. 2008;10(12):2483-2495. doi:10.1111/j.1462-5822.2008.01223.x.

10. Azevedo MF De, Gilson PR, Gabriel HB, et al. Systematic Analysis of FKBP Inducible Degradation Domain Tagging Strategies for the Human Malaria Parasite *Plasmodium falciparum*. *PLoS One*. 2012;7(7):e40981. doi:10.1371/journal.pone.0040981.

11. Banaszynski LA, Chen L chun, Maynard-Smith LA, Ooi AGL, Wandless TJ. A Rapid, Reversible, and Tunable Method to Regulate Protein Function in Living Cells Using Synthetic Small Molecules. *Cell*. 2006;126:995-1004. doi:10.1016/j.cell.2006.07.025.

12. Dvorin JD, Martyn DC, Patel SD, et al. A Plant-Like Kinase in *Plasmodium falciparum* Regulates Parasite Egress from Erythrocytes. *Science (80- )*. 2010;328(5980):910-912.

13. Russo I, Oksman A, Vaupel B, Goldberg DE. A calpain unique to alveolates is

essential in *Plasmodium falciparum* and its knockdown reveals an involvement in pre-S-phase development. *Proc Natl Acad Sci U S A*. 2009;106(5):1554-1559.

14. Tilley L, Mcfadden G, Cowman A, Klonis N. Illuminating *Plasmodium falciparum* - infected red blood cells. *TRENDS Parasitol*. 2007;23(6):268-277. doi:10.1016/j.pt.2007.04.001.

15. Klemba M, Gluzman I, Goldberg DE. A *Plasmodium falciparum* dipeptidyl aminopeptidase I participates in vacuolar hemoglobin degradation. *J Biol Chem*. 2004;279(41):43000-43007. doi:10.1074/jbc.M408123200.

16. Pedelacq J-D, Cabantous S, Tran T, Terwilliger TC, Waldo GS. Engineering and characterization of a superfolder green fluorescent protein. *Nat Biotechnol*. 2006;24(1):79-89. doi:10.1038/nbt1172.

17. Nkrumah LJ, Muhle R a, Moura P a, et al. Efficient site-specific integration in *Plasmodium falciparum* chromosomes mediated by mycobacteriophage Bxb1 integrase. *Nat Methods*. 2006;3(8):615-621. doi:10.1038/nmeth904.

18. Gisselberg JE, Dellibovi-Ragheb T a, Matthews K a, Bosch G, Prigge ST. The suf iron-sulfur cluster synthesis pathway is required for apicoplast maintenance in malaria parasites. *PLoS Pathog*. 2013;9(9):e1003655. doi:10.1371/journal.ppat.1003655.

19. Muench S, Rafferty J, Mcleod R, Rice D, Prigge S. Expression, purification and Crystallization of the *Plasmodium falciparum* enoyl reductase. *Biol Crystallogr*. 2003;59:1246-1248.

20. Allary M, Lu JZ, Zhu L, Prigge ST. Scavenging of the cofactor lipoate is essential for the survival of the malaria parasite *Plasmodium falciparum*. *Mol Microbiol*. 2007;63(5):1331-1344. doi:10.1111/j.1365-2958.2007.05592.x.

21. Afanador GA, Muench SP, McPhillie M, et al. Discrimination of potent inhibitors of *Toxoplasma gondii* Enoyl-Acyl carrier protein reductase by a thermal shift assay. *Biochemistry*. 2013;52:9155-9166. doi:10.1021/bi400945y.

22. Schneider C a, Rasband WS, Eliceiri KW. NIH Image to ImageJ: 25 years of image analysis. *Nat Methods*. 2012;9(7):671-675. doi:10.1038/nmeth.2089.

# Chapter 4

# Evaluation of Protein Trafficking by Conditional Localization Domains 1, 2, and 3

**ABSTRACT**

This chapter describes our analysis of protein trafficking dynamics for CLD1, 2, and 3. We analyzed protein trafficking by CLD1, 2, and 3 in immunofluorescence images of cells stained with antibodies to track the location of the cargo protein (SFG) in the presence and absence of the interacting ligand (Shield1). Our analysis revealed that CLD1 has a leaky apicoplast trafficking phenotype, CLD3 showed a slight tendency to traffic to the apicoplast in the presence of Shield1, and CLD2 trafficked most efficiently to both the apicoplast and secreted compartment.

We hypothesized that CLD1's leaky apicoplast trafficking phenotype could be caused by a higher level of protein stability compared to CLD2 or 3. To investigate this hypothesis we analyzed the thermal stability of CLD1, 2 and 3 using thermal shift assays to determine the melting temperature of each protein. Our analysis showed that as expected, CLD1 has a higher thermal stability than CLD2 or 3. CLD1's higher stability likely prevents it from sampling the unfolded state as often as CLD2 or 3 and causes it to be less efficiently trafficked to the apicoplast.

We also titrated Shield1 concentrations to determine the relative sensitivity of CLD1, 2, and 3 to low concentrations of the Shield1 ligand. We found that CLD1 was the most sensitive to low concentrations of Shield1. This is consistent with our thermal stability analysis, which showed that CLD1 is also the most stable domain, and likely the most competent to bind Shield1 *in vivo*. CLD2 and 3 have similar levels of sensitivity and were less sensitive to low concentrations of Shield1 than CLD1. All three of the CLDs respond to concentrations of Shield1 well below 1 μM.

Our analysis showed that CLD2 has the most efficient trafficking characteristics and will likely be ideal for use in most validation studies of our conditional localization system.

We further investigated the timing of localization change and the effect of higher concentrations of Shield1 on CLD2 trafficking. These studies showed that secretion is nearly complete at 24 hours with 500 nM Shield1 added to cell culture media. Although CLD1 and 3 did not have the most efficient trafficking characteristics, they may still be useful in studies of certain protein where exclusion of protein from one compartment or the other is desirable. This analysis of the trafficking dynamics of CLD1, 2, and 3 will be used to guide validation studies in the next chapter.

## INTRODUCTION

The goal of this study was to gain a better understanding of how CLD1, 2, and 3 differ in their ability to control protein trafficking. The development and initial studies of these CLDs are described in detail in Chapter 3. In this chapter we further characterized each domain to quantitatively analyze the trafficking efficiency and Shield1 sensitivity of each CLD. We also purified each CLD protein from *E. coli* to measure thermal stability of the domains.

To study protein trafficking we did a co-localization analysis that compared the localization of the CLD trafficked cargo protein (SFG) to the apicoplast marker ACP. We calculated co-localization statistics for each cell using the ImageJ image processing software developed by the National Institutes of Health[1]. In the absence of Shield 1 we expect a high level of co-localization between SFG and ACP to confirm the apicoplast trafficking pattern of CLD1, 2, and 3 observed in live fluorescence images (Chapter 3; Figures 3-4, 3-5, and 3-6). When Shield1 is added to cell culture media we expect to see a drop in co-localization as the SFG protein is diverted from the apicoplast and is secreted from the cell.

The Pearson's Correlation Coefficient (PCC) is a measure of co-localization that is often reported in image analysis studies[2,3]. The PCC is modeled visually by plotting the intensities of the two fluorochromes being analyzed (for example TRITC and FITC) on the x and y-axis of a scatter plot (Figure 4-1). The PCC estimates how well the relationship between two fluorochromes plotted on an intensity scatter plot matches a linear approximation. When there is co-localization between the two fluorochromes, a positive linear relationship is observed on the intensity scatter plot (Figure 4-1 A) and the PCC is near 1. When there is not significant overlap between the fluorochromes being analyzed there is a negative linear or no relationship on the intensity scatter plot (Figure 4-1 B) and the PCC value is closer to -1 or 0.

The PCC is impacted by the average intensity of the two fluorochromes analyzed. When there is a significant difference in average intensity between two fluorochromes, the PCC value tends to be lowered as data points on the scatter plot are skewed towards the more intense fluorochrome's axis; this decline in PCC value occurs even when there is significant co-localization observed in the images of the two channels analyzed[3]. In our co-localization data set we analyzed two proteins that are expressed from different promoters. The SFG protein is expressed from the ribosomal L2 protein promoter and ACP is expressed from its endogenous promoter. This caused the average intensity for the SFG and ACP channels to be quite different in some of our data. To avoid the effect of intensity on the PCC calculation, we analyzed the Mander's Overlap Coefficient ($M_1$) instead of the PCC value[4]. In our studies, $M_1$ measures the fraction of intensities from the SFG channel (TRITC) that overlap with intensities from the ACP channel (FITC). $M_1$ is not affected by the average intensity of the channels because it counts all SFG intensities for which the intensity in the ACP channel is above zero equally[3].

An example of this difference between PCC and $M_1$ calculations is shown in Figure 4-1 C. The intensity scatter plot in Figure 4-1 C represents the image of the cell to its right. For this cell, the average intensity in the FITC channel is higher than the average intensity in the TRITC channel. Although the ACP and SFG proteins appear to be mostly co-localized in the image, the PCC value calculated for this cell is lower than the $M_1$ value because of the skewing of the intensities towards the FITC axis. For images like this one where the average intensity of the two channels analyzed is not equal, the $M_1$ value more accurately reflects the visual co-localization observed between the ACP and SFG proteins because it does not take the average intensity into account. Although the $M_1$ value is not affected by differences in average intensity, it is sensitive to high levels of background intensity or noise in the image. The ImageJ software however, allows users to manually set thresholds to eliminate background intensities from the $M_1$ calculation and setting appropriate intensity thresholds for each image reduces the effect of noise on the $M_1$ calculation.

We calculated $M_1$ values to evaluate the level of co-localization between SFG and ACP for CLD1, 2, and 3 in the presence and absence of the interacting ligand, Shield1. Previous studies have shown that correct timing of expression is important for trafficking of proteins to secretory organelles in *P. falciparum*[5,6]. To investigate whether timing of expression might have an effect on CLD trafficking we broke the co-localization analysis data up by developmental stage (ring, trophozoite, or schizont) and analyzed trafficking to the apicoplast and secreted compartment. We did not detect strong trends towards a lowered trafficking efficiency at any particular stage but our co-localization analysis did reveal that CLD1 has a leaky apicoplast trafficking phenotype compared to CLD2 or 3. We hypothesized that CLD1's leaky apicoplast trafficking may be because CLD1 has a higher stability level than CLD 2 or 3, and we investigated this hypothesis by analyzing the stability

of each CLD protein using thermal shift assays. Our thermal stability analysis showed that CLD1 is more stable than CLD2 or 3 and this likely causes CLD1 to traffic to the apicoplast less efficiently than CLD2 or 3. As discussed in previous chapters, transit peptides must be unstructured to traffic to the apicoplast, and the destabilization of the CLD is what allows the domain to mimic this feature of transit peptides under permissive conditions.

Finally, we were interested in estimating the lower limit of Shield1 effectiveness for each CLD. Given that Shield1 is toxic at high concentrations, it may be ideal to use the lowest effective concentration of Shield1 in future experiments. We titrated down the concentration of Shield1 and evaluated the localization of CLD1, 2, and 3 at each concentration. We found that CLD1 is the most sensitive to low concentration of Shield1, while CLD2 and 3 are not as sensitive to low concentrations of Shield1. The analyses presented in this chapter will be used to help determine which CLD is most appropriate to tag cargo proteins in validation studies.

## RESULTS

### Analysis of protein trafficking by CLD1, CLD2, and CLD3

*Immunofluorescence assays and calculation of $M_1$ values*

To measure the trafficking efficiency of CLD1, 2 and 3 we did a co-localization analysis of fixed cells co-stained with antibodies against the apicoplast marker ACP and the CLD trafficked SFG protein. We analyzed images from untreated cell samples or cells that were synchronized and then treated with 500 nM Shield1 for 72 hours before staining. For CLD1 we observed only partial co-localization between SFG and ACP (Figure 4-2 A; top panel); some of the CLD1 trafficked SFG protein appears to accumulate in the

parasitophorous vacuole space in addition to the apicoplast. This observation is consistent with a leaky apicoplast trafficking phenotype for CLD1. We observed close co-localization however, between SFG and ACP in images of untreated cells expressing CLD2 or CLD3 (Figures 4-3 A, and 4-4 A; top panel). Analysis of immunofluorescence images collected after Shield1 treatment show that SFG accumulates in the parasitophorous vacuole space and little to no co-localization is observed between SFG and ACP for all three CLDs (Figures 4-2 A, 4-3 A, and 4-4 A; bottom panel). Some of the SFG protein in cells treated with Shield1 is observed in the cell but not in the apicoplast, this protein is presumed to be in the secretory pathway, en route to be secreted from the cell.

We collected images of cells from a minimum of two independent immunofluorescence assays done in the presence or absence of Shield1 for each CLD. We then calculated $M_1$ values for each cell and summarized the data points on the graphs shown in Figures 4-2 B, 4-3 B, and 4-4 B. In the absence of Shield1 CLD2 and 3 have $M_1$ values near one, indicating that the ACP and SFG proteins are co-localized. After the addition of Shield1, the average $M_1$ values of CLD2 and CLD3 declined due to a change in the localization of SFG so that its intensities no longer overlap with ACP (Figures 4-3 B and 4-4 B; compare "0 nM Shield1" graph to "500 nM Shield1" graph). For CLD1, the $M_1$ values calculated in the absence of Shield1 were not as high as for CLD2 and 3. This was expected, because of the leaky apicoplast trafficking observed in immunofluorescence images of CLD1 expressing cells. When we added Shield1 to the assay, the M1 values for CLD1 declined, but the difference was not as significant as was observed for CLD2 and 3 (Figures 4-2 B; compare "0 nM Shield1" graph to "500 nM Shield1" graph).

Although the calculated $M_1$ values for CLD1 in the absence of Shield1 are low, we believe that CLD1 does traffic some protein to the apicoplast because of the live fluorescent

images that show a characteristic apicoplast trafficking pattern for CLD1 (Figure 3-4). We also consistently observed a portion of SFG protein co-localized with ACP in images of parasites expressing CLD1 in the absence of Shield1. The leaky apicoplast trafficking phenotype of CLD1 is only evident in immunofluorescence images of fixed cells and is not discernable in live fluorescence images (compare live images in Figure 3-4 to immunofluorescence images in Figure 4-2 A). Secondary antibody staining enhances detection of SFG protein in immunofluorescence images and this enhancement could be what allows us to detect small amounts of SFG protein that is secreted by CLD1 in the absence of the interacting ligand.

*Development of protein trafficking controls and comparison of $M_1$ values*

We compared the $M_1$ values calculated for CLD1, 2, and 3 to those calculated from trafficking controls also expressed in parasites. As a control for apicoplast trafficking we expressed the signal sequence and transit peptide from ACP fused to SFG. This parasite line constitutively traffics SFG to the apicoplast. For a secreted trafficking control we expressed only the signal sequence from ACP fused to SFG. This parasite line constitutively secretes the SFG protein. Figure 4-5 A shows immunofluorescence images of both of the parasite lines that express these trafficking controls. We did two immunofluorescence assays for each of the trafficking controls and calculated $M_1$ values to analyze co-localization between the apicoplast marker ACP and the SFG protein ($M_1$ values for controls are graphed in Figure 4-5 B).

We compared the $M_1$ values calculated for the apicoplast trafficking control to those calculated for CLD1, 2, and 3 in the absence of Shield1. This comparison (Shown in Figure 4-6 A) revealed that CLD2 traffics SFG to the apicoplast at levels most similar to the

apicoplast trafficking control. As expected, CLD1 has the most leaky apicoplast trafficking and CLD3 traffics to the apicoplast at levels similar to CLD2. We also compared the $M_1$ values calculated for the secreted trafficking control to those calculated for CLD1, 2, and 3 in the presence of Shield1 (Also shown in Figure 4-6 A). The $M_1$ values calculated for CLD1 and 2 were not significantly different form the secreted trafficking control. Slightly higher $M_1$ values were calculated for CLD3 however, when compared to the secreted trafficking control.

The average $M_1$ values calculated for the apicoplast and secreted trafficking controls were used to normalize the $M_1$ values for CLD1, 2, and 3. We compared the normalized $M_1$ values for each CLD in the presence and absence of Shield1 in Figure 4-6 B. We calculated a 100 % decline in $M_1$ values after addition of Shield1 for the CLD2 trafficked protein. CLD1 had an 88 % decline and CLD3 had a 94 % decline in $M_1$ values after Shield1 was added to cell culture media.

Finally, we broke the normalized $M_1$ values down by developmental stage of the parasite in the red blood cell (ring, trophozoite, or schizont). We then analyzed protein trafficking for CLD1, 2, and 3 at each developmental stage in the presence and absence of Shield1 (Figure 4-7). We did not observe any strong trends of mislocalization at any specific stage of parasite development. There was a slight decline in $M_1$ values of schizonts for apicoplast trafficked CLD2 and 3 (- Shield1), which could be due to a smaller number of schizonts analyzed as compared to rings or trophozoites. Also, this decline in $M_1$ values of schizonts for CLD2 and 3 is not significantly different from the $M_1$ values calculated for schizonts from the apicoplast trafficking control parasite line.

*Further characterization of CLD2*

Based on our co-localization analysis, CLD2 traffics to the apicoplast and secreted compartment at levels most similar to the trafficking controls. This suggests that CLD2 has optimal trafficking characteristics to both compartments and may be ideal for use in future validation studies. We therefore, further characterized protein trafficking by CLD2. In Figure 4-8 A we analyzed cells treated with 500 nM Shield1 at an earlier time point and found that the decline in $M_1$ values is similar at 24 and 72 hours. We also looked at the effect of doubling the concentration of Shield1 on CLD2 secretion in Figure 4-8 B. There was no significant difference in the level of secretion at 500 nM and 1 μM Shield1. These studies suggest that the change in localization by CLD2 is reasonably complete after 24 hours of treatment with 500 nM Shield1.

**Analysis of stability of CLD1, CLD2, and CLD3**

We investigated the thermal stability of the CLD proteins to determine how stability of the CLD affects trafficking. Our hypothesis was that CLD1's leaky apicoplast trafficking phenotype, may be caused by a higher stability of the CLD1 protein compared to CLD2 or 3. We reasoned that a more stable CLD1 protein would be less able to mimic the unstructured feature of transit peptides. To investigate this hypothesis, we purified CLD1, 2, and 3 proteins for thermal shift assay analysis to determine the melting temperature of each protein.

We compared the melting temperature of the CLDs to the stable Shield1 binding FKBP mutant (sbFKBP). Our first observation from this experiment was that the destabilized CLD2 and CLD3 proteins could not be purified at concentrations high enough for thermal shift assays without adding Shield1 during protein purification. This suggests that CLD2 and 3 are more destabilized than CLD1 without a binding ligand. Because of this

feature of the purification process for these CLD proteins, only the assays done with Shield1 present are comparable. Table 4-1 shows that the melting temperatures of CLD2 and 3 are at least 3.8 °C less than the sbFKBP, while CLD1 is only 0.3 °C less. This confirms our hypothesis that CLD1 is more stable than CLD2 or 3. This analysis also revealed that the charge reversal mutation at residue six ($FKBP_{E6K}$) has a more destabilizing effect than the mutation at residue four ($FKBP_{Q4K}$) since $T_m$ values for sbFKBP and CLD1 are approximately equal and adding the Q4K mutation to CLD2 – to generate CLD3 – does not significantly change the melting temperature of the CLD.

In order to get an idea of whether the destabilized CLD proteins might be vulnerable to degradation, we compared their melting temperature to that of the published degradation domain FKBP mutant (dFKBP) [7]. dFKBP is destabilized without Shield1, which causes proteins tagged with dFKBP to be degraded. We purified dFKBP, and as discussed in Chapter 3, this protein could not be purified at high concentrations without adding Shield1 during protein purification. The difference in $T_m$ between dFKBP and sbFKBP was much larger than for any of the 3 CLDs. This suggests that the CLDs are unlikely to be degraded without Shield1 since they are at least 10 degrees more stable than the degradation domain and they are also trafficked through the secretory pathway where they do not interact with the proteasome in the cytosol.

**Analysis of sensitivity of CLD1, CLD2, and CLD3 to Shield1**

In our next set of experiments we titrated down the concentration of Shield1 to investigate the limit of sensitivity for each CLD. We added 5, 25, 125, or 500 nM Shield1 to cultures for 72 hours before live fluorescence imaging analysis. Because this experiment was done using live fluorescence imaging we did not calculate a quantitative number of parasites

with a secreted phenotype at each concentration but the images shown are representative images of the cells at each concentration. Figure 4-9 A shows that CLD1 was secreted at the lowest concentration of Shield1 added (5 nM Shield1). This is consistent with the thermal stability analysis from Table 4-1, showing that CLD1 is the most stable domain, and thus the most competent to bind Shield1 *in vivo*. CLD2 and 3 have similar levels of sensitivity to Shield1 and secrete some protein at concentrations as low as 25 nM (Figure 4-9 B and C). This is also consistent with thermal stability data showing that CLD2 and 3 have similar melting temperatures. CLD3 however, exhibits a partially secreted phenotype at 25 nM Shield1 while CLD2's secretion at this concentration is more complete. This slight difference between the responsiveness of CLD2 and 3 could be because of the difference in net positive charge near the N-terminus of the two proteins. Since CLD3 has a more positively charged N-terminus, it may be more inclined to traffic to the apicoplast in the presence of low concentrations of Shield1.

## CONCLUSIONS AND DISCUSSION

This chapter describes our characterization of the protein trafficking dynamics of CLD1, 2 and 3. Figure 4-10 summarizes the main analyses of CLD1, 2, and 3 that were presented in this chapter. The order of the domains in Figure 4-10 shows how the CLDs behaved relative to each other for each analysis. Co-localization analysis revealed that CLD1, 2, and 3 do not traffic equally well to the apicoplast and secreted compartments (co-localization data from figures 4-2, 4-3, 4-4, 4-5, and 4-6 is summarized Figure 4-10 A). Most notably, CLD1 has a leaky apicoplast trafficking phenotype that was observed as partial co-localization in immunofluorescence images and reflected in the lower $M_1$ values calculated

for CLD1 compared to CLD2 or 3. We investigated whether the leaky apicoplast trafficking phenotype of CLD1 is due to a higher level of protein stability compared to CLD2 or 3, by measuring the melting temperature of each CLD protein and comparing them to stable and unstable FKBP controls (thermal stability analysis from Table 4-1 is summarized in Figure 4-10 B). Our thermal stability analysis showed that CLD1 has a higher level of stability than CLD2 or 3 and supported our hypothesis that CLD1 may be too stable to be effectively trafficked to the apicoplast in the absence of Shield1.

We also analyzed Shield1 sensitivity for each CLD (sensitivity analysis from Figure 4-9 is summarized in Figure 4-10 C). This analysis showed that CLD1 is more sensitive to low concentrations of Shield1 than CLD 2 or 3. This is consistent with our thermal stability analysis because CLD1 is more stable than CLD2 or 3 and is likely more competent to bind Shield1 *in vivo*. Both CLD2 and 3 are less sensitive to low concentrations of Shield1 than CLD1. CLD2 has a limit of sensitivity around 25 nM, while CLD3 exhibited a partially secreted phenotype at 25 nM, and was fully secreted at 125 nM. The low sensitivity of CLD3 to Shield1 combined with the slightly higher $M_1$ values calculated for CLD3 in the presence of Shield1 (Figure 4-6 A) suggests that CLD3 may have a higher preference for trafficking to the apicoplast in the presence of Shield1 than CLD2. This difference in trafficking could be because of the higher net positive charge of CLD3 near the N-terminus - CLD3 has an increased net positive charge near the N-terminus of +3, while CLD2 only increases +2.

Because CLD2 exhibited the most efficient trafficking to the apicoplast and secreted compartments, and is sensitive to concentrations of Shield1 well below the 1μM inhibitory concentration, CLD2 is likely to be the optimal domain for use in most validation studies. CLD3 appears to have a slight preference toward trafficking to the apicoplast in the presence of low levels of Shield1, and is less sensitive to Shield1 than CLD2. These features put

CLD3 in second place behind CLD2, in terms of its attractiveness for use in validations studies of the conditional localization system. CLD1 has a leaky apicoplast trafficking phenotype and may be the least attractive candidate for some validation studies. CLD1 however, could be an ideal domain to tag exogenously expressed proteins that are not normally active in the apicoplast. Whenever a protein is over expressed in the apicoplast there is a risk that it will not be tolerated at high levels in the organelle due to its activity. Tagging an exogenously expressed protein with CLD1 could prevent the toxic effects of overexpression because the protein is not trafficked to the apicoplast as efficiently as it would be with CLD2 or 3. This puts CLD1 in a unique position to be useful in some overexpression studies that traffic proteins to the apicoplast in *P. falciparum*.

All of the features of CLD1, 2, and 3 evaluated in this chapter are useful to get an idea of how effectively each CLD traffics an ideal cargo protein, but they may vary in implementation studies with parasite proteins. Studies of FKBP fusion proteins have found that in general, C-terminal tags tend to destabilize FKBP[8]. The destabilizing effect of C-terminal fusions on the CLD should have a positive effect on the domain's ability to traffic to the apicoplast by allowing the domain to more closely mimic an unstructured apicoplast transit peptide. The positive effect of this destabilization is only useful however, if the CLD maintains the ability to bind Shield1 and change localization. The analysis of protein trafficking by CLD1, 2, and 3 described in this chapter are a useful guide for use of the domains but the size and stability of cargo proteins could cause trafficking dynamics of each CLD to vary slightly with different cargo proteins.

## METHODS

**Generation of plasmid constructs for expression of CLD1, 2, and 3 in *E. coli***

Plasmids used for protein expression in *E. coli* were generated by PCR amplifying the human FKBP gene with Shield1 binding mutation [7] using forward primers that contain nucleotide changes to produce lysine mutations at residues 4, 6, or both (to generate CLD1, 2 or 3 respectively). Fk4e6.EcoRI.LIC.for was used to generate CLD1, Fq4k6.EcoRI.LIC.for was used for CLD2, and Fkk.EcoRI.LIC.for was used for CLD3. One reverse primer (FKBP.P107L.HindIII.LIC.rev) was used to amplify the FKBP gene in all three reactions. PCR amplicons were then inserted into the pMALcHT [9] *E. coli* expression vector using ligase independent cloning with T4 DNA polymerase.

**Synchronization of parasites**

For experiments where parasites were synchronized, a homemade magnet with field strength of about 8,000 G was used to separate schizonts from mixed stage cultures. Briefly, a MACS LS Column (Miltenyi Biotec) was inserted into the homemade magnet and infected red blood cell culture was pipetted into the top of the column. When the column is attached to the magnet, schizonts stick to the magnetized beads while trophozoites and rings flow through. Schizonts were eluted from the column by taking it off of the magnet and running an additional 5 mL of media through the column.

**Statistical Analyses**

In experiments where only two groups were compared, we conducted the Mann-Whitney U test for analysis of non-normal, unpaired data sets. Comparisons of three or more groups were conducted using the Kruskal-Wallis one-way analysis of variance for non-

normal, unpaired data sets. For both of these analyses, tests were considered statistically significant if the P-value was less than 0.05.

- Immunofluorescence assays and live fluorescence imaging methods are the same as for Chapter 3.
- Thermal Shift Assays and protein purification methods are the same as for chapter 3.
- Parasite culture methods are the same as for Chapter 2.

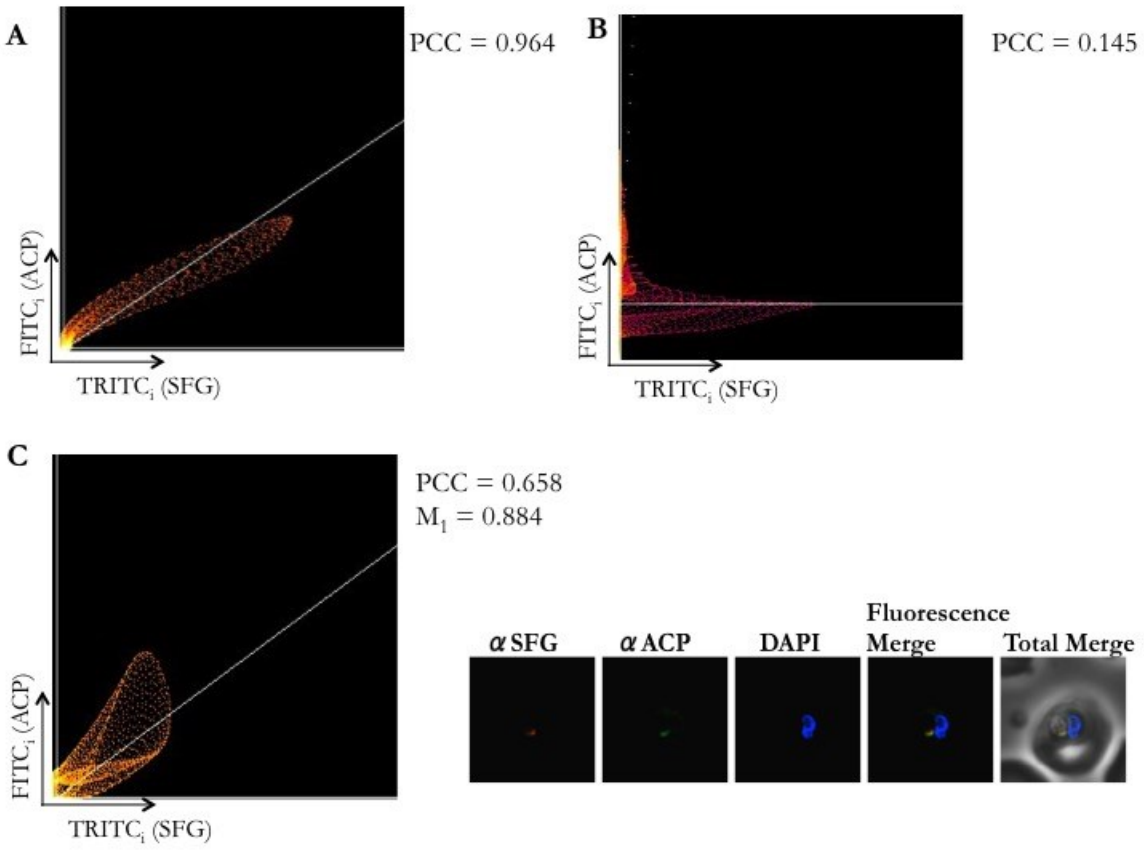


**Figure 4-1 Introduction to co-localization analysis**

A) Intensity scatter plot that represents an image of a cell with significant co-localization between ACP and SFG. The scatter plot shows a positive correlation between the two fluorochromes analyzed.

B) Intensity scatter plot that represents an image of a cell that does not have significant co-localization between ACP and SFG. The intensity scatter plot shows a lack of correlation between the two fluorochromes analyzed.

C) The intensity scatter plot was generated from the images to its right. The FITC channel has a higher average intensity than the TRITC channel and so the points on the scatter plot are skewed towards the FITC axis. The $M_1$ value for this image is higher than the PCC value because the $M_1$ calculation does not take average intensity into account. Microscopy images are 10μm long by 10μm wide.

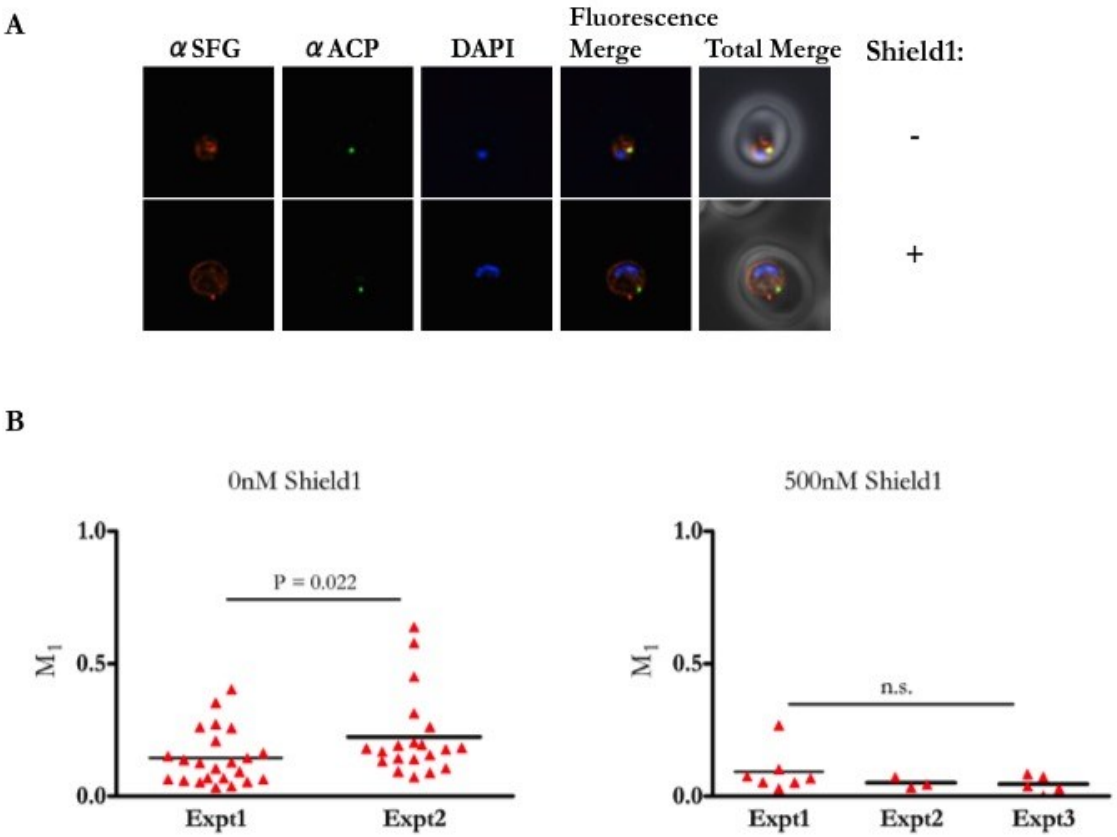


**Figure 4-2 Co-localization analyses for CLD1**

A) Immunofluorescence images of a transgenic parasite line that expresses CLD1 fused to SFG. The row labeled "-" shows a cell that has not been treated with Shield1 and the row labeled "+" shows a cell that was treated with 500 nM Shield1 for 72 hours before imaging. Images are 10 μm long by 10 μm wide.

B) Mander's Overlap Coefficients ($M_1$) were calculated for immunofluorescence images similar to the ones shown in in part A. At least two independent immunofluorescence assays were done in the absence (left side graph) or presence (right side graph) of Shield1 and the $M_1$ values were calculated for each cell.

The Mann-Whitney U test was used to compare the $M_1$ values from the two experiments done with 0 nM Shield1 and the Kruskal-Wallis one-way analysis of variance test was used to compare the three experiments done with 500 nM Shield1. Expt = Experiment

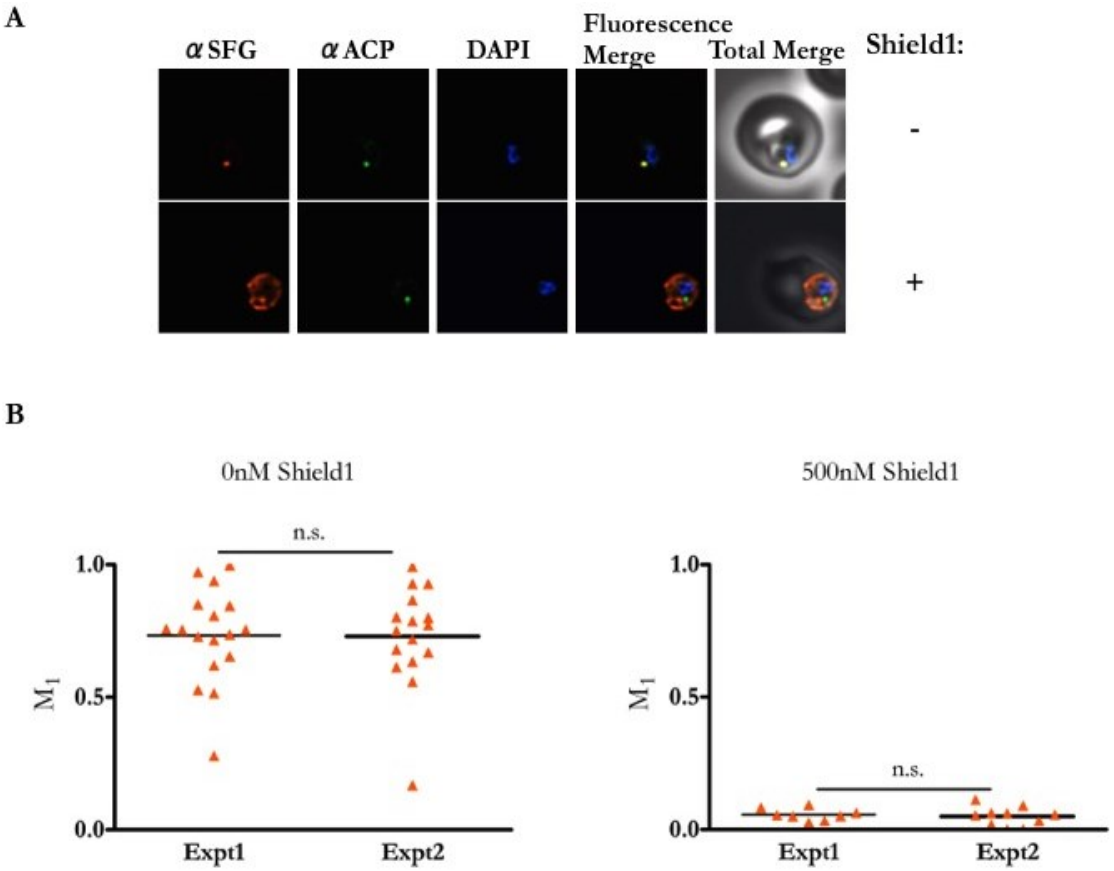


**Figure 4-3 Co-localization analyses for CLD2**

A) Immunofluorescence images of a transgenic parasite line that expresses CLD2 fused to SFG. The row labeled "-" shows a cell that has not been treated with Shield1 and the row labeled "+" shows a cell that was treated with 500 nM Shield1 for 72 hours before imaging. Images are 10 μm long by 10 μm wide.

B) Mander's Overlap Coefficients ($M_1$) were calculated for immunofluorescence images similar to the ones shown in in part A. At least two independent immunofluorescence assays were done in the absence (left side graph) or presence (right side graph) of Shield1 and the $M_1$ values were calculated for each cell.

The Mann-Whitney U test was used to compare the $M_1$ values.

Expt = Experiment

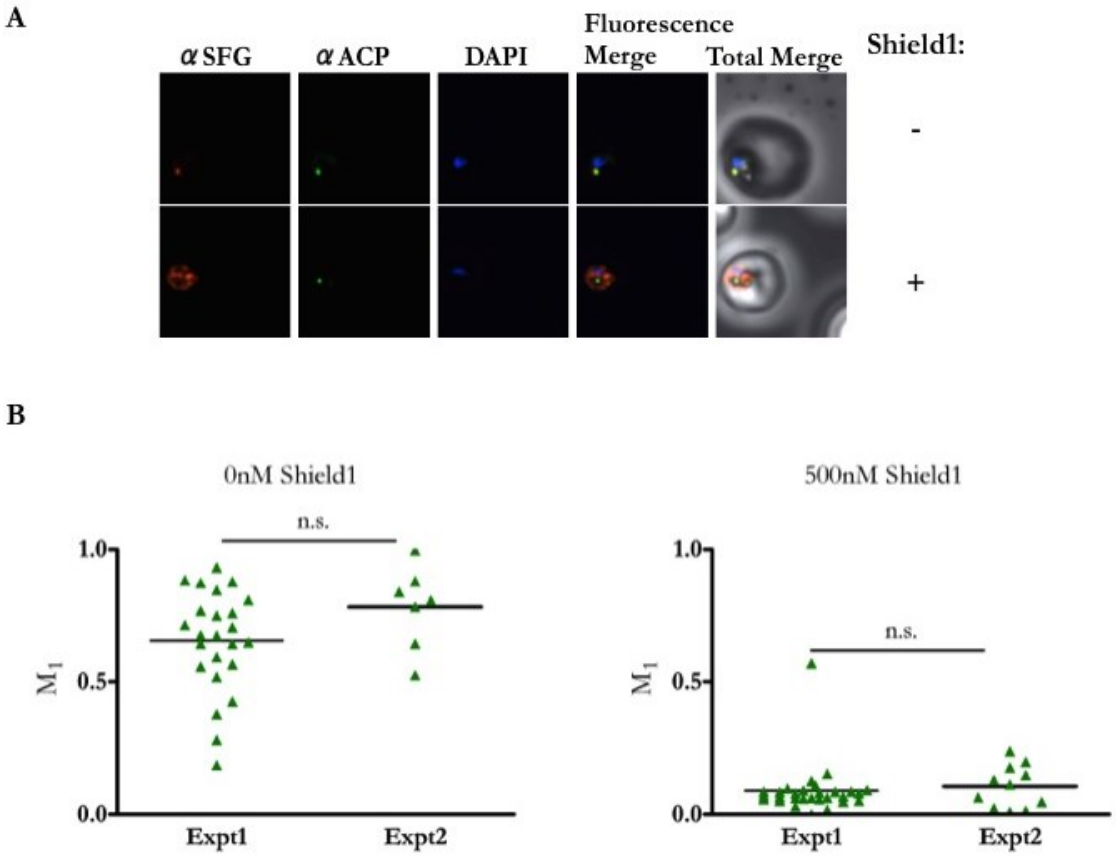


**Figure 4-4 Co-localization analyses for CLD3**

A) Immunofluorescence images of a transgenic parasite line that expresses CLD3 fused to SFG. The row labeled "-" shows a cell that has not been treated with Shield1 and the row labeled "+" shows a cell that was treated with 500 nM Shield1 for 72 hours before imaging. Images are 10 μm long by 10 μm wide.

B) Mander's Overlap Coefficients ($M_1$) were calculated for immunofluorescence images similar to the ones shown in in part A. At least two independent immunofluorescence assays were done in the absence (left side graph) or presence (right side graph) of Shield1 and the $M_1$ values were calculated for each cell.

The Mann-Whitney U test was used to compare the $M_1$ values.

Expt = Experiment

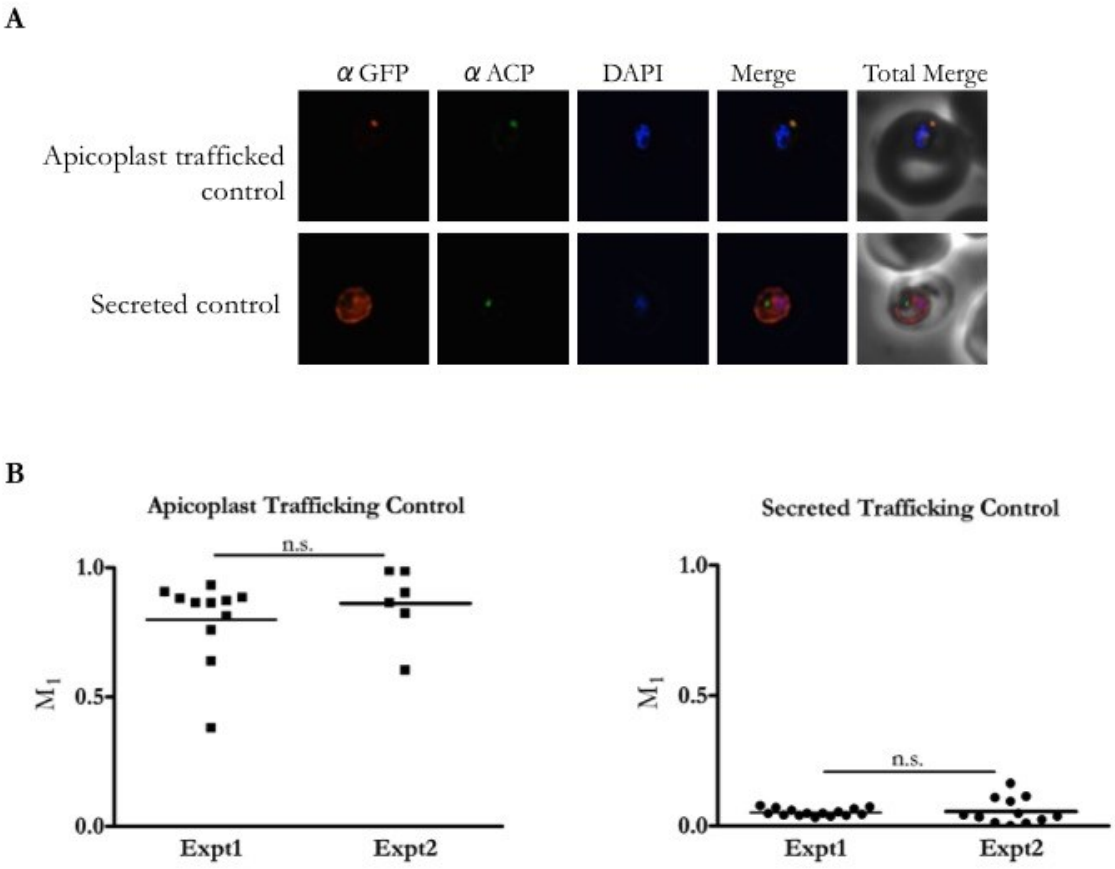


**Figure 4-5 Co-localization analyses for protein trafficking controls**

A) Immunofluorescence images of transgenic parasites that expresses a constitutively apicoplast trafficked SFG protein (top row) or a constitutively secreted SFG protein (bottom row). Images are 10 μm long by 10 μm wide.

B) Mander's Overlap Coefficients ($M_1$) were calculated for immunofluorescence images similar to the ones shown in part A. Two independent immunofluorescence assays were done for each control line and the $M_1$ values were calculated for each cell.

The average $M_1$ value for the apicoplast trafficking control is 0.821 and the average $M_1$ value for the secreted trafficking control is 0.053.

The Mann-Whitney U test was used to compare the $M_1$ values. Expt = Experiment

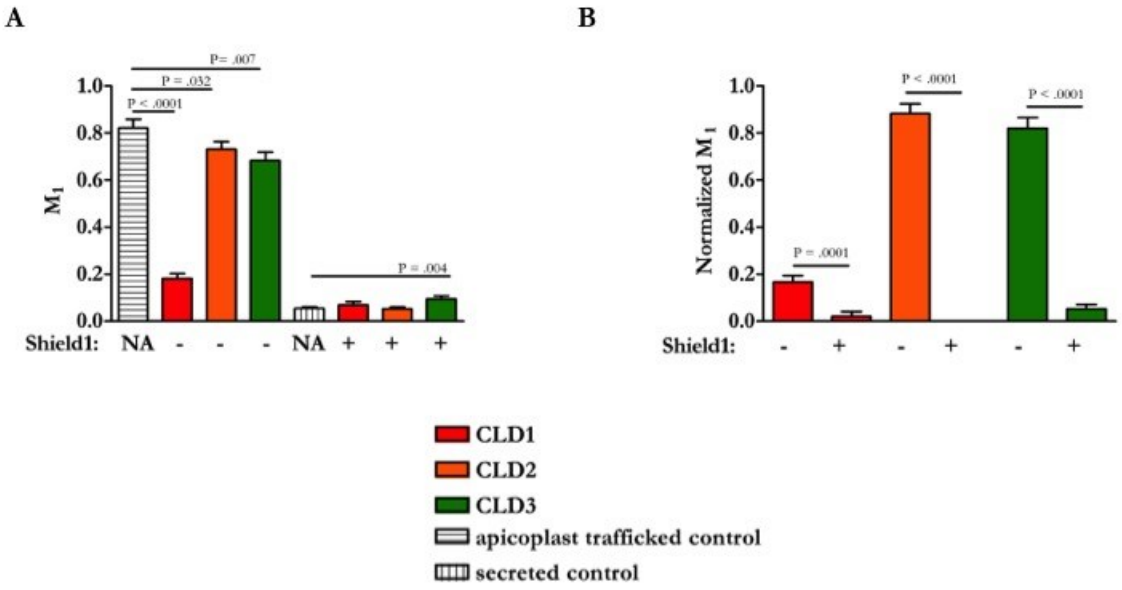


**Figure 4-6 Analysis of $M_1$ values for CLD1, 2, and 3, compared to control trafficking constructs**

A) The $M_1$ values calculated in the absence of Shield1 (- Shield1) for each CLD are compared to the apicoplast trafficking control (signal seq.$_{ACP}$-transit pep.$_{ACP}$-SFG) and the $M_1$ values calculated in the presence of Shield1 (+ Shield1) for each CLD are compared to the secreted trafficking control (signal seq.$_{ACP}$-SFG). The $M_1$ values for each CLD are compared to the appropriate control using the Mann-Whitney U test.

B) Normalized co-localization values calculated for each CLD in the absence of Shield1 or after addition of 500 nM Shield1. The CLD data are normalized to the average of $M_1$ values calculated for the trafficking controls presented in Figure 4-5. Normalized $M_1$ values are compared using the Mann-Whitney U test.

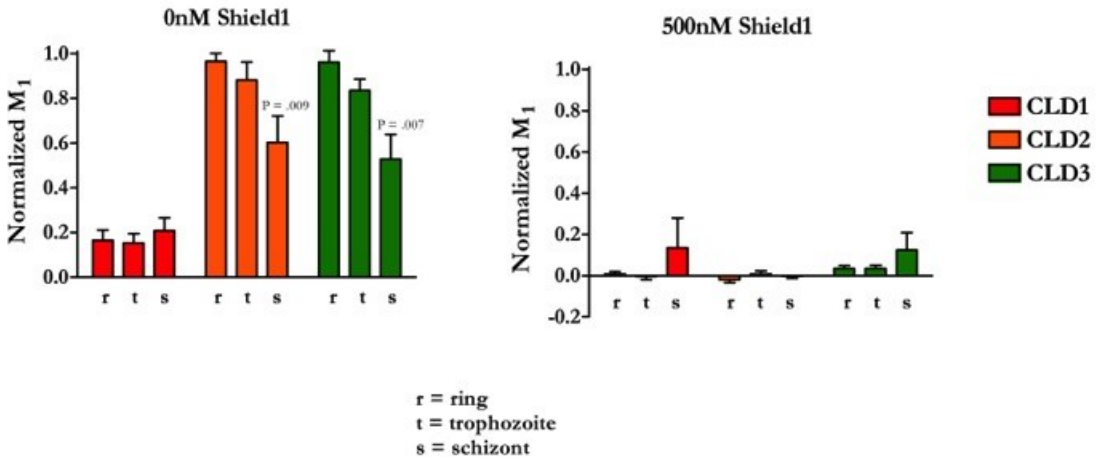


**Figure 4-7 Analysis of protein trafficking at each parasite developmental stage in the red blood cell**

The bar graph on the left compares apicoplast trafficking efficiency of each CLD at the ring, trophozoite, and schizont stage of development. There data are collected from cells that were not treated with Shield1 before imaging.

The bar graph on the right compares secreted trafficking efficiency at the ring, trophozoite, and schizont stage of development. There data are collected from cells that were synchronized and then treated with 500 nM Shield1 for 72 hours before imaging.

Both graphs show $M_1$ values for CLD1, 2, and 3 that have been normalized to the average $M_1$ values for trafficking controls presented in Figure 4-5. $M_1$ values are compared for rings, trophozoites, and schizonts using the Kruskal-Wallis one-way analysis of variance test.

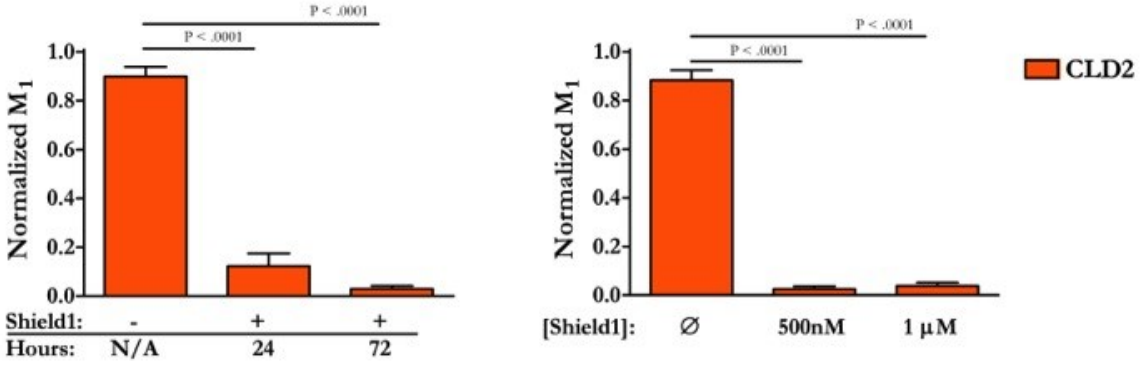


**Figure 4-8 Further analysis of the change in localization by CLD2**

The bar graph on the left shows the change in localization for CLD2 after 24 or 72 hours of treatment with 500 nM Shield1. The bar graph on the right shows the change in localization of CLD2 after 72 hours of treatment with 500 nM or 1uM Shield1. Cells were not synchronized for these experiments.

For both experiments, the cells were stained with antibodies to track the location of SFG and ACP using the same methods described for Figure 4-3a. Co-localization analysis was done to calculate $M_1$ values that were then normalized to the average $M_1$ values of the trafficking controls presented in Figure 4-5.

The Mann-Whitney U-test was used to compare the $M_1$ values for each of the test conditions (+ Shield1 samples) to untreated cells.

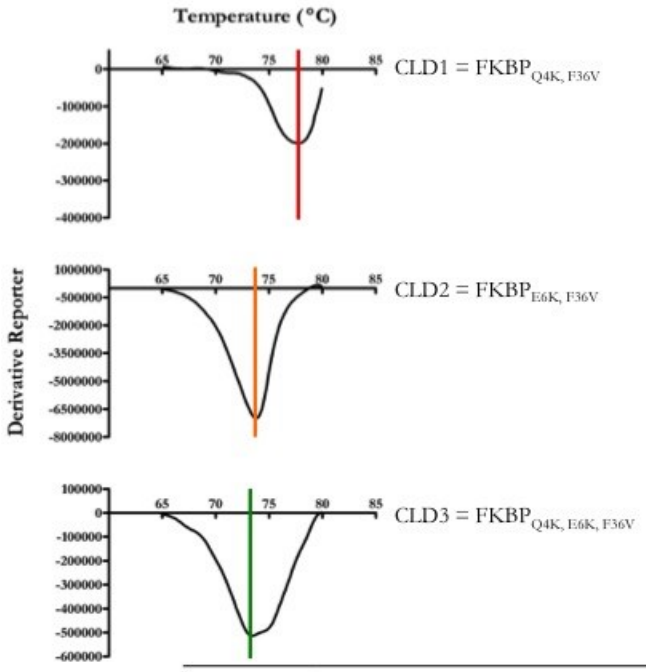


| | sbFKBP | CLD1 | CLD2 | CLD3 | dFKBP |
|---|---|---|---|---|---|
| - Shield1 | 54 ± 2.1 °C | – | – | – | – |
| + Shield1 | 77.5 ± 0.4 °C | 77.2 ± 0.9 °C | 73.7 ± 0.7 °C | 73.6 ± 1.2 °C | 62.9 ± 0.2°C |
| $\Delta T_m$ | – | -0.3°C | -3.8°C | -3.9°C | -14.6°C |

**Table 4-1 Thermal stability analysis of CLD1, 2, and 3**

Thermal shift assays were done to determine the melting temperature of purified proteins. The change in melting temperature ($\Delta T_m$) is calculated by subtracting the $T_m$ of CLD1, 2, 3 or dFKBP from the $T_m$ of sbFKBP. Melting temperatures are shown with standard deviations calculated from triplicate biological replicates.

Derivative reporter plots show representative data curves generated for each protein.

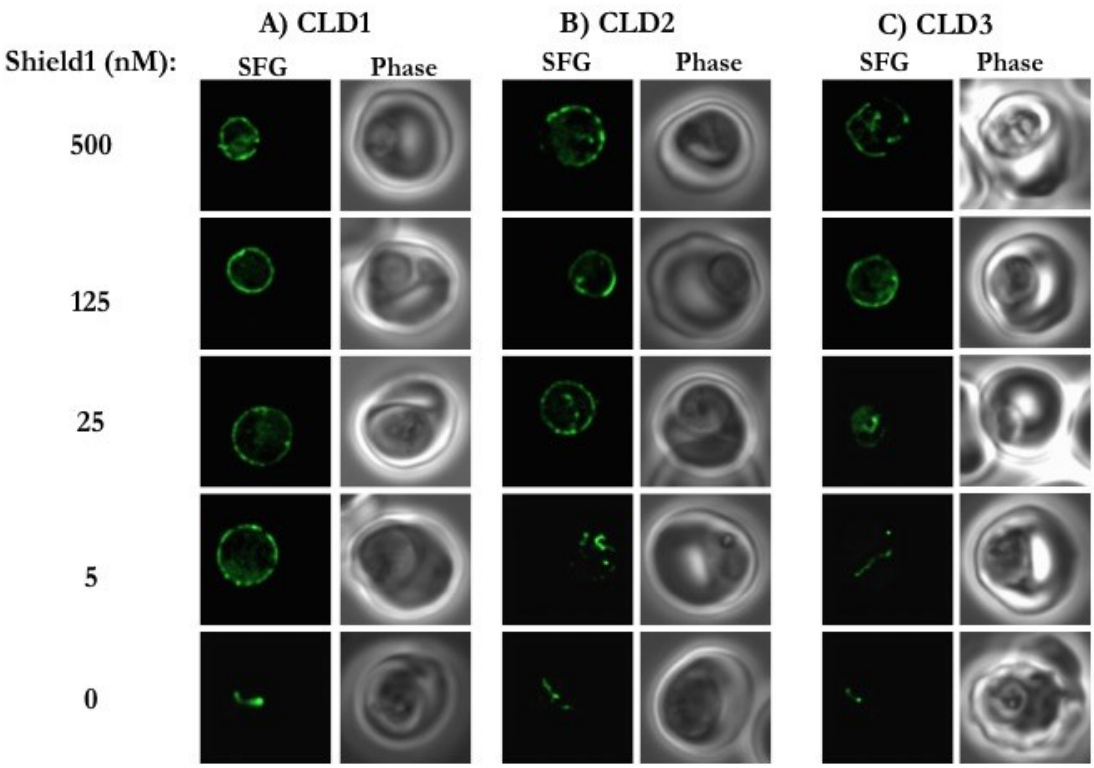


**Figure 4-9 Sensitivity analysis of CLD1, 2, and 3**

Live fluorescence images of CLD1 (a), CLD2 (b), and CLD3 (c) with varying concentrations of Shield1 added to the culture media. Shield1 was added at appropriate concentrations for 72 hours before imaging. Images are 10 μm long by 10 μm wide.

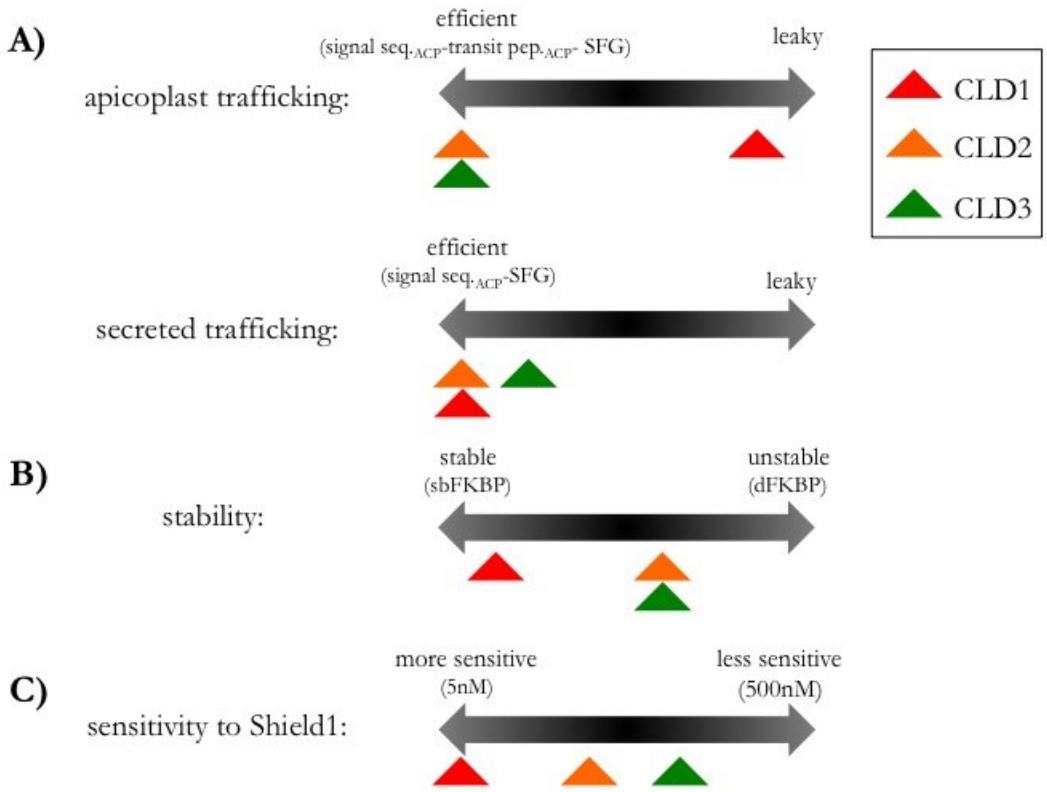


**Figure 4-10 Summary of the analyses of protein trafficking by CLD1, 2, and 3 presented in this chapter**

A) Apicoplast and secreted trafficking efficiency of each CLD is summarized. CLD2 and 3 traffic to the apicoplast at similar levels while CLD1 has a leaky apicoplast trafficking phenotype. CLD1 and 2 are secreted at similar levels in the presence of Shield1 while CLD3 is slightly less efficiently secreted in the presence of Shield1.

B) Thermal stability analysis of each CLD is summarized compared to stable and unstable FKBP controls. CLD2 and 3 are similarly destabilized while CLD1 is the most stable domain.

C) Analysis of the sensitivity of each CLD to concentrations of Shield1 below 500 nM is summarized. CLD1 was sensitive to the lowest concentrations of Shield1 tested (5 nM). CLD2 is sensitive to slightly higher concentrations (25 nM) and CLD3 was the least sensitive to Shield1 (125 nM).

| Primer name | Primer sequence |
|---|---|
| Fk4e6.EcoRI.LIC.for | CATCACCATCACGAATTCAAAAATCATATGGGAGTGAAGGTGGAAACCATC |
| Fq4k6.EcoRI.LIC.for | CATCACCATCACGAATTCAAAAATCATATGGGAGTGCAGGTGAAAACCATC |
| Fkk.EcoRI.LIC.for | CATCACCATCACGAATTCAAAAATCATATGGGAGTGAAGGTGAAAACCATC |
| FKBP.P107L.HindIII.LIC.rev | GCCAGTGCCAAGCTTCTATTCCAGTTTTAGAAGCTCCACATCGAAGACG |

**Table 4-2 Primers used to generate CLD1, 2, and 3 sequences for expression in *E. coli***

## REFERENCES


1. Schneider C a, Rasband WS, Eliceiri KW. NIH Image to ImageJ: 25 years of image analysis. *Nat Methods*. 2012;9(7):671-675. doi:10.1038/nmeth.2089.

2. Mcdonald JH, Dunn KW. Statistical tests for measures of colocalization in biological microscopy. *J Microsc*. 2013;252(3):295-302. doi:10.1111/jmi.12093.

3. Bolte S, Cordelieres FP. A guided tour into subcellular colocalisation analysis in light microscopy. *J Microsc*. 2006;224(3):213-232. doi:10.1111/j.1365-2818.2006.01706.x.

4. Manders EMM, Verbeek FJ, Aten JA. Measurement of co-localization of objects in dual-colour confocal images. *J Microsc*. 1993;169(3):375-382.

5. Rug M, Wickham ME, Foley M, et al. Correct Promoter Control Is Needed for Trafficking of the Ring-Infected Erythrocyte Surface Antigen to the Host Cytosol in Transfected Malaria Parasites. *Infect Immun*. 2004;72(10):6095-6105. doi:10.1128/IAI.72.10.6095.

6. Przyborski JM, Lanzer M. Protein transport and trafficking in *Plasmodium falciparum* -infected. *Parasitology*. 2005;130:373-388. doi:10.1017/S0031182004006729.

7. Armstrong CM, Goldberg DE. An FKBP destabilization domain modulates protein levels in *Plasmodium falciparum*. *Nat Methods*. 2007;4(12):1007-1009. doi:10.1038/nmeth1132.

8. Sekiguchi M, Kobashigawa Y, Kawasaki M, et al. An evaluation tool for FKBP12-dependent and -independent mTOR inhibitors using a combination of FKBP-mTOR fusion protein, DSC and NMR. *Protein Eng Des Sel*. 2011;24(11):811-817. doi:10.1093/protein/gzr045.

9. Muench S, Rafferty J, Mcleod R, Rice D, Prigge S. Expression, purification and Crystallization of the *Plasmodium falciparum* enoyl reductase. *Biol Crystallogr*. 2003;59:1246-1248.

# Chapter 5

# Validation of the Conditional Localization Domain by Tagging an Active Parasite Biotin Ligase

**ABSTRACT**

To validate our conditional localization system we tested whether two of the CLDs analyzed in Chapter 4 could control the localization of a *P. falciparum* biotin ligase called Holocarboxylase Synthetase 1 (HCS1) without interfering with the function of the enzyme.

HCS1 is primarily localized in the cytosol but was shown to be the main ligase responsible for biotinylating the apicoplast targeted Acetyl-Coenzyme A Carboxylase (ACC) in liver stage Plasmodium parasites. Blood stage parasites also express HCS1 in the cytosol but at this stage the ligase is not active against the ACC. In this study we used the CLD to conditionally express HCS1 in the apicoplast to determine if localization of HCS1 controls its activity in blood stage parasites. In order to avoid potentially toxic effects of HCS1 overexpression in the apicoplast we tagged HCS1 with CLD1, which has a leaky apicoplast trafficking phenotype. CLD1 was able to control the localization of HCS1 and HCS1 does not appear to be toxic in the apicoplast when trafficked by CLD1. We also showed that protein biotinylation in the apicoplast is controlled by altering the localization of HCS1 with Shield1. This experiment shows that CLD1 is able to control the localization of HCS1 without affecting its biotin ligase activity.

In our next experiment we investigated whether HCS1 activity in the apicoplast could activate downstream pathways, specifically the Type II Fatty Acid Synthesis (FAS II) pathway in the apicoplast. For this experiment we tagged HCS1 with CLD2, which traffics more efficiently to the apicoplast than CLD1. We confirmed that protein biotinylation in the apicoplast is also controlled in a ligand-dependent manner with the CLD2 tagged HCS1 protein (CLD2-HCS1). To detect FAS II pathway products we radiolabeled newly synthesized fatty acids in parasites using [1-$^{14}$C] -acetate and generated fatty acid methyl esters from parasite lysates that were analyzed by thin layer chromatography. We compared

fatty acid products produced by the CLD2-HCS1 expressing parasites in the absence and presence of Shield1 to products produced by the control parental parasite line and found no difference in fatty acids synthesized in any of the samples. This result suggests that HCS1 activity may not be sufficient to activate the FASII pathway in blood stage parasites. Alternatively, [1-$^{14}$C]-acetate may not be effectively absorbed into the apicoplast and this could also explain why we don't see a difference in FAS II pathway activity.

The validation experiments in this chapter demonstrate the full functionality of the conditional localization domain developed in this thesis. These CLDs may be used to tag other proteins of interest in future experiments and answer questions about apicoplast biology.

## INTRODUCTION

We validated the conditional localization system by tagging an exogenous copy of the biotin ligase, Holocarboxylase Synthetase 1 (HCS1; PlasmoDB PF3D7_1026900). We chose this enzyme for our validation experiments because of previous studies in our lab that investigated the role of HCS1 in fatty acid metabolism. Fatty acids that are obtained from the host cell or synthesized *de novo* are important at all stages of the parasite life cycle to support the formation of membranes at morphologically and biochemically distinct stages[1–3]. *P. falciparum* has a Type II Fatty Acid Synthesis (FAS II) pathway located in the apicoplast and a fatty acid elongation pathway in the endoplasmic reticulum. Unlike *Toxoplasma gondii* – a related apicomplexan parasite – *Plasmodium falciparum* do not contain a Type I Fatty Acid Synthesis pathway in the cytosol[4]. (Figure 5-1 summarizes fatty acid synthesis and elongation pathways in *P. falciparum*) Previous studies from our group and others have shown that

HCS1 biotinylates the Acetyl-Coenzyme A Carboxylase (ACC). The ACC is a biotin dependent enzyme that performs the rate-limiting step in initiation of the FASII pathway. The ACC converts Acetyl-Coenzyme A (Acetyl-CoA) into malonyl-Coenzyme A (malonyl-CoA), which is tethered to the Acyl Carrier Protein (ACP) and extended by the FASII elongation enzymes to generate long chain fatty acids. Our lab found that HCS1 activity is important for the initiation of fatty acid synthesis and normal liver stage parasite development but HCS1 is not active against the ACC in blood stage parasites[5]. Additionally, studies from other groups have shown that fatty acid synthesis is essential for parasite progression from liver to blood stage but it is not essential for continuation of the erythrocytic cycle[3,6].

Localization studies of HCS1 and the ACC showed that in liver and blood stage parasites HCS1 is primarily localized in the cytosol, while the ACC is trafficked to the apicoplast. HCS1 and the ACC are not expected to meet at any point during trafficking to their separate compartments in blood stage parasites and so we reasoned that some method of alternative trafficking must allow HCS1 to encounter and activate the ACC in the liver stage but not the blood stage. We therefore hypothesized that differential localization of HCS1 and the ACC during the blood stage of parasite development might control activity of HCS1 and possibly also activation of the downstream FASII pathway. To investigate this hypothesis we tagged an exogenous copy of HCS1 with the CLD to allow us to express HCS1 in the apicoplast of blood stage parasites in a ligand dependent manner.

We first investigated whether HCS1 activity in the apicoplast is dependent on the localization of the enzyme by using the CLD1 tag to conditionally express HCS1 in the apicoplast. We used anti-biotin antibodies to probe for biotinylation activity in the apicoplast of parasites expressing CLD1 tagged HCS1(CLD1-HCS1). We detected biotinylation of

apicoplast resident proteins in the absence of Shield1, and this activity was removed by adding Shield1 to cell culture media to change the localization of HCS1.

In our next experiment we wanted to determine if activation of biotinylation in the apicoplast of blood stage parasites was sufficient to activate the FASII pathway. We generated an independent transgenic parasite line that expresses HCS1 fused to CLD2 (CLD2-HCS1). To assay for FASII pathway activity we radiolabeled newly synthesized fatty acids in the CLD2-HCS1 expressing parasite line. We expected that because CLD2 traffics to the apicoplast more efficiently than CLD1, using the CLD2-HCS1 parasite line in these experiments would improve our chances of detecting FASII pathway products. We confirmed that CLD2 is able to control the localization and activity of HCS1 in blood stage parasites in a similar manner to CLD1 and proceeded to radiolabel (with [1-$^{14}$C]-acetate) newly synthesized fatty acids in the presence and absence of Sheild1. We hypothesized that we might see different lengths of fatty acid products in samples that have not been treated with Shield1 if HCS1 activity in the apicoplast is sufficient to activate the FASII pathway. We did not however, detect any differences in fatty acids produced in parasites with HCS1 active in the apicoplast (- Shield1) compared to those that did not have HCS activity in the apicoplast (+ Shield1) or the parental parasite line.

These experiments show that controlling the localization of HCS1 with CLD1or 2 can control the activity of this enzyme. We were not able to detect activation of the downstream FASII pathway in parasites with an active HCS1 in the apicoplast using radiolabeled acetate. This suggests that there may be other factors limiting the activation of the FASII pathway in blood stage parasites or that acetate does not enter the apicoplast. These studies however, have shown that the CLD can be used to control the location and

activity of a parasite enzyme. This provides proof of principle for future studies that will use the CLD to investigate other proteins of interest in the parasite.

## RESULTS

### Validation of CLD1 by tagging the biotin ligase HCS1

*Analysis of protein trafficking*

Previous attempts in our lab to constitutively traffic HCS1 to the apicoplast from a high strength overexpression promoter (the *P. falciparum* Calmodulin promoter) failed and so we suspected that HCS1 might be toxic in the apicoplast compartment. For our experiments we switched to a lower strength promoter (the *P. falciparum* ribosomal L2 protein promoter) to express HCS1 fused to CLD1. We chose CLD1 because it has a leaky apicoplast trafficking phenotype and we reasoned that expressing HCS1 from a lower strength promoter, trafficked by a low efficiency CLD, could allow this ligase that is not normally expressed in the apicoplast compartment to be better tolerated by the cell.

We analyzed protein trafficking in live fluorescence images of cells expressing CLD1 tagged HCS1 (CLD1-HCS1; protein expression construct is diagramed in the top part of Figure 5-2). In the absence of Shield1 ("- Shield1" rows in Figure 5-2) we observed a trafficking pattern that is characteristic of apicoplast localization at each stage in parasite development in the red blood cell. In the ring stage the apicoplast is a single dot-like organelle that is located on the edge of the cell, in the trophozoite stage the apicoplast branches out, and in the schizont stage the apicoplast divides into multiple daughter organelles that get packaged into each new merozoite. When we added Shield1 to cell culture media ("+ Shield1 rows in Figure 5-2), the CLD1-HCS1 protein changes localization to

become secreted from the cell at all three stages of parasite development. The secreted protein accumulates in the parasitophorous vacuole space that separates the parasite from the red blood cell cytosol. In later stages (trophozoites and schizonts) some of the protein also appears to be taken back into the cell and accumulates in the digestive vacuole. This trafficking pattern of accumulation in the digestive vacuole as well as the parasitophorous vacuole after the addition of Shield1 to cell culture media was also observed for the CLD1 test construct described in Chapter 3 (Figure 3-4).

We confirmed the trafficking patterns observed in Figure 5-2 by staining cells in immunofluorescence assays with antibodies to track the location of the CLD trafficked HCS1-SFG protein and the apicoplast marker ACP (Figure 5-3 A). The top row in Figure 5-3 A shows cells that have not been treated with Shield1; under this condition the SFG protein partially co-localizes with ACP. Some of the HCS1-SFG protein also accumulates in the parasitophorous vacuole space. This trafficking pattern is consistent with the leaky apicoplast trafficking phenotype previously described for CLD1. When we added 500 nM Shield1 to cell culture media for 72 hours, we no longer observed significant co-localization between the ACP and SFG proteins (Figure 5-3 A bottom row). After Shield1 is added to cell culture media the SFG signal accumulates outside the cell in the parasitophorous vacuole space. Some protein is also observed inside the cell but not co-localized with ACP and is presumably en route to be secreted from the cell.

To quantitatively analyze the level of co-localization between SFG and ACP in immunofluorescence images, we calculated the Mander's Overlap Coefficient ($M_1$ is described in detail in Chapter 4) to determine the fraction of SFG intensities that overlap with ACP in the presence or absence of Shield1 (Figure 5-3 B). In the absence of Shield1 we observed partial co-localization between SFG and ACP in immunofluorescence images

(Figure 5-3 A) and consistent with this observation, we also calculated higher $M_1$ values for these cells compared to cells that were treated with Shield1 (Figure 5-3 B). The $M_1$ values calculated from immunofluorescence images of cells treated with Shield1 declined significantly (Figure 5-3 B), indicating that the HCS1-SFG protein is secreted from the cell and no longer traffics to the apicoplast. These analyses of protein trafficking in live (Figure 5-2) and fixed (Figure 5-3) cell samples show that CLD1 is able to control the localization of the HCS1-SFG cargo protein.

*Analysis of biotinylation activity*

In our next experiment we investigated whether localization of HCS1 controls its activity. HCS1 has only one predicted target protein in the parasite, which is the ACC. The ACC is an apicoplast resident protein and so we expected to observe biotinylation activity when HCS1 is trafficked to the apicoplast (- Shield1) and no activity in the apicoplast when HCS1 is removed (+ Shield1). We assayed for biotinylation activity in the apicoplast by staining cells in immunofluorescence assays with antibodies against biotin and the apicoplast marker ACP. The top row in Figure 5-4 shows that when HCS1 is trafficked to the apicoplast (- Shield1) we detect biotinylation activity that co-localizes with the apicoplast marker protein (ACP). This activity is absent when we change the localization of HCS1 by adding Shield1 to cell culture media. In the bottom 2 rows of Figure 5-4, cells have been treated with 500 nM Shield1 for 72 hours before immunofluorescence analysis. We did not detect biotinylation in the apicoplast of samples treated with Shield1. The image in the third row in Figure 5-4 is the same cell in the second row but the FITC channel has been brightened to show that there is no detectable enhancement of biotinylation signal above background in the apicoplast organelle.

This analysis shows that altering the localization of HCS1 can control the activity of the enzyme. When we traffic HCS1 to the apicoplast using CLD1 it is able to biotinylate an apicoplast resident protein that is presumably the ACC. In our next study we investigated whether HCS1 activity in the apicoplast is sufficient to activate the downstream FASII pathway. We reasoned that to improve our chances of detecting FASII pathway activity in parasites we should tag HCS1 with a CLD that traffics more efficiently to the apicoplast organelle. For this study we generated a second parasite line that expresses an exogenous copy of HCS1 tagged with CLD2 instead of CLD1.

**Validation of CLD2 by tagging the biotin ligase HCS1**

*Analysis of protein trafficking*

We generated a transgenic parasite line that expresses the HCS1 biotin ligase fused to CLD2 (CLD2-HCS1; protein expression construct is diagramed in top part of Figure 5-5) and analyzed protein trafficking in live fluorescence images of this cell line. In the absence of Shield1 ("- Shield1" rows in Figure 5-5) we observed a trafficking pattern that is consistent with apicoplast trafficking at all three stages of parasite development in the red blood cell (typical apicoplast trafficking characteristics were reviewed in the previous section and described in detail in Chapter 1). When Shield1 was added to cell culture media ("+ Shield1" rows in Figure 5-5) we observed a change in SFG localization as the HCS1-SFG protein is secreted from the cell and accumulates in the parasitophorous vacuole space. We also observed some protein that is taken back into the cell's digestive vacuole after secretion, which is consistent with our previous analysis of CLD2 trafficking in the presence of Shield1 described in Chapter 3 (Figure 3-5).

We confirmed the trafficking patterns observed in live fluorescence images of the CLD2-HCS1 parasite line by staining cells in immunofluorescence assays. We analyzed localization of the CLD2 trafficked HCS1-SFG and the apicoplast marker ACP. Figure 5-6 A shows representative images from our analysis of cells left untreated ("- Shield1") or treated with 500 nM Shield1 for 72 hours before analysis ("+ Shield1"). In the absence of Shield1 we observed co-localization between ACP and SFG (Figure 5-6 A top row). When we added Shield1 to cell culture media we no longer detect significant co-localization between ACP and SFG and the SFG protein is accumulated in the parasitophorous vacuole space (Figure 5-6 A bottom row).

We quantified the level of co-localization between ACP and SFG by calculating $M_1$ values ($M_1$ is a colocalization statistic that was described in detail in Chapter 4) for each cell analyzed in immunofluorescence assays done in the absence or presence of Shield1. The bar graph in Figure 5-6 B shows that in the absence of Shield1 the $M_1$ values are higher, indicating that CLD2 traffics the HCS1-SFG protein to the apicoplast. When we treated cells with Shield1 we observed a decline in co-localization between ACP and SFG as the CLD2 tag causes HCS1-SFG to be secreted from the cell. The average $M_1$ value calculated for the CLD2-HCS1 line in the absence of Shield1 is higher than the average $M_1$ value calculated for the CLD1-HCS1 line. This confirms that CLD2 traffics HCS1 to the apicoplast more efficiently than CLD1.

*Analysis of biotinylation activity*

In our next experiment we confirmed that controlling the localization of HCS1 with CLD2 controls the activity of the ligase – as was observed with CLD1. We assayed for biotinylation activity in the apicoplast by staining cells in immunofluorescence assays with a

streptavidin-FITC molecule and antibodies against the apicoplast marker ACP. Figure 5-7 shows that when HCS1 is trafficked to the apicoplast ("- Shield1", top row) we can detect biotinylation activity that co-localizes with the apicoplast. This is presumably biotinylation of the ACC, since the ACC is the only known target of HCS1 in the apicoplast. When we added Shield1 to cell culture media to change the localization of HCS1 (Figure 5-7 bottom two rows), the biotinylation activity is removed from the apicoplast organelle. The third row in Figure 5-7 is the same cell as in the second row, except the FITC channel has been brightened to show that there is no detectable enhancement of biotinylation signal in the apicoplast.

Our analysis of biotinylation activity in the CLD1-HCS1 and CLD2-HCS1 expressing parasite lines (Figure 5-4 and 5-7) shows that altering the localization of HCS1 using Shield1 can control HCS1 activity in the apicoplast. Since CLD2 traffics HCS1 to the apicoplast more efficiently than CLD1 and does not interfere with the biotin ligase activity of HCS1, we proceeded with studies to investigate whether the downstream FASII pathway is activated when an active HCS1 enzyme is trafficked to the apicoplast by CLD2.

*Analysis of FASII pathway activity*

We assayed for FASII pathway activity in the CLD2-HCS1 parasite line by labeling newly synthesized fatty acids with [1-$^{14}$C]-acetate. We hypothesized that the labeled acetate could be converted to acetyl-CoA by the parasites and serve as a substrate for the FASII pathway in the apicoplast (Figure 5-8 shows a model of how [1-$^{14}$C]-acetate might label FASII pathway products in the parasite). After 24 hours of labeling with [1-$^{14}$C]-acetate we lysed the parasites, extracted fatty acids, and generated fatty acid methyl esters (FAMEs) to resolve on a high performance thin layer chromatography (HPTLC) silica gel. The gel was

exposed to an imaging plate and then imaged on a phosphoimager to detect radiolabeled fatty acid species.

For this experiment we labeled the CLD2-HCS1 parasite line in the presence and absence of Shield1 and also a control parental parasite line (dd2attB) that does not express an exogenous copy of HCS1. Figure 5-9 (left side) shows the FAME species detected on the imaging plate after one week of exposure to the HPTLC gel. The same FAME species are detected in the dd2attB control parasites as in the CLD2-HCS1 parasite lines with 0 or 500 nM Shield1 added to cell culture media. The difference in intensity of the FAME species generated in each sample is likely because of the slightly different final parasitemias reached by each culture after three days of incubation in the presence or absence of Shield1 and then 24 hours of radiolabeling.

Previous studies have shown that in parasites that lack a critical enzyme for FASII pathway activity – a FabI knock out parasite line – C16 and C18 are still synthesized, presumably through the fatty acid elongation pathway in the endoplasmic reticulum[3]. All of the FAME species detected in the CLD2-HCS1 samples are likely synthesized by the fatty acid elongation pathway since they are also present in the parental parasite strain sample which does not have an active FASII pathway. Flux though the fatty acid elongation pathway could mask low levels of FASII pathway activity in the '- Shield1' CLD2-HCS1 sample. To address this concern we exposed the HPTLC gel to the imaging plate for an additional two and a half months (Figure 5-9 right side) to try to detect low levels of FASII pathway products. We did not however see any difference in fatty acid products produced after this longer exposure compared to the one-week exposure.

## CONCLUSIONS AND DISCUSSION

Previous studies from our lab have shown that HCS1 is active in the apicoplast of liver stage parasites[5]. HCS1 biotinylates the ACC which then generates substrates for fatty acid synthesis that are essential for normal liver stage parasite development [3,5–7]. In blood stage parasites HCS1 is not active and studies have shown that fatty acid synthesis is dispensable at this stage of parasite development[3,5]. Localization studies of HCS1 and its substrate, found that in both liver and blood stage parasites the ACC is trafficked to the apicoplast while HCS1 is primarily cytosolic. We hypothesized that differential HCS1 localization in blood stage parasites might control its activity. We reasoned that since HCS1 does not encounter the ACC in blood stage parasites it is inhibited form activating the ACC and initiating FASII pathway activity. We tagged HCS1 with the CLD to test if changing the localization of HCS1 so that it encounters the ACC in blood stage parasites is sufficient to allow HCS1 to biotinylate the ACC and activate fatty acid synthesis at this stage.

Both CLD1 and CLD2 were able to control the localization of HCS1 (Figures 5-2, 5-3, 5-5, and 5-6) and independently confirm that altering the localization of HCS1 can control its activity in blood stage *P. falciparum*. HCS1 is active against an apicoplast-targeted substrate that is presumably the ACC, and this activity is removed when HCS1 is removed from the apicoplast (Figures 5-4 and 5-7). We tested whether HCS1 activity was sufficient to activate the FASII pathway by radiolabeling fatty acids in parasites that express HCS1 in the apicoplast (- Shield1) or secreted compartments (+ Shield1). We found no difference in fatty acid species produced in parasites that had an active HCS1 enzyme in the apicoplast compared to those in which the enzyme was secreted (Figure 5-9). This result could indicate that [1-$^{14}$C]-acetate is not effectively taken into the apicoplast. Studies in trypanosomes – another protozoan parasite – found that [1-$^{14}$C]-acetate had a lower capacity for cellular

uptake compared to pyruvate or glucose[8]. Future experiment with this parasite line could attempt to label fatty acids with glucose instead of acetate. Figure 5-8 shows how glucose could also be used to label FASII pathway products in *P. falciparum*. Briefly, in the cytosol glucose is converted into phosphoenolpyruvate (PEP), which can be taken into the apicoplast via a membrane transporter (the PEP/phosphate translocator; PPT)[9]. PEP is converted to pyruvate, which is used to generate the substrate for the ACC, acetyl-CoA[7,10].

A third experiment that could detect FASII pathway activity and does not rely on metabolic labeling is to pull down the Acyl-Carrier Protein (ACP). ACP anchors the growing fatty acid chain during the elongation cycle of fatty acid synthesis[7]. We expect that if we pull down the ACP in parasites that have HCS1 expressed in the apicoplast – and the FASII pathway is active – we should be able to detect fatty acids attached to the protein using mass spectrometry. In parasites that have HCS1 secreted from the cell (+ Shield1) or the parental parasite strain, we expect that we would not detect fatty acids attached to ACP since the FASII pathway is not thought to be active in blood stage parasites when HCS1 is not trafficked to the apicoplast.

An alternative explanation for the lack of FASII pathway activity detected in Figure 5-9 is that HCS1 activity alone is not sufficient to activate the downstream FASII pathway. Several other enzymes and substrates are required for activation of the FASII elongation cycle and we cannot rule out the possibility that there are other rate limiting steps that prevent FASII from being activated in blood stage parasites. Although the question of whether HCS1 activity in the apicoplast is sufficient to activate the FASII pathway could be further investigated in future experiments, this study has met the goal of validating the conditional localization system developed in this thesis. In this chapter we showed that the CLD could be used to control the activity of a parasite protein (HCS1) without interfering

with the function of the enzyme (biotinylation activity). This study sets the stage for future experiments in our lab that will use the CLD to investigate the function of other parasite proteins.

## METHODS

### Generation of plasmid constructs for parasite expression of CLD1-HCS1 and CLD2-HCS1

The HCS1 gene was amplified from plasmid DNA [5] using BsrG1.HCS10.for and BsiWI.HCS10.rev (Table 5-1) and digested with BsiWI and BsrGI. pRL2 parasite expression vectors described in Chapter 3 to express CLD1 and CLD2 were then also digested with BsiWI. The HCS1 gene was ligated into the CLD1 and CLD2 vectors for parasite expression using Quick Ligase (New England BioLabs). DNA sequences were confirmed by sequencing after insertion.

### Anti-biotin and Streptavidin-FITC Immunofluorescence Assays

Microscope slides were set up for immunofluorescence assays by drawing wells on the slide with a Super Pap Pen Liquid Blocker (Ted Pella, inc.). A .01 % poly-L-Lysine solution (Sigma-Aldrich) in water was added to each well and allowed to dry for at least 30 minutes. 300µl of parasite culture was then spun down and resuspended in an equal volume of fixative (4 % paraformaldehyde and .0075 % glutaraldehyde in PBS). Cells were added to each well on the slide and then incubated for 30 minutes at room temperature. After incubation, fixed cells were permeabilized by incubation in 1 % Triton for ten minutes. The samples were then reduced by incubation in 100 µg/ml $NaBH_4$ for 10 minutes. Next the cells

were incubated in blocking solution (3 % BSA in PBS) for two hours. Before applying primary antibodies cells were washed in PBS and then incubated with appropriate antibodies at 4°C. For anti-biotin IFA experiments, cells were left in primary antibodies over the weekend and if streptavidin-FITC was used the cells were left in the primary antibody overnight. [Rabbit polyclonal αACP 1:500, raised against the *P. falciparum* antigen; monoclonal mouse αBiotin 1:50(Sigma)]. Cells were then washed three times in PBS and then once in 3 % BSA. Appropriate secondary antibodies [goat αrabbit AlexaFluor 594 1:1000 (Life Technologies); goat αmouse AlexaFluor 488 1:1000 (Life Technologies)] or streptavidin-FITC reagent (1:50) was added to cells and incubated for 2 hours in the dark at room temperature. Finally cells were washed in PBS three times and sealed with ProLong Gold antifade reagent with DAPI (Life Technologies) under a coverslip sealed with nail polish. Slides were allowed to sit overnight at room temperature before imaging analysis on the Zeiss AxioImager M2 microscope.

**[1-$^{14}$C]-acetate labeling and extraction/generation of FAMEs**

After 3 days of culture in 0 nM or 500 nM Shield1, parasites were synchronized using a magnetic column (as previously described in Chapter 4) and 50 μCi of [1-$^{14}$C]-acetate was added to 5mL of cell culture media. Parasite were allowed to grow in the presence of radiolabeled acetate for 24 hours before cell pellets were collected, snap frozen in liquid nitrogen and stored in the -80 °C freezer overnight.

The next day the cells were saponin lysed in 0.05 % saponin and washed in Phosphate Buffered Saline twice. Parasite pellets were then resuspended in 400μl 5M KOH/10 % Methanol and heated at 80 °C for one hour to extract free fatty acids. 400 μL of 5M $H_2SO_4$ was added to the solution and fatty acids were extracted using 1 mL of Hexane.

Fatty acids were evaporated under Nitrogen gas and then dissolved in 750 µl 1.25 M methanolic HCl and heated for 1 hour at 80 °C. 750 µl 0.15 M NaCl was added to the solution and FAMEs were extracted using hexane and evaporated under nitrogen gas again. The FAMEs were finally resuspended in 50 µl chloroform and resolved on a HPTLC-RP18 reversed phase unibond octadecyl modified silica gel using 5:15:1 $CHCl_3$: MeOH : $H_2O$. Radiolabeled FAME product were exposed to an imaging plate for 1 week or 2.5 months and then imaged using a phosphoimager.

- All other immunofluorescence assays and live fluorescence imaging methods are the same as for Chapter 3.
- Parasite culture methods are the same as for Chapter 2.
- Statistical analysis methods are the same as for Chapter 4.

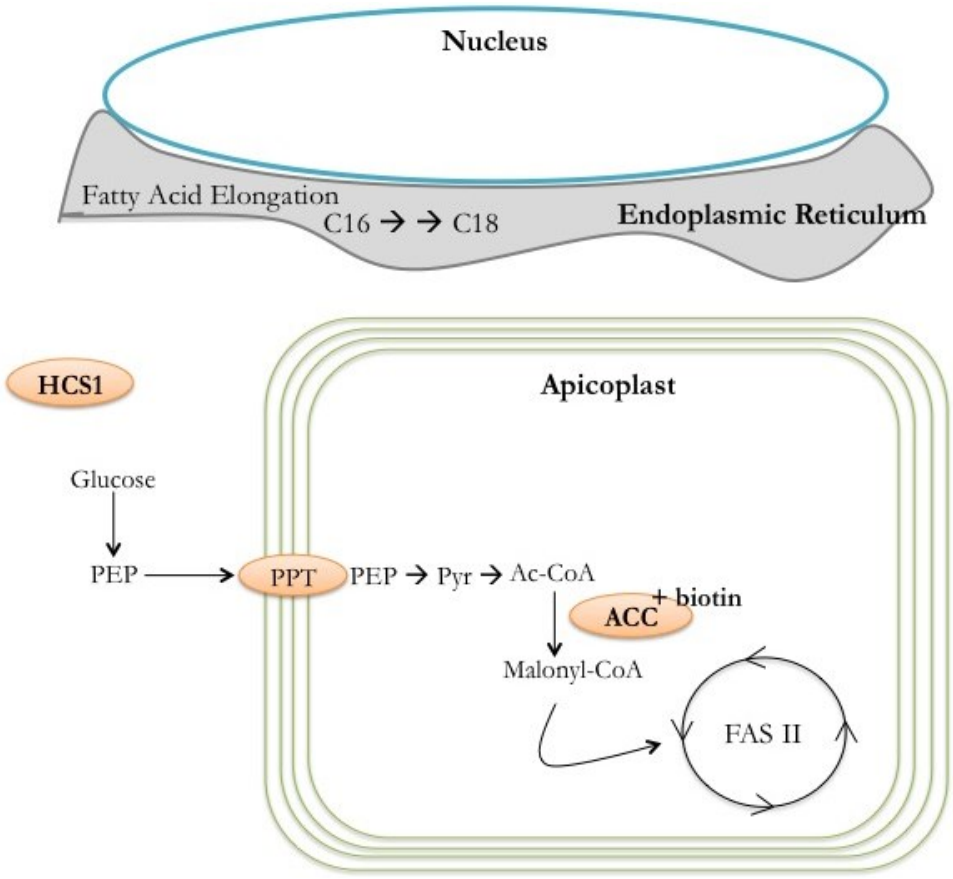


**Figure 5-1 Fatty Acid Metabolism in *P. falciparum***

*P. falciparum* has a fatty acid elongation pathway in the endoplasmic reticulum that can elongate C16 to C18 in blood stage parasites[11]. *P. falciparum* also has a Type II Fatty Acid Synthesis (FASII) pathway in the apicoplast that is required for liver stage parasite development but not the erythrocytic cycle[3,6]. Glucose metabolism in the cytosol produces phosphoenolpyruvate (PEP), which is taken into the apicoplast by the PEP/phosphate translocator (PPT). PEP is converted to pyruvate (Pyr), which is used to generate acetyl-Coenzyme A (Ac-CoA). The Acetyl-CoA Carboxylase (ACC) is a biotin dependent enzyme that converts Ac-CoA into malonyl-CoA, which is attached to the holo-Acyl Carrier Protein and modified by FASII pathway elongation enzymes to generate long chain fatty acids. The ACC is biotinylated by a biotin ligase that is primarily localized in the cytosol of blood stage parasites called the Holocarboxylase Synthetase 1 (HCS1).

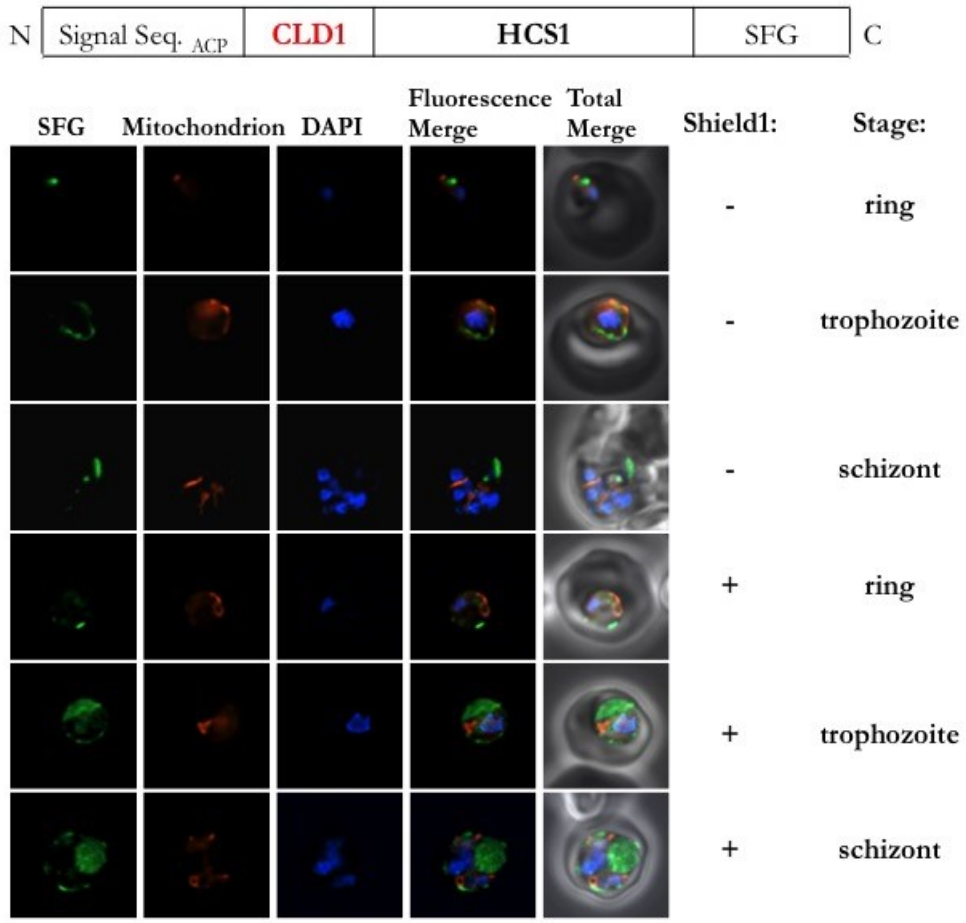


**Figure 5-2 Analysis of protein trafficking by CLD1-HCS1**

The diagram on the top shows the protein expression construct for CLD1-HCS1.

Signal Seq.$_{ACP}$ = signal sequence from the Acyl Carrier Protein
CLD1 = conditional localization domain 1 (FKBP$_{Q4K, F36V}$)
HCS1 = holocarboxylase synthetase 1
SFG = super folder green

The cell images are live fluorescence images of transgenic parasites that express CLD1-HCS1. The rows labeled "-" are cells that have not been treated with Shield1 and rows labeled "+" are cells that have been treated with 500 nM Shield1 for 24 hours. The development stage of each parasite is estimated based on the number of nuclei and the size of the parasite relative to the red blood cell.

Images are 10μm long by 10μm wide.

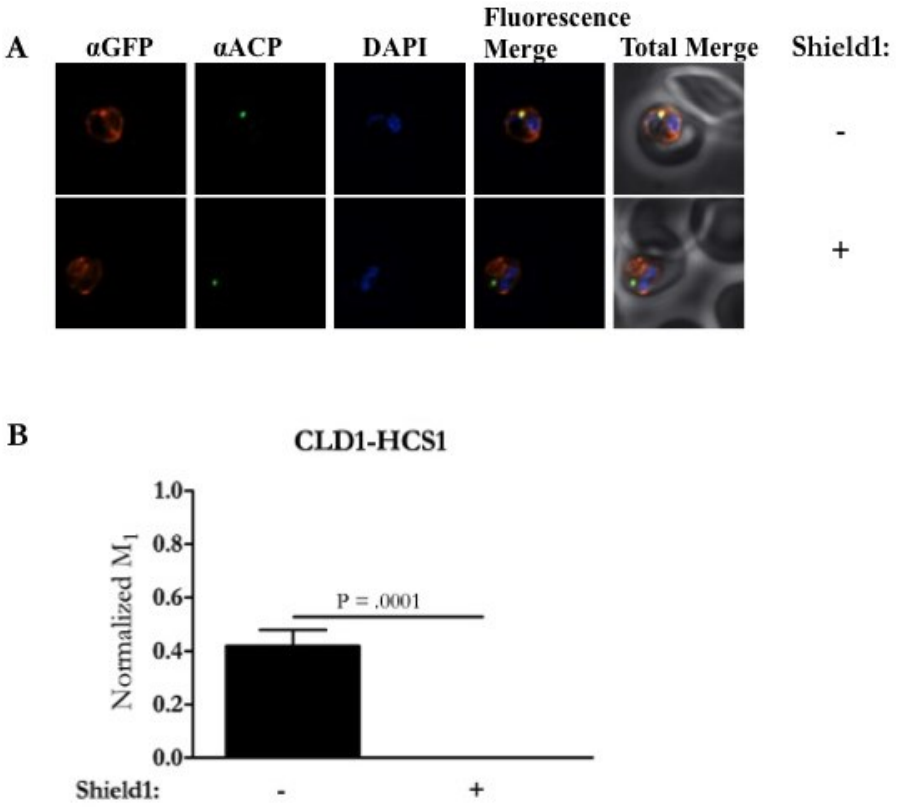


**Figure 5-3 Co-localization analyses for CLD1-HCS1**

A) Immunofluorescence images of a transgenic parasite line that expresses CLD1 fused to HCS1-SFG. The row labeled "-" shows a cell that has not been treated with Shield1 and the row labeled "+" shows a cell that was treated with 500 nM Shield1 for 72 hours before imaging. Images are 10μm long by 10μm wide.

B) Mander's Overlap Coefficients ($M_1$) were calculated for immunofluorescence images similar to the ones shown in in part A. $M_1$ values were calculated for each cell and all values were normalized to the average of the trafficking controls presented in Chapter 4 (Figure 4-5).

The Mann-Whitney U test was used to compare the $M_1$ values from the – and + Shield1 groups.

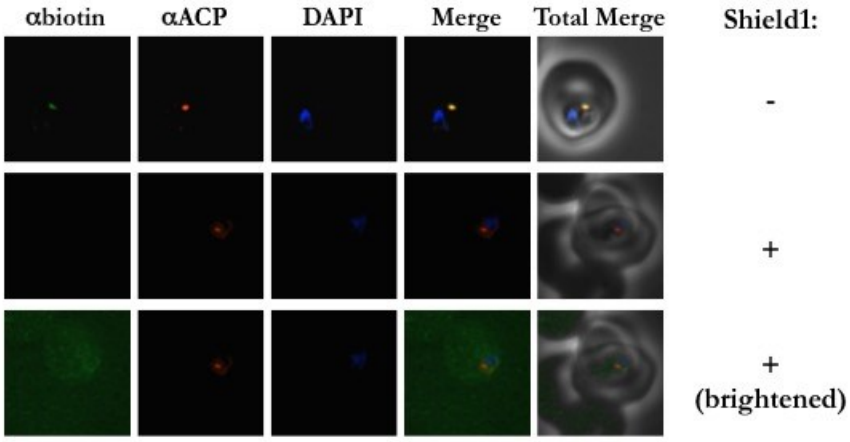


**Figure 5-4 Analysis of biotinylation activity in the CLD1-HCS1 expressing parasite line**

Immunofluorescence images of cells with no Shield1 added to culture (- Shield1) or 500 nM Shield1 added for 72hours (+ Shield1). The bottom row shows the same image in the second row with brightness enhanced in FITC channel. Images are 10μm long by 10μm wide.

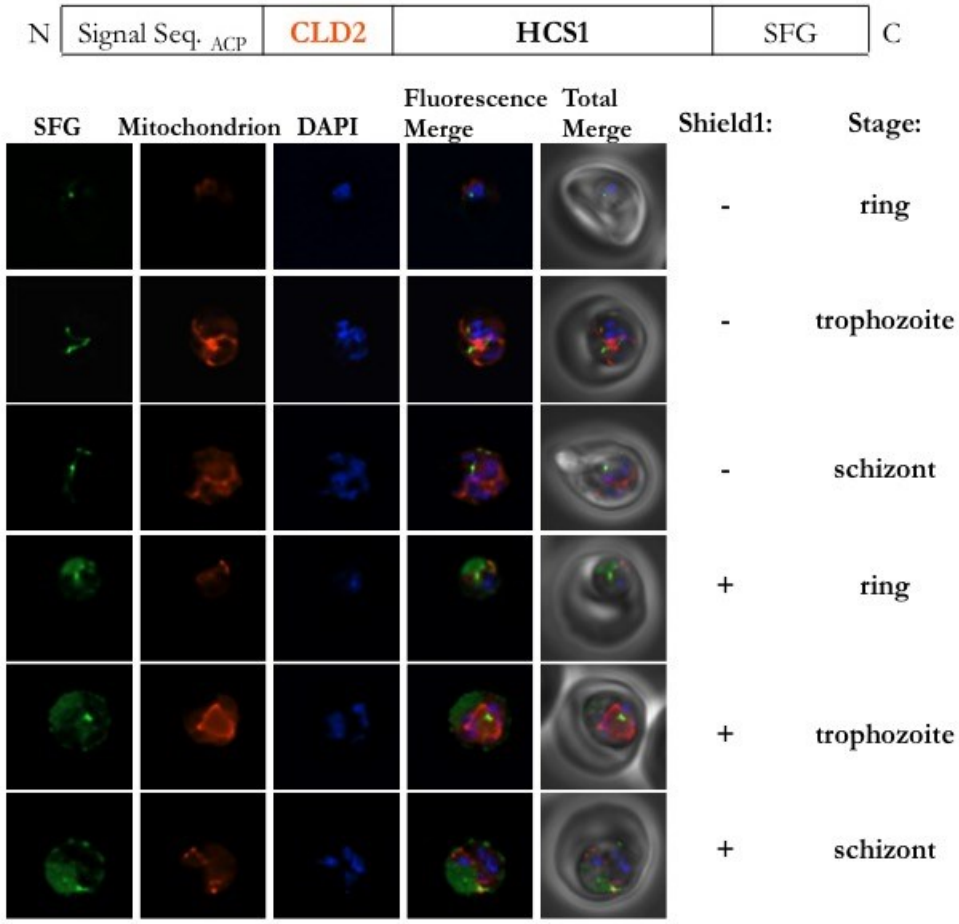


**Figure 5-5 Analysis of protein trafficking by CLD2-HCS1**

The diagram on the top shows the protein expression construct for CLD2-HCS1.

Signal Seq.$_{ACP}$ = signal sequence from the Acyl Carrier Protein
CLD2 = conditional localization domain 2 (FKBP$_{E6K, F36V}$)
HCS1 = holocarboxylase synthetase 1
SFG = super folder green

The cell images are live fluorescence images of transgenic parasites that express CLD2-HCS1. The rows labeled "-" are cells that have not been treated with Shield1 and rows labeled "+" are cells that have been treated with 500 nM Shield1 for 24 hours. The development stage of each parasite is estimated based on the number of nuclei and the size of the parasite relative to the red blood cell. Images are 10μm long by 10μm wide.

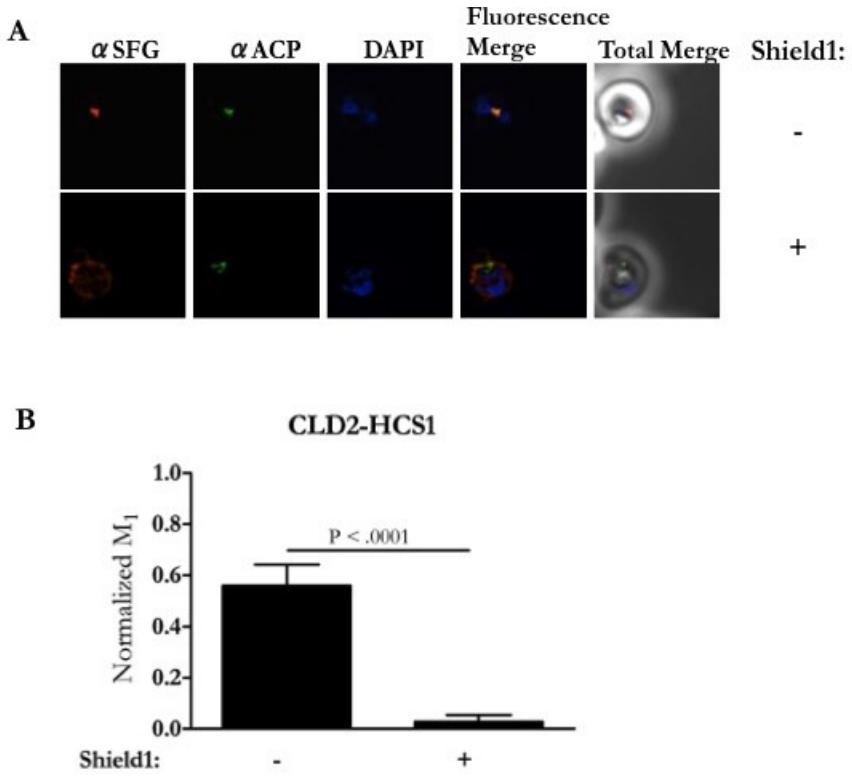


**Figure 5-6 Co-localization analyses for CLD2-HCS1**

A) Immunofluorescence images of a transgenic parasite line that expresses CLD2 fused to HCS1-SFG. The row labeled "-" shows a cell that has not been treated with Shield1 and the row labeled "+" shows a cell that was treated with 500 nM Shield1 for 72 hours before imaging. Images are 10 μm long by 10 μm wide.

B) Mander's Overlap Coefficients ($M_1$) were calculated for immunofluorescence images similar to the ones shown in in part A. $M_1$ values were calculated for each cell and all values were normalized to the average of the trafficking controls presented in Chapter 4 (Figure 4-5).

The Mann-Whitney U test was used to compare the $M_1$ values from the – and + Shield1 groups.

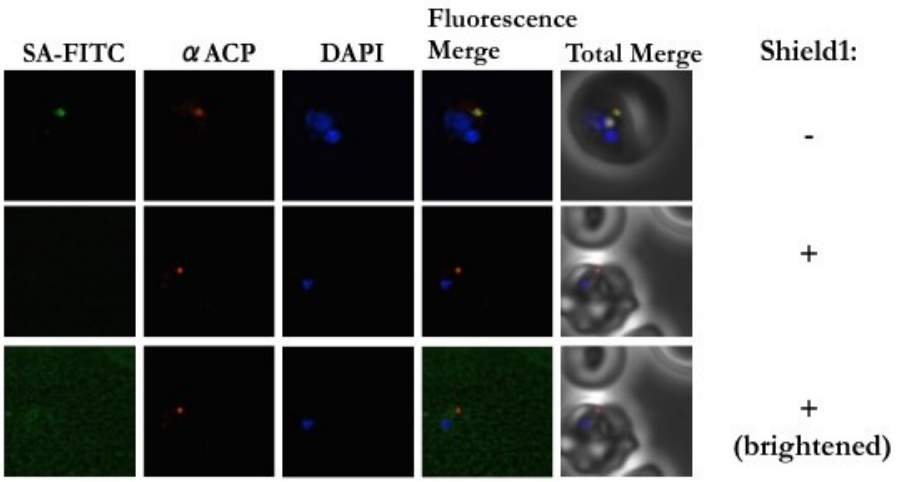


**Figure 5-7 Analysis of biotinylation activity in the CLD2-HCS1 expressing parasite line**

Immunofluorescence images of cells with no Shield1 added to culture (- Shield1) or 500 nM Shield1 added for 72hours (+ Shield1). The bottom row shows the same image in the second row with brightness enhanced in FITC channel. Images are 10μm long by 10μm wide.

SA = Streptavidin

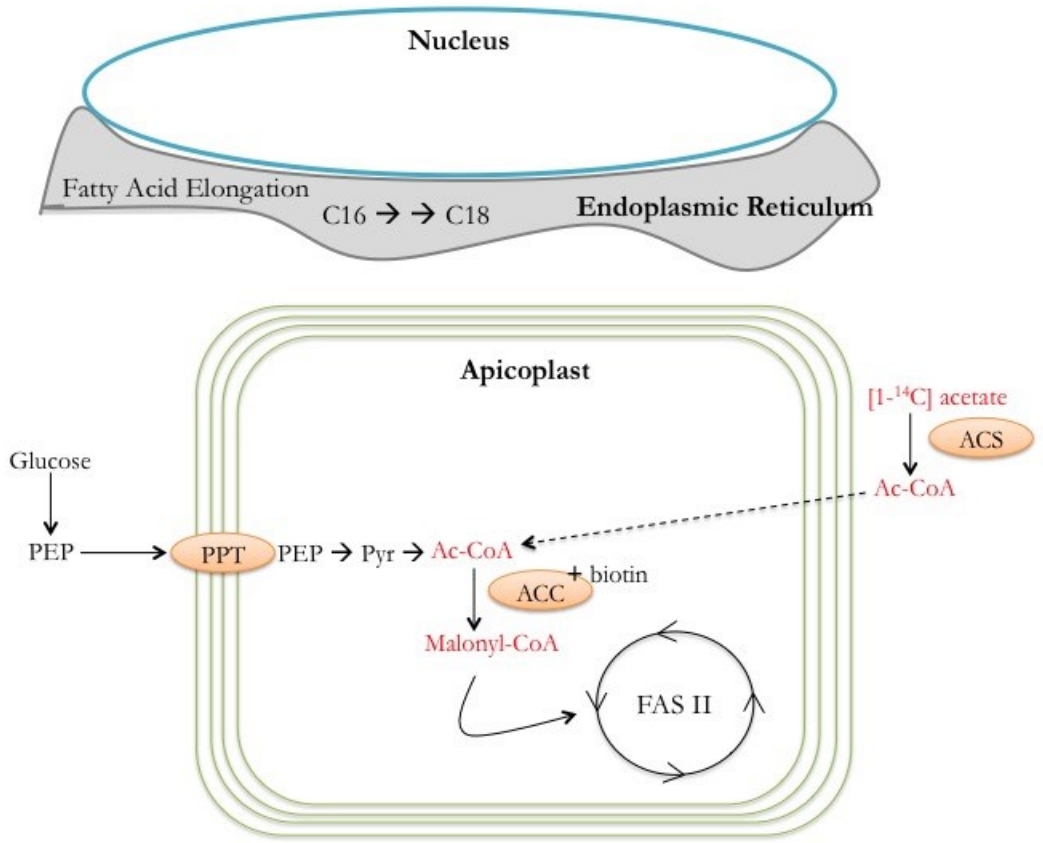


**Figure 5-8 Model of how [1-$^{14}$C]-acetate could be used to label FASII pathway products**

[1-$^{14}$C]-acetate is taken into the infected red blood cell and converted into Acetyl-Coenzyme A (Ac-CoA) by the Ac-CoA Synthetase (ACS) in the cytosol. This molecule must then be imported into the apicoplast into order to be used as a substrate for the FASII pathway. All other abbreviations and details are the same in this diagram as was described in Figure 5-1.

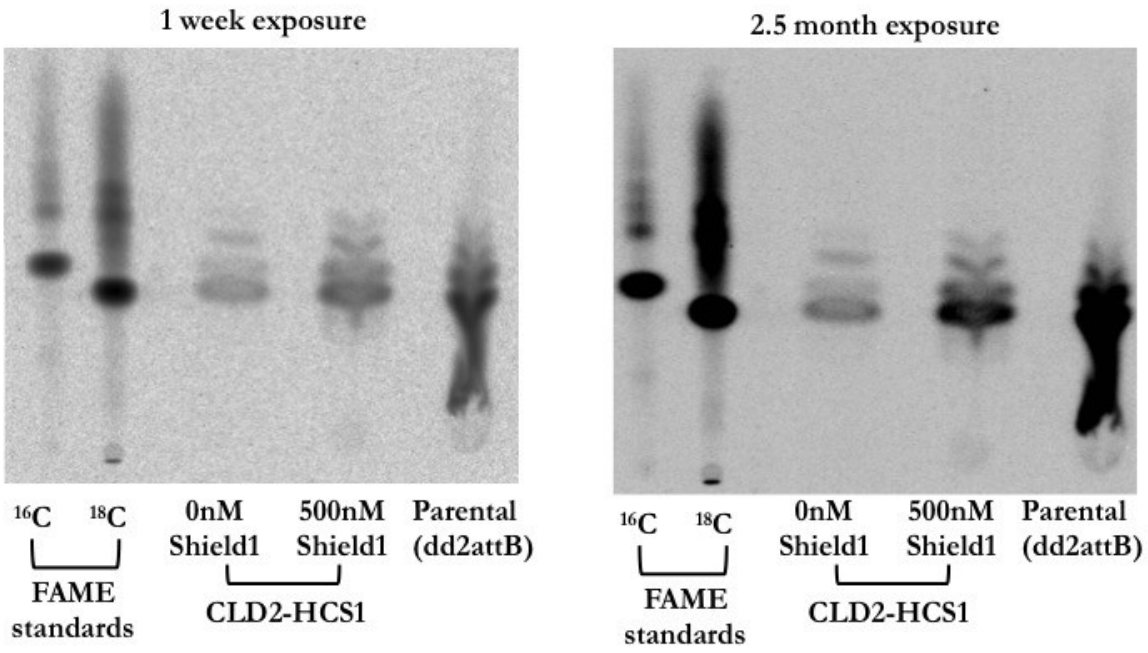


**Figure 5-9 Analysis of FASII pathway activity in the CLD2-HCS1 parasite line**

After treatment with 0 nM or 500 nM Shield1 for 72 hours parasites were synchronized and then radiolabeled with [1-$^{14}$C] acetate for 24 hours to label newly synthesized fatty acids. Fatty acids were extracted to generate fatty acid methyl esters (FAMEs) and resolved on an HPTLC silica gel. The gel was exposed to an imaging plate for one week (left) or 2.5 months (right).

- CLD2-HCS1 samples treated with 0 nM Shield1 have an active HCS1 enzyme expressed in the apicoplast.
- CLD2-HCS1 samples treated with 500 nM Shield1 do not have an active HCS1 enzyme in the apicoplast
- The parental dd2attB strain does not overexpress HCS1 and is not expected to have an active FASII pathway since the FASII pathway is dispensable in blood stage parasites.

| Primer name | Primer sequence |
|---|---|
| **BsrG1.HCS10.for** | GGTTGTACAACGCGTATGGAGGAAGGTCGCAAA ATTTTTG |
| **BsiWI.HCS10.rev** | GGTCGTACGGTCATCATCCTTTAC |

**Table 5-1 Primers used to amplify the HCS1 sequence**

## REFERENCES


1. Tran PN, Brown SHJ, Rug M, Ridgway MC, Mitchell TW, Maier AG. Changes in lipid composition during sexual development of the malaria parasite *Plasmodium falciparum*. *Malar J*. 2016;15(73):1-13. doi:10.1186/s12936-016-1130-z.

2. Schaijk BCL Van, Kumar TRS, Vos MW, et al. Type II Fatty Acid Biosynthesis Is Essential for *Plasmodium falciparum* Sporozoite Development in the Midgut of Anopheles Mosquitoes. *Eukaryot Cell*. 2014;13(5):550-559. doi:10.1128/EC.00264-13.

3. Yu M, Kumar TRS, Nkrumah LJ, et al. The fatty acid biosynthesis enzyme FabI plays a key role in the development of liver-stage malarial parasites. *Cell Host Microbe*. 2008;4:567-578. doi:10.1016/j.chom.2008.11.001.

4. Ramakrishnan S, Serricchio M, Striepen B, Bütikofer P. Lipid synthesis in protozoan parasites: A comparison between kinetoplastids and apicomplexans. *Prog Lipid Res*. 2013;52:488-512. doi:10.1016/j.plipres.2013.06.003.

5. Dellibovi-Ragheb T, Goodman C, Walters M, et al. *Host Biotin Is Required for Liver Stage Development in Malaria Parasites*.

6. Vaughan AM, O'neill MT, Tarun AS, et al. Type II fatty acid synthesis is essential only for malaria parasite late liver stage development. *Cell Microbiol*. 2009;11(3):506-520. doi:10.1111/j.1462-5822.2008.01270.x.

7. Shears MJ, Botté CY, McFadden GI. Fatty acid metabolism in the Plasmodium apicoplast: Drugs, doubts and knockouts. *Mol Biochem Parasitol*. 2015;199:34-50. doi:10.1016/j.molbiopara.2015.03.004.

8. John P. Barnard and Peter L. Pedersen BR. Glucose Catabolism in African Trypanosomes. *J Biol Chem*. 1993;268(5):3654-3661.

9. Mullin KA, Lim L, Ralph SA, Spurck TP, Handman E, Mcfadden GI. Membrane transporters in the relict plastid of malaria parasites. *Proc Natl Acad Sci U S A*. 2006;103(25):9572-9577.

10. Ralph SA, Dooren GG Van, Waller RF, et al. Metabolic Maps and Function of the *Plasmodium Falciparum* Apicoplast. *Nat Rev Microbiol*. 2004;2:203-216. doi:10.1038/nrmicro843.

11. Mi-Ichi F, Kita K, Mitamura T. Intraerythrocytic *Plasmodium falciparum* utilize a broad range of serum-derived fatty acids with limited modification for their growth. *Parasitology*. 2006;133:399-410. doi:10.1017/S0031182006000540.

# Chapter 6

# Conclusions and Future Directions

**Development and Future Studies of the Conditional Localization Domain**

This thesis describes the design, characterization, and validation of a novel molecular tool that can be used to control the localization of apicoplast targeted proteins. We designed a conditional localization domain (CLD) that can be added as an amino-terminal tag to a protein of interest and to control its localization. The CLD mimics the features of natural *P. falciparum* transit peptides and is destabilized without an interacting ligand, which allows it to traffic to the apicoplast. When a ligand is added to cell culture media, it stabilizes the structure of the CLD and causes the domain to be secreted from the cell.

We tested Dihydrofolate Reductase (DHFR) and FK-506 Binding Protein (FKBP) as candidate CLDs in Chapters 2 and 3 respectively. Our DHFR variants were not suitable CLDs because they did not traffic to the apicoplast. There are several reasons why DHFR may have performed poorly as a CLD. Our analysis suggests that DHFR's ability to bind multiple ligands, its enzymatic activity, or its complex amino-terminal structure may have contributed to its inability to traffic to the apicoplast. We then moved on to design our next candidate CLDs, which were ultimately successful, from FKBP. FKBP has been used as a molecular tool in many eukaryotic cell systems including multiple tools designed for use in *P. falciparum* and has been engineered to bind a synthetic ligand (Shield1) with higher affinity than endogenous ligands[1–4]. We designed three CLDs – CLD1, CLD2, and CLD3 – that are able to traffic to the apicoplast and secreted compartment in a ligand dependent manner. In Chapter 4 we conducted an analysis of trafficking dynamics, structural stability, and sensitivity of each of the CLDs (A summary of these analyses is diagramed in Figure 4-10). Most notably, we found that CLD1 has a leaky apicoplast trafficking phenotype that is linked to its higher protein stability compared to CLD2 or 3. We also showed that CLD2 has the most optimal trafficking efficiency to the apicoplast and secreted compartments.

In the final portion of this thesis we validated the conditional localization system by tagging a parasite biotin ligase (Holocarboxylase Synthetase 1; HCS1) with CLD1 and then CLD2. We showed that altering the localization of the HCS1 enzyme controls HCS1 activity in the apicoplast. This study proved that the CLD can be used to control the localization of a parasite enzyme without interfering with the function of the protein and demonstrates the full functionality of the CLD tool.

There are some characteristics of the CLDs that could be further modified in future studies to improve the domains. One feature that could be further studied is the CLD cleavage site. Natural transit peptides are cleaved after they are imported into the apicoplast lumen by a metalloprotease called the Stromal Processing Peptidase (SPP; PF3D7_1440200.1)[5]. The signal for transit peptide recognition and cleavage by *Pf*SPP is currently unknown. Studies of similar transit peptide cleavage enzymes in chloroplasts however, have identified two short consensus sequences (between four and six amino acids long) that appear to be involved in recognition of some transit peptides in plants [6]. While no such consensus sequence has been identified for *P. falciparum* transit peptides, the exact site of transit peptide cleavage for the apicoplast marker Acyl-Carrier Protein (ACP) has been mapped (see ACP cleavage site in Figure 6-1 A)[5].

Since we do not know what the exact sequence recognition signal is for the *Pf*SPP, we decided to insert the three amino acid residues around the ACP cleavage site after the CLD sequence (see CLD cleavage site in Figure 6-1 B) as an artificial transit peptide cleavage site that would hopefully allow the CLD to be cleaved from the mature protein after import into the apicoplast. Preliminary studies of the CLD cleavage site showed that the CLDs are cleaved from SFG when the domain traffics to the apicoplast (- Shield1) and also when the domain traffics to the parasitophorous vacuole (+ Shield1). This suggests that the *Pf*SPP in

the apicoplast is not the only protease capable of cleaving the artificial cleavage site we inserted after the CLD. Additionally, studies from other groups have shown that proteases are among the most abundant proteins in the parasitophorous vacuole[7]. It is plausible that one or more of the proteases present in the parasitophorous vacuole space is able to cleave the artificial transit peptide cleavage site that we inserted after the CLD. Further studies to improve the CLD could test longer sequences for the CLD cleavage site to generate a cut site for the CLD that is exclusively recognized by the SPP in the apicoplast. This would allow future studies that implement the CLD to track protein localization by analyzing the size of the target protein on a western blot in addition to visualizing localization using microscopy.

**Implementation of the Conditional Localization Domain in Future Studies**

There are over 500 proteins that are predicted to be targeted to the apicoplast in *P. falciparum*[8]. Many of these proteins participate in biochemical pathways that perform essential functions in the apicoplast such as the Type II fatty acid synthesis pathway and the isoprenoid precursor synthesis pathway. Other proteins are involved in maintenance of the apicoplast genome, organelle morphology, or protein import to the apicoplast. Any of these proteins may be of interest in future studies that could use the CLD to probe their function or viability as a drug target.

There are however, some limitations on the use of the CLD, in particular for tagging proteins that are trafficked to the apicoplast membrane. Four membranes surround the apicoplast and only a few studies have characterized proteins that are trafficked to these membranes[9,10]. These studies have shown that some proteins that traffic to the apicoplast membrane do not contain a canonical bipartite apicoplast trafficking motif. The molecular

mechanism for apicoplast targeting without a transit peptide motif is still unknown and it is difficult to predict how adding a CLD to the amino-terminus a membrane protein that does not contain a transit peptide would affect its trafficking. Use of the CLD is therefore likely limited to proteins that are soluble and trafficked to the apicoplast lumen by a canonical signal sequence and transit peptide motif.

The CLD could also be used to tag soluble proteins in the parasitophorous vacuole. A proteomic study of the parasitophorous vacuole revealed that proteases and chaperones are the most abundant proteins in the parasitophorous vacuole space[7]. Some of these proteases are likely to be involved in release of mature merozoites from the red blood cell. Future studies could use the CLD to mislocalize proteases in the parasitophorous vacuole and determine which enzymes are important for parasite egress. This type of study can only be successful however if the protease is not toxic when trafficked to the apicoplast compartment.

Currently our lab is in the process of tagging several proteins with the CLD at their endogenous locus. Our goal is to use the CLD to mislocalize a protein that is important for apicoplast maintenance and then follow the metabolic and morphological changes that occur in the cell, as the protein is mislocalized (by adding Shield1) and the apicoplast is lost. We are also interested in disseminating the conditional localization domain to other labs. Some labs have expressed interest in applying the CLD to control apicoplast-targeted proteins in *Toxoplasma gondii* (a related apicomplexan parasite). This may be feasible since *T. gondii* has similar amino-terminal targeting motif requirements for trafficking to the apicoplast as *P. falciparum*[11,12]. It is not clear however whether the structural features of *T. gondii* transit peptides are similar to those of *P. falciparum* and this would be a key determinant for the successful use of the CLD in other plastid containing organisms.

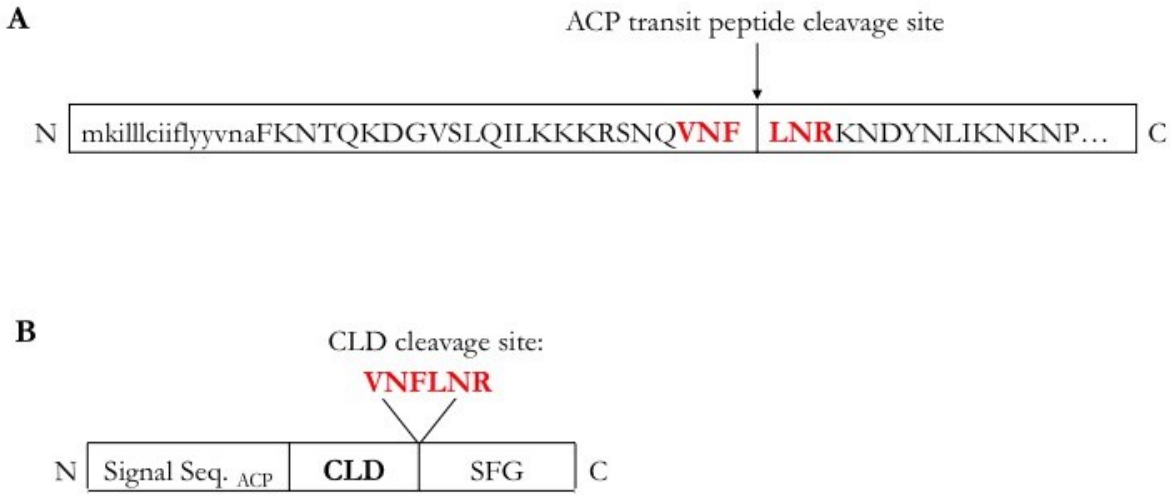


**Figure 6-1 Stromal Processing Peptidase cleavage sites for ACP and the CLD**

A) The amino-terminal sequence of the Acyl-Carrier Protein (ACP) is shown[5]. The arrow indicates where the *P. falciparum* Stromal Processing Peptidase (*Pf*SPP) cleaves this sequence as the protein is imported into the apicoplast lumen.

B) We inserted the six amino acid sequence around the transit peptide cleavage site of ACP after the CLD sequence to serve as an artificial CLD cleavage site.

## REFERENCES


1. Armstrong CM, Goldberg DE. An FKBP destabilization domain modulates protein levels in *Plasmodium falciparum*. *Nat Methods*. 2007;4(12):1007-1009. doi:10.1038/nmeth1132.

2. Birnbaum J, Flemming S, Reichard N, et al. A genetic system to study *Plasmodium falciparum* protein function. *Nat Methods*. 2017:1-7. doi:10.1038/nmeth.4223.

3. Saridaki T, Sanchez CP, Pfahler J, Lanzer M. A conditional export system provides new insights into protein export in *Plasmodium falciparum*-infected erythrocytes. *Cell Microbiol*. 2008;10(12):2483-2495. doi:10.1111/j.1462-5822.2008.01223.x.

4. Clackson T, Yang W, Rozamus LW, et al. Redesigning an FKBP-ligand interface to generate chemical dimerizers with novel specificity. *Proc Natl Acad Sci U S A*. 1998;95:10437-10442. doi:10.1073/pnas.95.18.10437.

5. van Dooren GG, Su V, D'Ombrain MC, Mcfadden GI. Processing of an Apicoplast Leader Sequence in *Plasmodium falciparum* and the Identification of a Putative Leader Cleavage Enzyme. *J Biol Chem*. 2002;277(26):23612-23619. doi:10.1074/jbc.M201748200.

6. Bruce BD. The paradox of plastid transit peptides : conservation of function despite divergence in primary structure. *Biochim Biophyrica Acta*. 2001;1541:2-21.

7. Nyalwidhe J, Lingelbach K. Proteases and chaperones are the most abundant proteins in the parasitophorous vacuole of *Plasmodium falciparum* -infected erythrocytes. *Proteomics*. 2006;6:1563-1573. doi:10.1002/pmic.200500379.

8. Ralph SA, Dooren GG Van, Waller RF, et al. Metabolic Maps and Function of the *Plasmodium Falciparum* Apicoplast. *Nat Rev Microbiol*. 2004;2:203-216. doi:10.1038/nrmicro843.

9. Spork S, Hiss J a, Mandel K, et al. An unusual ERAD-like complex is targeted to the apicoplast of *Plasmodium falciparum*. *Eukaryot Cell*. 2009;8(8):1134-1145. doi:10.1128/EC.00083-09.

10. Mullin KA, Lim L, Ralph SA, Spurck TP, Handman E, Mcfadden GI. Membrane transporters in the relict plastid of malaria parasites. *Proc Natl Acad Sci U S A*. 2006;103(25):9572-9577.

11. Waller RF, Keeling PJ, Donald RG, et al. Nuclear-encoded proteins target to the plastid in *Toxoplasma gondii* and *Plasmodium falciparum*. *Proc Natl Acad Sci U S A*. 1998;95:12352-12357. doi:10.1073/pnas.95.21.12352.

12. Derocher A, Hagen CB, Froehlich JE, Feagin JE, Parsons M. Analysis of targeting sequences demonstrates that trafficking to the *Toxoplasma gondii* plastid branches off

the secretory system. *J Cell Sci*. 2000;113:3969-3977.

# Appendix

## Localization of the *Plasmodium falciparum* Lipoate Ligase 2

## INTRODUCTION

The study described in this appendix was a part of a larger line of research in our lab that interrogates the role of lipoate in the parasite mitochondrion. Lipoate is an enzyme cofactor that is scavenged by the parasite for use in the mitochondrion and is essential for blood stage parasite development [1]. Lipoate is attached to three parasite proteins in the mitochondrion that each function as a part of larger multi-enzyme complexes[2]. One of these lipoylated proteins is the H-protein, which is a part of the glycine cleavage complex of enzymes. And the other two lipoylated proteins are the mitochondrial pyruvate dehydrogenase (mPDH) and the α-ketoglutarate dehydrogenase (KDH). Both the mPDH and KDH are members of multi-enzyme complexes that generate products used by the tricarboxylic acid (TCA) cycle[2].

A former student in our lab investigated how lipoate is attached to each of its target proteins in the mitochondrion. There are two predicted lipoate ligases in *P. falciparum* called Lipoate Ligase 1 and 2 (Lipl1 and Lipl2). Studies of these two enzymes showed that Lipl1 is able to lipoylate the H-protein independent of Lipl2 activity. Lipl2 however, does not appear to have the expected lipoate ligase activity. Lipl2 instead acts as a transferase that takes activated lipoate from Lipl1 and attaches it to the target proteins: KDH and mPDH[3].

Previous studies form other groups have localized the Lipl1 and Lipl2 proteins to different compartments in the cell. Using episomal over-expression methods, Lipl1 was localized exclusively to the mitochondrion while Lipl2 was localized to both the mitochondrion and the apicoplast[4,5]. Given our studies showing that Lipl2 is not a ligase and requires Lipl1 for activity, it is unclear what the function of Lipl2 would be in the apicoplast without Lipl1. I began this study to try to confirm the reported dual localization of Lipl2

with an improved overexpression technique. We generated transgenic parasites that express the full-length Lipl2 protein integrated at a non-essential locus in blood stage parasites using the Bxb1 integrase system for site specific recombination in parasites[6]. Using this method to over express Lipl2 we observed consistent co-localization of Lipl2 with the mitochondrion and no colocalization with the apicoplast.

## RESULTS

### Lipl2 Expression and Localization

*Lipl2-GFP expression and localization*

We generated a parasite line that expresses the Lipl2 protein fused to a C-terminal Green Fluorescent Protein (Lipl2-GFP) tag. Lipl2-GFP is expressed from the moderate strength *P. falciparum* ribosomal L2 promoter in this experiment. We stained cells with the Mitotracker Red (Invitrogen) dye, which stains the mitochondria of the parasite, and observed colocalization between Lipl2-GFP and the Mitotracker Red dye (Figure A-1 A). This suggests that Lipl2 traffics to the mitochondria in blood stage parasites. In all of the live fluorescence cell images that we collected, Lipl2 appears to be co-localized with the mitochondria. Figure A-1 A shows a representative image at each stage of parasite development in the red blood cell (ring, trophozoite, and schizont). Lipl2 colocalizes with the mitochondria at all three stages.

To further interrogate whether Lipl2 also traffics to the apicoplast we stained fixed cells in immunofluorescence assays with antibodies to track the location of Lipl2-GFP and the apicoplast marker Acyl-Carrier Protein (ACP). We did not observe significant colocalization between Lipl2 and ACP in any of the images we collected (Figure A-1B).

Finally we confirmed expression of Lipl2-GFP by western blot. Lipl2-GFP is about 74kD and we observed a band at the correct size in our analysis of Lipl2-GFP parasite lysates (Figure A-1 C). We also observed a smaller band around 50kD. Further experiments should be done to determine whether the band at 50kD is an artifact of the cell lysis protocol or if it is a cleaved version of the protein that is present in the cell.

*Lipl2-mCherry expression and localization*

We generated a second parasite line that expresses Lipl2 fused to a C-terminal mCherry (Lipl2-mCherry) fluorophore. Lipl2-mCherry is expressed from the high strength *P. falciparum* Calmodulin promoter in this parasite line. We stained cells with a Mitotracker Green (Invitrogen) dye that stains the mitochondrion of the parasite and again observed colocalization between Lipl2 and the Mitotracker dye (Figure A-2). This supports our initial observation that Lipl2 traffics to the mitochondria in blood stage parasites. In all of the live cell images that we collected, with the Lipl2-mCherry line, Lipl2 appears to be co-localized with the mitochondria.

*Dual expression of Lipl2-GFP and an apicoplast marker*

In our final attempt to interrogate whether Lipl2 traffics to the apicoplast we designed a plasmid to express Lipl2-GFP and a fluorescent apicoplast marker in parasites. We reasoned that this parasite line would allow us to detect Lipl2-GFP colocalized with the apicoplast in live fluorescence images.

The apicoplast marker protein in this experiment is the targeting motif from ACP fused to mCherry. We expressed this apicoplast marker from the same promoter as the resistance cassette by appending a skip peptide sequence followed by the apicoplast marker

sequence to the end of the open reading frame for the resistance cassette (See plasmid map in Figure A-3 A). Skip peptides are short amino acid sequences that RNA viruses use to express multiple genes from one open reading frame[7]. When translated, the skip peptide sequence impairs formation of a specific peptide bond in its own sequence without affecting translation of the next residue. This allows the ribosome to "skip" formation of one peptide bond after the first protein in the open reading frame and continue translating the second protein[7].

We transfected parasites with the plasmid in Figure A-3 A and analyzed cells for expression of Lipl2-GFP and the apicoplast marker. We did not detect expression of Lipl2-GFP in this parasite line, which suggests that the parasites have turned off expression of the transgene while maintaining the resistance cassette. We did detect the cleaved apicoplast marker protein in the western blot shown in Figure A-3 B. This blot shows that the skip peptide is able to facilitate cleavage of the apicoplast marker protein from Blasticidin S Deaminase (BSD), which mediates resistance to blasticidin in parasites. If the skip peptide had not worked, we would expect to see a larger band at 49kD on the western blot because the BSD protein would still be attached to the apicoplast marker. Although this parasite line could not be used to localize Lipl2, it does confirm that the skip peptide is functional in *P. falciparum*.

## DISCUSSION AND FUTURE DIRECTIONS

In this study we over-expressed Lipl2 in parasites in two independent experiments using the Bxb1 integrase system to generate transgenic parasites that have integrated Lipl2 at a specific locus in the nuclear genome. Studies from another group reported that Lipl2 is

dually localized to the apicoplast and the mitochondrion but we did not observe apicoplast localization in either of our overexpression lines. In our hands, Lipl2 appears to be exclusively localized to the mitochondrion. This result is consistent with our previously described functional studies of Lipl2, which showed that Lipl2 has transferase activity and works in conjunction with Lipl1.

Differences in localization between our study and the published report may be due to the different methods of overexpression that were utilized in these studies. The previous study expressed Lipl2 episomally, which is not ideal for protein over expression in *P. falciparum* because the parasite does not efficiently maintain episomes. Parasites that maintain episomes often do not effectively pass the plasmid from one generation to the next and so growth of cultures expressing episomal plasmids is significantly slower that normal. Parasites can also maintain more than one plasmid and so expression levels may vary between cells[8–10].

Another option to localize the Lipl2 protein is to tag it at its endogenous locus. We cannot rule out the possibility that correct timing of expression or protein levels in the cell affect trafficking of Lipl2. Tagging Lipl2 at its endogenous locus and analyzing localization could provide more insight into the true localization of Lipl2.

## METHODS

### Generation of plasmid constructs

The Lipl2 gene was PCR amplified from plasmid DNA and then digested with AvrII and BsiWI. Vector DNA pLN-mCherry or pRL2-GFP were then also digested with AvrII and BsiWI restriction enzymes. Inserts were ligated into the appropriate vector to generate plasmids described in this appendix using Quick Ligase (New England BioLabs). DNA sequences were confirmed by sequencing after insertion.

The P2A skip peptide and TA-mCherry genes were added to the C-terminus of the Blasticidin S Deaminase coding region on the pRL2-Lipl2-GFP plasmid. The TA-mCherry gene with an N-terminal P2A sequence fragment was PCR amplified from plasmid DNA using TAmCh.P2A.F and TAmCh.Bsu36I.R. The C-terminus of Blasticidin S Deaminase was then PCR amplified from plasmid DNA with an overlapping C-terminal P2A fragment using BSD.EagI.P2A and BSD.P2A.R. The P2A-TAmCherry and BSD-P2A fragments with overlapping P2A sequences were then put into a final PCR reaction with primers to amplify the entire BSD-P2A-TAmCherry insert form the ends (BSD.Syn.F and TAmCherry.Syn.R). The final PCR product was digested with EagI and Bsu36I and inserted into the pRL2-Lipl2-GFP vector (also digested with EagI and Bsu36I). The final DNA sequence was confirmed by sequencing after insertion.

**Western blots**

5mL parasite cultures at 2 % hematocrit were lysed in 0.2 % saponin and washed in PBS. Cell pellets were then re-suspended in 5x SDS running buffer. Samples were run on a NuPage 4– 12 % Bis-Tris reducing gel (Invitrogen) and then transferred to nitrocellulose. The nitrocellulose membrane was then blocked in 5 % milk for 1hour before probing with a primary antibody overnight at 4 °C. Nitrocellulose membranes were probed with Living Colors mouse anti-GFP JL-8 (Clonetech) used at 1:5000 or rabbit anti-dsRed used at 1:5000. The membranes were then washed and probed with appropriate secondary (anti-rabbit Horse Radish Peroxidase (HRP) or anti-mouse HRP at 1:5000) antibodies for 1 hour. The membranes were then washed again and treated with Super Signal West Pico PLUS (Thermo Scientific) reagent before exposure to film.

- Live cell imaging and immunofluorescence assays were done using the same methods described in chapter 2
- Parasite transfections methods are the same as in Chapter 2.
- Parasite culture methods are the same as for Chapter 2 except that these parasites were grown in human serum instead of albumax.

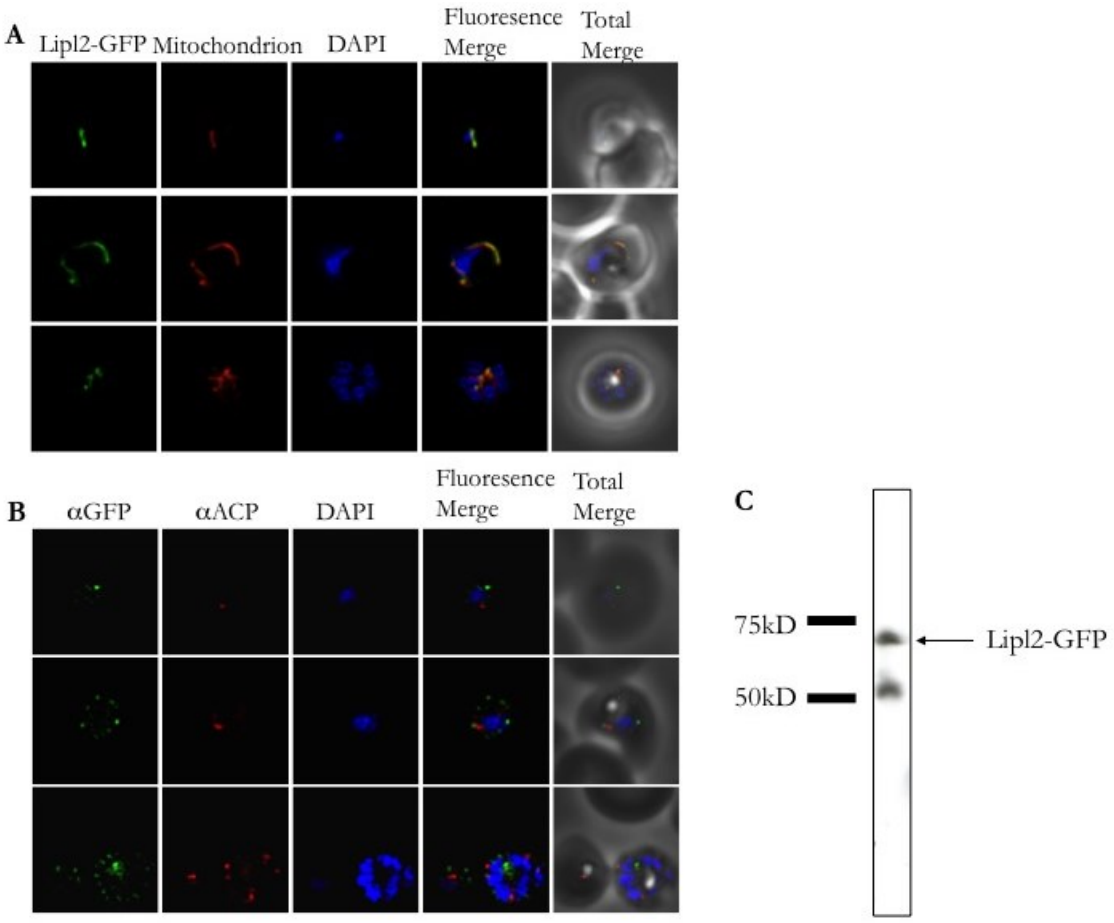


**Figure A-1 Lipl2-GFP Localization**

A) Live fluorescence images of a transgenic parasite line expressing Lipl2 fused to GFP. The mitochondrion is stained with Mitotracker Red (Invitrogen).

B) Immunofluorescence images of the same parasite line in part A.

C) Western blot analysis of parasites expressing Lipl2 fused to GFP. Parasite lysates have been probed with an anti-GFP primary antibody.

Images are 10μm long by 10μm wide.

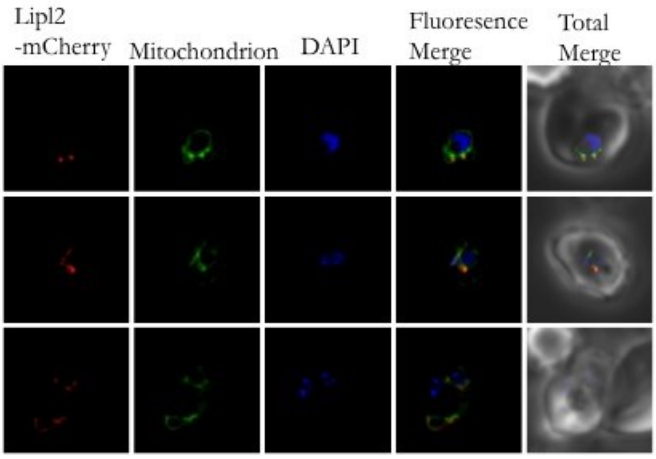


**Figure A-2 Lipl2-mCherry Localization**

Live fluorescence images of a transgenic parasite line expressing Lipl2 fused to mCherry.

The mitochondrion is stained with Mitotracker Green (Invitrogen).

Images are 10μm long by 10μm wide.

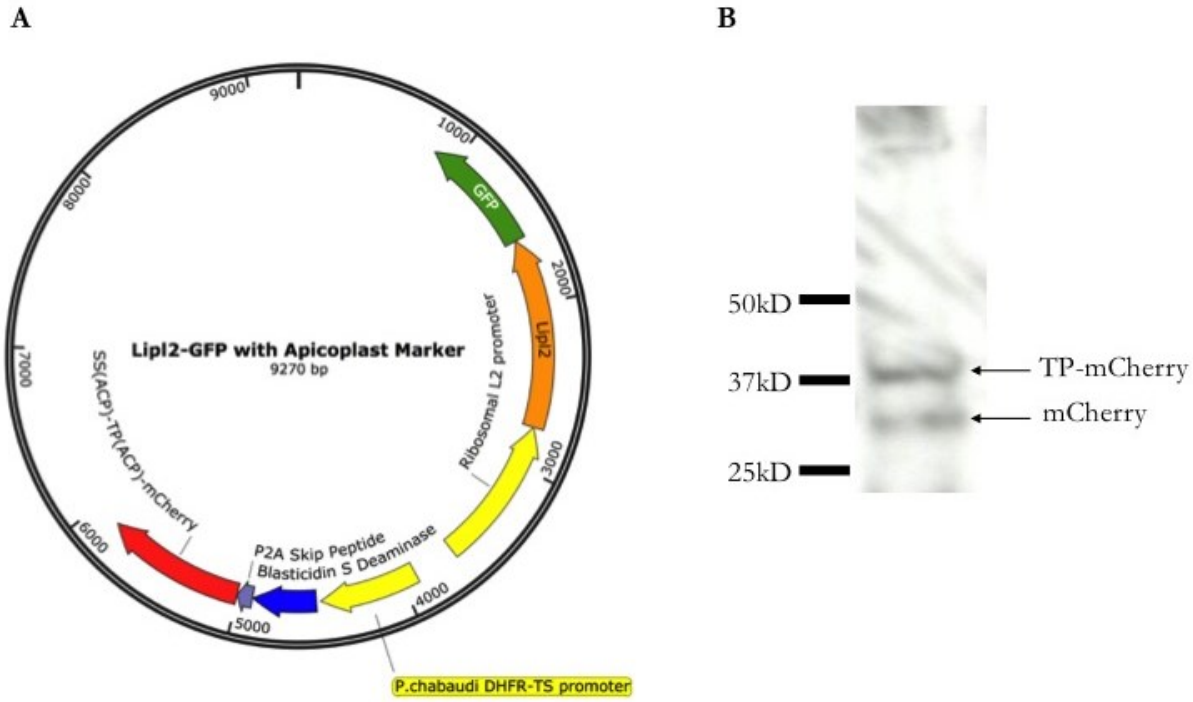


**Figure A-3 Dual expression of Lipl2-GFP and an apicoplast marker**

A) Map of the parasite expression vector we used to attempt to generate a parasite line that expresses Lipl2-GFP and a fluorescent apicoplast marker (mCherry).

B) Western blot analysis of parasites selected after transfection with the plasmid in part A. Parasite lysate was probed with an anti-dsRed primary antibody.

| Primer name | Primer sequence |
|---|---|
| **BSD.EagI.F** | GGTGGTCGGCCGCATCTTCACTGG |
| **BSD.P2A.R** | CTTCTACATCTCCTGCTTGCTTTAAAAGAGAAAAATTTGTAGCTCCGGAGCCCTCCCACACATA ACCAG |
| **TAmCh.P2A.F** | CTTTTAAAGCAAGCAGGAGATGTAGAAGAAAATCCCGGGCCTATGAAGATCTTATTACTTTGT ATAATTTTTC |
| **TAmCh.Bsu36I.R** | GGTGCACCTTAGGACGCGTTTACTTGTACAGCTCGTCCATGCCG |
| **BSD.syn.F** | GGGATTCGTGAATTGCTGCCCTCTGGTTATGTGTGGGAGG**GC**TC |
| **TAmCh.syn.R** | GCGTTAACATAATATAGAAAAATTATACAAAGTAATAAGATCTTCATAGGC |

**Table A-1 Primers used to add an apicoplast marker to the pRL2-Lipl2-GFP plasmid**

## REFERENCES


1. Allary M, Lu JZ, Zhu L, Prigge ST. Scavenging of the cofactor lipoate is essential for the survival of the malaria parasite *Plasmodium falciparum*. *Mol Microbiol*. 2007;63(5):1331-1344. doi:10.1111/j.1365-2958.2007.05592.x.

2. Spalding MD, Prigge ST. Lipoic acid metabolism in microbial pathogens. *Microbiol Mol Biol Rev*. 2010;74(2):200-228. doi:10.1128/MMBR.00008-10.

3. Afanador GA, Matthews KA, Bartee D, et al. Redox-dependent lipoylation of mitochondrial proteins in *Plasmodium falciparum*. *Mol Microbiol*. 2014;94(1):156-171. doi:10.1111/mmi.12753.

4. Wrenger C, Müller S. The human malaria parasite *Plasmodium falciparum* has distinct organelle-specific lipoylation pathways. *Mol Microbiol*. 2004;53(1):103-113. doi:10.1111/j.1365-2958.2004.04112.x.

5. Günther S, Wallace L, Patzewitz E-M, et al. Apicoplast lipoic acid protein ligase B is not essential for *Plasmodium falciparum*. *PLoS Pathog*. 2007;3(12):e189. doi:10.1371/journal.ppat.0030189.

6. Nkrumah LJ, Muhle R a, Moura P a, et al. Efficient site-specific integration in *Plasmodium falciparum* chromosomes mediated by mycobacteriophage Bxb1 integrase. *Nat Methods*. 2006;3(8):615-621. doi:10.1038/nmeth904.

7. Szymczak-Workman AL, Vignali KM, Vignali D a a. Design and construction of 2A peptide-linked multicistronic vectors. *Cold Spring Harb Protoc*. February 2012:199-204. doi:10.1101/pdb.ip067876.

8. Donnell RAO, Preiser PR, Williamson DH, Moore PW, Cowman AF, Crabb BS. An alteration in concatameric structure is associated with efficient segregation of plasmids in transfected *Plasmodium falciparum* parasites. *Nucleic Acids Res*. 2001;29(3):716-724.

9. Donnell RAO, Freitas-junior ÂH, Preiser PR, et al. A genetic screen for improved plasmid segregation reveals a role for Rep20 in the interaction of *Plasmodium falciparum* chromosomes. *The EMBO Journal*. 2002;21(5):1231-1239.

10. Crabb BS, Rug M, Gilberger T-W, et al. *Transfection of the Human Malaria Parasite Plasmodium Falciparum*.; 2004.

**Curriculum Vitae**

# ALEAH D. ROBERTS

Department of Molecular Microbiology and Immunology
Johns Hopkins University School of Public Health
615 N Wolfe St Room E4410
Baltimore MD 21210
E-mail: arober43@jhu.edu

## EDUCATION

**Dept. of Molecular Microbiology and Immunology**, Johns Hopkins University School of Public Health
PhD Candidate **–** Project: Developing a conditional localization tool to control protein trafficking in *Plasmodium falciparum*
**Advisor** – Dr. Sean Prigge

**2010-present**

School of Engineering and Applied Science, University of Virginia
**BS in Engineering Science & Minor in Biomedical Engineering**

**2004-2008**

## RESEARCH EXPERIENCE

**Research Assistant** in the laboratory of Dr. Phillip Scott at the Dept. of Pathobiology, University of Pennsylvania
Project: Characterizing the role human monocyte subsets in *Leishmania braziliensis* infection

**2009-2010**

**Research Assistant** in the laboratory of Dr. Edward Pearce at the Dept. of Pathobiology, University of Pennsylvania
Project: Characterizing the role of Notch signaling in alternative macrophage activation

**2008-2009**

**Undergraduate Researcher** in the laboratory of Dr. Jason Papin at the Dept. of Biomedical Engineering, University of Virginia
Project: Worked on an agent based computer model of *Xenopus laevis* embryogenesis and designed a sensitivity analysis to test the model

**2007-2008**

## AWARDS

**Outstanding Turbo Talk Award Winner**
Molecular Parasitology Meeting at the Marine Biological Laboratory in Woods Hole, MA

**2016**

**Johns Hopkins Malaria Research Institute Pre-Doctoral Fellowship Award**
This award supports pre- doctoral students interested in studying malaria

**2015**

**Russell Military Scholars Program Grant**
The focus of this program is to support research that is relevant to the health and healthcare of service members, veterans, and their family members.

**2014**

## TEACHING EXPERIENCE

**Teachers Assistant** for the graduate Biology of Parasitism course offered in the department of Molecular Microbiology and Immunology at Johns Hopkins School of Public Health. Independently lead journal club portion of the course in 2015, which involved facilitating online and in person discussions of research articles among students.

**2013, 2014, & 2015**

**Laboratory Rotation Mentor** for Amanda Balaban, Molecular Microbiology and Immunology, Johns Hopkins Bloomberg School of Public Health

**Fall 2012**

## PRESENTATIONS

**Poster** at the Future of Malaria Research Symposium, Rockville MD
Development and validation of a conditional localization domain (CLD) to control trafficking of apicoplast targeted proteins in *Plasmodium falciparum*
Aleah Roberts, Alfredo Guerra, PhD., and Sean T. Prigge, PhD.
Department of Molecular Microbiology and Immunology, Johns Hopkins School of Public Health, Baltimore, MD 21205.

**November 2016**

**Poster and Turbo Talk** at the Molecular Parasitology Meeting, Woods Hole, MA
Development and validation of a conditional localization domain (CLD) to control trafficking of apicoplast targeted proteins in *Plasmodium falciparum*
Aleah Roberts, Alfredo Guerra, PhD., and Sean T. Prigge, PhD.
Department of Molecular Microbiology and Immunology, Johns Hopkins School of Public Health, Baltimore, MD 21205.

**September 2016**

**Poster** at the Future of Malaria Research: A Young Scientists' Meeting, Rockville MD
Development and validation of a conditional localization tool to control trafficking of apicoplast targeted proteins in *Plasmodium falciparum*
Aleah Roberts and Sean T. Prigge
Department of Molecular Microbiology and Immunology, Johns Hopkins School of Public Health, Baltimore, MD 21205.

**October 2015**

**Poster** at the JHMRI World Malaria Day Meeting, Baltimore, MD
Developing a Conditional Localization Tool to Control Trafficking of Apicoplast Targeted Proteins in *Plasmodium falciparum*.
Aleah Roberts, Sean T. Prigge, PhD.
Department of Molecular Microbiology and Immunology, Johns Hopkins School of Public Health, Baltimore, MD 21205.

**April 2013**

**Poster** at the *Annual Biomedical Research Conference for Minority Students, Phoenix, AZ*
A Role for Notch Signaling in Mediating Alternative Activation of Macrophages.
Aleah Roberts, Edward J. Pearce, Ph.D., and Lucas Carvalho, Ph.D.

**November 2009**